

Development of Bacterial RNA Polymerase (RNAP) and Steroid 11- β -hydroxylase (CYP11B1) Inhibitors for Wound Healing

Dissertation

zur Erlangung des Grades des Doktors der Naturwissenschaften
der Naturwissenschaftlich-Technischen Fakultät III
Chemie, Pharmazie, Bio- und Werkstoffwissenschaften
der Universität des Saarlandes

von

MMed Weixing ZHU

Saarbrücken, 2014

Die vorliegende Arbeit wurde von September 2010 bis Mai 2014 unter Anleitung von Herrn Prof. Dr. Rolf W. Hartmann am Helmholtz Institut für Pharmazeutische Forschung Saarland und in der Fachrichtung 8.2 Pharmazeutische und Medizinische Chemie der Naturwissenschaftlich-Technischen Fakultät III der Universität des Saarlandes angefertigt.

Tag des Kolloquiums:	29. 08.2014
Dekan:	----- Professor Dr.Volkhard Helms
Berichterstatter:	----- Prof. Dr. Rolf W. Hartmann ----- Prof. Dr. Claus-Michael Lehr -----
Vorsitz:	----- Professor Dr. Claus Jacob
Akad. Mitarbeiter:	----- Dr. Ksenia Astanina -----

Abstract

This dissertation describes development of inhibitors targeting two enzymes regarding bacterial RNA polymerase (RNAP) and steroid 11 β -hydroxylase (CYP11B1) for wound healing.

During our quest for novel bacterial RNAP inhibitors as infective agents, two studies have been launched and involved in artifacts. In one study, compound **I-1** was identified as a hit compound. Later, an impurity with a structure of polymeric carboxylic acids originating from **I-1** was discovered and proven to be responsible for the biological activity. The polymer acted as a negatively charged ligand interacting very efficiently with the protein surface of *E. coli* RNAP *via* electrostatic interaction and blocking the DNA channel. In the other study, we focused on CBR703, which was reported to inhibit bacterial RNAP and biofilm formation, considering it to be a good candidate for further optimization. While synthesized derivatives of CBR703 did not result in more active RNAP inhibitors, we observed promising antibacterial activities. These again correlated with a significant cytotoxicity towards mammalian cells. Furthermore, the promising effects on biofilm formation were uncovered to be artifacts.

Topical application of CYP11B1 inhibitors to reduce cutaneous cortisol is a novel strategy to promote chronic wound healing. To satisfy this application, inhibitors were developed to possess specific metabolic profile: stable in wound fluid and unstable in liver. The potent inhibitor **III-34** ($IC_{50} = 5$ nM) was very stable in plasma ($t_{1/2} \gg 150$ min), which is similar to wound fluid in composition, whereas it was fast metabolized in human liver S9 fraction ($t_{1/2} = 16$ min) to avoid impairing adrenal steroidogenesis. It also showed no mutagenic effects and was selective CYP17 and CYP19. Therefore it is a promising candidate for further *in vivo* evaluation.

Zusammenfassung

In der vorliegenden Dissertation wird daher sowohl die Entwicklung von bakteriellen RNA Polymerase (RNAP) Inhibitoren als auch 11 β -hydroxylase (CYP11B1) Inhibitoren für die Wundheilung beschrieben.

Während unserer Suche nach neuartigen Hemmstoffen der bakteriellen RNAP zur Behandlung von Infektionskrankheiten sind wir in zwei Studien auf Artefakte gestoßen. In einer der beiden Studien identifizierten wir die Verbindung **I-1** als Hit. Später stellte sich jedoch heraus, dass die biologische Aktivität nicht auf der Verbindung selbst beruht, sondern auf eine Verunreinigung mit einem – unter physiologischen Bedingungen negativ geladenen – Polymer. Via elektrostatische Wechselwirkungen und Blockierung des DNA-Kanals interagiert dieses Polymer höchst effizient mit der Proteinoberfläche der *E. coli* RNAP. In einer weiteren Studie fokussierten wir uns auf die Verbindung CBR703, die in der Literatur als Hemmstoff der RNAP und bakterieller Biofilme beschrieben ist, was sie aus unserer Sicht attraktiv für eine weitere Optimierung machte. Obwohl die von uns synthetisierten Derivate nicht zu aktiveren RNAP-Hemmstoffen führten, beobachteten wir vielversprechende antibakterielle Aktivitäten. Diese korrelierten jedoch mit einer signifikanten Zytotoxizität in Säugerzellen. Zudem klärten wir auf, dass es sich bei den beschriebenen Effekten bezüglich Biofilmhemmung um Artefakte handelt.

Die topische Applikation von CYP11B1- Hemmstoffen zur Reduktion der Cortisol-Spiegel in der Haut ist eine neue Strategie zur Förderung der Heilung chronischer Wunden. Um diese Applikation gerecht zu werden, wurden Inhibitoren entwickelt, um durch spezifische metabolische Profil (stabil in Wundflüssigkeit aber instabil in Leber). Der sehr aktive Inhibitor **III-34** (IC_{50} = 5 nM) zeigte dabei eine sehr hohe Stabilität in Plasma ($t_{1/2}$ >> 150 min), dessen Komponenten ähnlich zu denen der Wundflüssigkeit sind, wohingegen er in humanen Leber-S9-mix schnell metabolisiert wurde ($t_{1/2}$ = 16 min), was wiederum die Steroidgenese in den Nebennieren weitgehend unbeeinträchtigt lässt. Die Verbindung zeigte keine mutagenen Effekte und keine signifikante Hemmung der Enzyme CYP17 und CYP19. Daher ist sie ein geeigneter Kandidat für weitere Untersuchungen *in vivo*.

Composition of this Dissertation

This doctoral dissertation comprises two published papers (I and II) and one submitted chapter (III), which are referred to in the text by their Roman numerals.

I. A detective story in drug discovery: elucidation of a screening artifact reveals polymeric carboxylic acids as potent inhibitors of RNA polymerase.

Weixing Zhu, Matthias Groh, Joerg Haupenthal, Rolf W Hartmann.

Chemistry-a European Journal **2013**, 19, 8397–400.

II. New insights into the bacterial RNA polymerase inhibitor CBR703 as a starting point for optimization as an anti-infective agent

Weixing Zhu, Joerg Haupenthal, Matthias Groh, Michelle Fountain, Rolf W Hartmann.

Antimicrob. Agents Chemother. **2014**, 58, 4242–4245.

III. Potent 11 β -Hydroxylase Inhibitors with Inverse Metabolic Stability in Human Plasma and Hepatic S9 Fractions to Promote Wound Healing

This chapter has been submitted to *J. Med. Chem.* recently.

Contribution Report

The author wishes to clarify her contributions to the papers **I** and **II**, and chapter **III** composing this dissertation.

- I.** Syntheses of the compounds (**1–5**) and polymers (**P1–P5**); significant contribution to elucidation of the polymers responsible for activity; significant contribution to the composition of manuscript.
- II.** Significant contribution to the inhibitor design conception; syntheses and characterization of the compounds (**1–27** and **1a–26a**), with compounds **28–30** synthesized by Dr. Matthias Groh; significant contribution to the composition of manuscript.
- III.** Significant contribution to the inhibitor design conception; syntheses and characterization of the compounds (**9–34**), with compounds **3–8** supplied by ElexoPharm; significant contribution to the interpretation of the results to SAR and test of metabolic stability; significant contribution to the composition of manuscript.

Acknowledgement

This dissertation is not only a summary of my work, but also condenses a lot of people's efforts and expectations. Now I would like to express my gratitude as a full stop to my PhD study.

I hereby extend my thanks to my doctoral advisor, Prof. Dr. Rolf W. Hartmann. I am a very ordinary student of yours, but you are the most respectable Professor to me in my eyes. No method can be used to calculate your devotion, no poems and songs to express my heartfelt gratitude and respect to you. It is you that cultivate my minds with your extensive knowledge and your noble spirits and catalyze me to enter the door to the field of drug development.

I thank China Scholarship Council for a PhD fellowship.

I express my sincere gratitude to Prof. Dr. Claus Jacob for being the chairman of the promotion committee.

I gratefully acknowledge my Berichterstatter Prof. Dr. Claus-Michael Lehr for the review of this dissertation.

I would like to thank Dr. Ksenia Astanina for being the member of the promotion committee.

Special appreciation is given to Jörg Haupenthal, Qingzhong Hu and Katrin Schmitt, who have suggested a lot to improve the dissertation in writing skills.

I appreciate Dr. Jörg Haupenthal, Dr. Matthias Groh and Dr. Qingzhong Hu as excellent group leaders. Thank you for your trust, instruction and encouragement.

The full support from Dr. Qingzhong Hu, Dr. Matthias Groh, Dr. Stefan Boettcher, and Dr. Josef Zapp in structure study as well as LC-MS and NMR measurement and resolution, respectively, is effusive in my gratitude.

I would like to thank Dr. Jörg Haupenthal, Dr. Nina Hanke, Ms. Jeannine Jung, and Ms. Jannine Ludwig for their kind help in biological evaluation of synthesized compounds.

I am grateful to Dr. Matthias Engel, Dr. Stefan Boettcher, Dr. Martin Frotscher, Mr. Lothar Jager, Ms. Katrin Schmitt, Ms. Martina Schwarz and Ms. Barbara Boeffel for their help with my accommodation and in coping with all kinds of bureaucratic procedures as I came here for the first time.

I appreciate all other members in Prof. Dr. Rolf W. Hartmann group.

Finally, I would like to express my deep love to my family. I thank my beloved parents, your love is a ship, carrying me from juvenile to mature and has given a well-being of the harbor, encouraging me during the whole voyage of the sailing. I would also like to say one sentence to my husband that I feel so lucky to hold your hand.

Abbreviations

RNAP	RNA Polymerase
CYP11B1	Steroid 11- β -hydroxylase
HTS	High-throughput screening
WHO	World Health Organization
MccJ25	microcin J25
<i>E. coli</i>	<i>Escherichia coli</i>
<i>P. aeruginosa</i>	<i>Pseudomonas aeruginosa</i>
SAR	structure-activity relationship
CYP51	lanosterol 14 α -demethylase
CYP19	aromatase
11 β -HSD1	11 β -hydroxysteroid dehydrogenase
CYP11B2	aldosterone synthase
MOA	mechanism of action
IC ₅₀	half maximal inhibitory concentration
SF	selectivity factor
GPC	gel permeation chromatography
CYP17	17 α -hydroxylase-17,20-lyase
<i>B. subtilis</i>	<i>Bacillus subtilis</i>
<i>S. aureus</i>	<i>Staphylococcus aureus</i>
FAD286	<i>R</i> -fadrozole
HEK	human embryonic kidney
FCS	fetal calf serum
M _w	weight-average molecular weight
PAINS	pan assay interference compounds
eq.	equivalent
DMAP	4-dimethylaminopyridine
phenyl-furanylrhodanines	SB series

Contents

1	Introduction	1
1.1	General	1
1.2	Bacterial RNAP and the inhibitors	2
1.2.1	Bacterial RNAP: an attractive target for combating infections	2
1.2.2	RNAP inhibitors and their binding sites	3
1.3	CYP11B1 and the inhibitors	11
1.3.1	CYP11B1: a promising target for cortisol dependent diseases	11
1.3.2	CYP11B1 inhibitors	13
2	Work Strategy	18
2.1	Design of RNAP inhibitors for anti-infection	18
2.2	Design of CYP11B1 inhibitors for wound healing	18
2.3	Biological Evaluation of Synthesized RNAP inhibitors	19
2.4	Biological Evaluation of Synthesized CYP11B1 inhibitors	19
3	Results and Discussions	20
3.1.	Paper I: A detective story in drug discovery: elucidation of a screening artifact reveals polymeric carboxylic acids as potent inhibitors of RNA polymerase.	20
3.2.	Paper II: New insights into the bacterial RNA polymerase inhibitor CBR703 as a starting point for optimization as an anti-infective agent	25
3.3.	Chapter III: Potent 11 β -Hydroxylase Inhibitors with Inverse Metabolic Stability in Human Plasma and Hepatic S9 Fractions to Promote Wound Healing	30
4	Summary and Conclusions	38
4.1	RNAP inhibitors	38
4.2	CYP11B1 inhibitors	39
5	References	41
6	Appendix	48
6.1	Supplemental Information for Paper I	48

	XI
6.2 Supplemental Information for Paper II	55
6.3 Supplemental Information for Chapter III	75
6.4 Curriculum Vitae	90

1 Introduction

1.1 General

Enzymes are considered as the most attractive targets in drug discovery. The attractiveness of enzymes as drug targets results not only from the essentiality of their catalytic activities in life processes and pathophysiology but also from the fact that enzymes, by their very nature, are highly amenable to inhibition by small molecular weight, drug-like molecules (Copeland, 2005). The most convincing evidence is that almost half the clinically used drugs today are enzyme inhibitors (Hopkins and Groom, 2002). Worldwide sales of small molecule drugs that function as enzyme inhibitors exceeded 104 billion dollars in 2011, and this market has been expected to grow to more than 127 billion dollars by 2016. It is forecasted that the worldwide market will grow at a rate of about 4% as of 2011 (Business Communications Company, Inc., 2012, <http://www.bccresearch.com/market-research/biotechnology/enzyme-inhibitors-global-markets-bio057b.html>) and therefore it is certain that specific enzyme inhibition will remain a major focus of pharmaceutical research for the foreseeable future.

Developing an enzyme inhibitor as new drug from the original idea to clinical use is a complex process which can take 12–15 years and cost over \$1 billion. Once a target has been chosen, the pharmaceutical industry and academic centers have streamlined a number of early processes to identify molecules which possess suitable properties as drugs. Due to the ability of rapid screening of diverse compounds, high-throughput screening (HTS) led to an explosion in the rate of data generated in recent years (Howe et al., 2008). “Gold can't be hundred percent pure.” It is worth mentioning that in spite of HTS’ tremendous success in drug discovery especially in hit-to-lead process, in many cases, some compounds were identified as active but later proved to be artifacts and represented false starts (Baell, 2010; Shoichet, 2006) due to their acting *via* an unspecific inhibition mode like aggregation (Coan and Shoichet, 2008; McGovern et al., 2002) or interfering with the bioassay (Auld et al., 2008; Inglese et al., 2007; Jadhav et al., 2010). Indeed, to avoid such situations, many researchers offered their experiences to give artifact alerts (Baker, 2010).

Chronic wounds torment around 2% (6.5 million) of the general population in the United States. They frequently appear as a comorbid condition and occur with increased risk of aging population, diabetes and obesity worldwide. The burden of treatment for wound healing is growing rapidly, thus it has been considered as a major and snowballing threat to public health and the economy (Sen

et al., 2009). However, the current treatment of chronic wounds is not satisfactory and novel therapy strategies are therefore urgently needed.

Wound healing is a complex process with many potential factors that can delay healing. Infection is detrimental to wound healing and all chronic wounds are colonized by bacteria. It is validated that low levels of bacteria are beneficial for wound healing (Edwards and Harding, 2004). It is also known that elevated levels of cortisol induced by stress or other reasons impair wound healing, whereas down-regulated levels of cortisol speed up wound healing (Ebrecht et al., 2004). Consequently, this work involves two parts of studies to explore novel therapy strategies regarding wound healing: the development of bacterial RNAP inhibitors combating infection and CYP11B1 inhibitors blocking cortisol synthesis.

1.2 Bacterial RNAP and the inhibitors

1.2.1 Bacterial RNAP: an attractive target for combating infections

According to the recent report of the World Health Organization (WHO), antibiotic resistance causes common infections (e.g. urinary tract, lung, bloodstream and skin infections) in all regions of the world and becomes an increasingly serious threat to global public health. A high percentage of hospital-acquired infections are caused by highly resistant bacteria. In 2012, there were about 450 000 new cases of multidrug-resistant tuberculosis. Patients with infections caused by drug-resistant bacteria are generally at increased risk of worse clinical outcomes and death, and consume more healthcare resources than patients infected with the same bacteria that are not resistant. The development of new chemicals with antibiotic properties has been considered as one of the most promising strategies for combating antibiotic resistance (Wright and Sutherland, 2007).

RNA polymerases (RNAPs) are enzymes that construct RNA chains by transcribing genes from a DNA or RNA template. This enzyme is essential for all living cells. Three reasons underline bacterial RNAP as an attractive target for combating bacterial infections (Mukhopadhyay et al., 2008): first, it is an essential enzyme for growth and survival to achieve efficacy; second, the RNAP-subunit sequences are highly conserved among bacteria to permit broad-spectrum activity; last but not least, bacterial RNAP does not share extensive sequence homology with eukaryotic RNAP to obtain therapeutic selectivity. Nowadays, bacterial RNAP is a well-validated target for broad-spectrum antibacterial including anti-tuberculosis therapy (Campbell et al., 2001b; Chopra,

2007; Darst, 2004) and highlighted by the rifamycins, which are applied as first line anti-tuberculosis drugs.

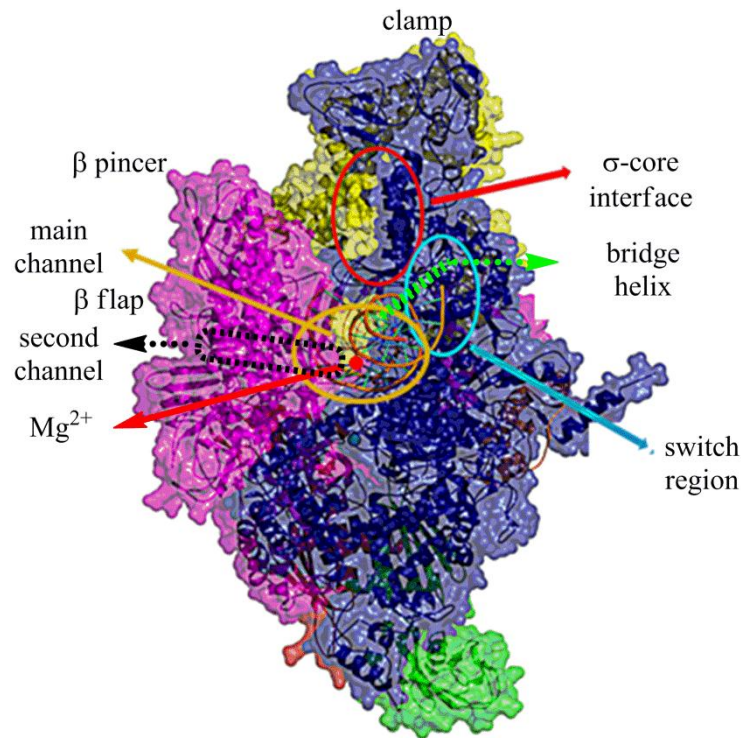


Figure 1 A model of the structure of σ factor and core enzyme. Subunits are color-coded as follows:

β , pink, β' , purple, α , green, σ , yellow, ω , brown.

1.2.2 RNAP inhibitors and their binding sites

The bacterial RNAP (~450 kDa) is a remarkable molecular machinery, consisting of a σ factor and the core enzyme, which is involved in the complicated transcription process of three stages: initiation, elongation and termination. The core enzyme (~400 kDa) of this large polymerase is composed of five subunits: α_2 , β , β' and ω , which resemble a 'crab claw'-like shape, consisting of four massive, rigid modules with additional smaller domains: the core, shelf, clamp and jaw-lobe modules. The core and shelf modules constitute the central part of RNAP, between which there are two channels, the main and the secondary channel. The clamp and jaw-lobe modules protrude from the shelf and core modules, respectively, like the pincers of a crab claw, and form parts of the main channel (Cramer et al., 2001; Zhang et al., 1999). Among these modules, the subunits connection is also revealed. The two α subunits form a dimer and play non-equivalent roles as one contacts exclusively the β' subunit whereas the other contacts β . β' and β are the largest subunits and interact with each other extensively and part of them together forms the floor of the active center cleft. Meanwhile, part of the β' subunit forms one pincer of the crab claw and part of β forms the other.

The ω subunit wraps around the carboxy-terminal tail of the β' subunit and contacts β' conserved regions. The active center of RNAP is located on the floor of the active center cleft and surrounded by five domains: the β' -clamp, β' -jaw, β -flap and the β upstream and downstream lobes. These domains are able to move independently as rigid bodies and enable binding to the transcription initiation factor σ and promoter DNA (Murakami and Darst, 2003; Murakami et al., 2002a; Murakami et al., 2002b; Wigneshweraraj et al., 2008; Wigneshweraraj et al., 2006), which is important for transcription initiation since the RNAP core must first associate with σ factor to form an RNA polymerase holoenzyme and then be activated to bind to the DNA promoter. So far, there is still little knowledge about the very initial stages of transcription activation and what the precise conformational changes and dynamics of RNAP during the transcription process are. Nevertheless, there are many known natural or synthesized molecules binding to different sites of bacterial RNAP and further blocking its function in transcription and finally inhibit bacterial growth. Some well studied binding sites for RNAP inhibitors and their locations are shown in Figure 1. The active center contains a tightly bound catalytic Mg^{2+} ion, which is adjacent to the junction of the active center cleft and the secondary channel. The downstream face of the active center is formed by the “bridge helix” (also referred to as “F helix”), which spans the active center cleft. The active center cleft and the secondary channel are divided by the bridge helix and the “trigger loop”, which interacts with each other. The “switch region”, which is located at the base of the clamp, serves as the hinge that mediates the opening and closing of the RNAP active center cleft (Cramer et al., 2001; Gnatt et al., 2001; Mukhopadhyay et al., 2008).

Rifamycins

The class of rifamycins specifically inhibiting bacterial RNAP are particularly effective against mycobacteria and are therefore used to treat tuberculosis, leprosy and mycobacterium avium complex infections. They belong to the ansamycin family of antibiotics, which have been first discovered in 1959 from an actinomycete, *Amycolatopsis mediterranei* (Sensi et al., 1959). They share a unique structure, comprising an aromatic moiety bridged by an aliphatic chain (Prelog and Oppolzer, 1973). Due to their main difference of the aromatic moiety, the various derivatives of ansamycins are divided into four classes: rifamycins possessing a naphthalene ring, naphthomycins with a naphthoquinone ring, ingeldanamycin bearing a benzene ring and ansamitocin having a benzoquinone ring (Balerna et al., 1969). The 3- and 4- positions of rifamycins have been

extensively modified by semisynthesis to improve the pharmacological properties and to yield commercial antibiotics such as rifampicin (Figure 2).

At the beginning, the mechanism of rifampicin activity was thought to depend on the allosteric inhibition of RNA polymerase (Schulz and Zillig, 1981). Based on the determination of the X-ray structure of rifampicin-RNAP, it was suggested that rifampicin binds to the DNA channel 12 Å away from the active site and acting by directly blocking the path of the elongating RNA when the transcript is 2–3 nucleotides long (Campbell et al., 2001). However, Artsimovitch et al hold a new view. In their study, rifampicin has appeared to be closer to the region 3 of factor σ than expected from the crystal structure of the rifampicin-core complex. Rifampicin changes the conformation of region 3 of σ , thereby inducing propagation of an allosteric effect along the DNA to the active site (Artsimovitch et al., 2005). Recently, another new binding model of rifampicin and its amino analogues has also been proposed as rifampicin acts as zwitterions (Pyta et al., 2012).

Sorangicin

Sorangicin (Figure 2) is a macrolide antibiotic, first obtained from the myxobacterium *Sorangium cellulosum* (Jansen et al., 1985). Sorangicin is a potent inhibitor of bacterial RNAP but has little or no effect on eukaryotic RNAPs. Its main antibacterial activity is directed against Gram-positive species (Irschik et al., 1987).

Co-crystallization of sorangicin with the *Thermus aquaticus* RNAP shows that sorangicin binds to the same β subunit pocket as rifampicin, with an almost complete overlap of RNAP binding determinants (Campbell et al., 2005).

Fidaxomicin

Fidaxomicin (Figure 2), also known as lipiarmycin, OPT-80 or PAR-101, is a macrocyclic antibiotic produced by *Actinoplanes deccanensis* (Coronelli et al., 1975). It is a novel antimicrobial agent with narrow-spectrum and particularly active against various *Clostridium* species (Swanson et al., 1991), approved by FDA for the treatment of *Clostridium difficile*-associated diarrhea in clinic. It is a specific inhibitor of transcription initiation and has no effect on middle or late transcription steps (Osburne and Sonenshein, 1980). After a fidaxomicin-resistant mutant of *Bacillus subtilis* (*B. subtilis*), which carries a mutation in the RNAP β' subunit (R326L) located in the DNA channel, opposite to the rifampicin-binding site and proximal to region 3 of σ , was isolated and characterized, the mechanism of fidaxomicin was proposed to affect transcription depending on the σ factor; moreover, region 3 is one of the most diverging domains of σ (Gualtieri et al., 2006b). More

recently, by using genetic and biochemical approaches, it was shown that fidaxomicin targets the σ^{70} subunit region 3.2 and the RNAP β' subunit switch-2 element, which controls the clamping of promoter DNA in the RNAP active-site cleft (Tupin et al., 2010).

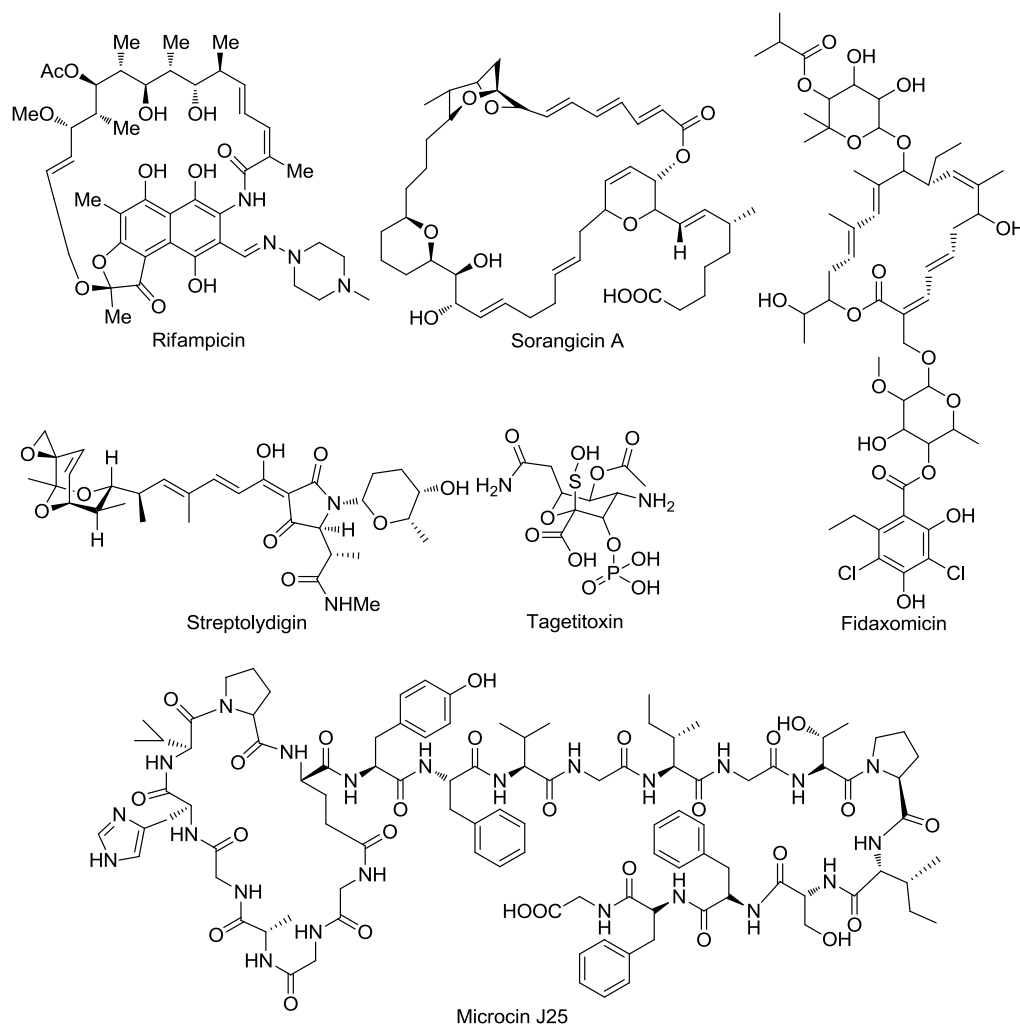


Figure 2 RNAP inhibitors (I)

Streptolydigin

Streptolydigin (Figure 2) is a member of the acyl tetramic acids (3-acyl-2,4-pyrrolidinediones) group of natural products, which inhibits bacterial RNAP and is involved in the processes of initiation, elongation and pyrophosphorolysis (Cassani et al., 1971; McClure, 1980; Siddhikol et al., 1969). It possesses high selectivity to eukaryotic RNAPI, RNAPII and RNAPIII (Cramer, 2002; Darst, 2001; Ebright, 2000). The different resistance spectra of streptolydigin compared to other RNAP inhibitors make it a compelling molecule: it exhibits only limited crossresistance with rifamycins, the only bacterial RNAP inhibitors applied in current clinical use for anti-tuberculosis (Campbell et al., 2001a) and shows only limited or no crossresistance with other RNAP inhibitors,

such as microcin J25 (Adelman et al., 2004; Mukhopadhyay et al., 2004; Yuzenkova et al., 2002), CBR703 (Artsimovitch et al., 2003) and sorangicin (Campbell et al., 2005).

The binding site of streptolydigin was determined by a combination of genetic, biochemical, and crystallographic approaches. It was uncovered that the compound binds a site adjacent to- but not overlaps the active center and stabilizes an RNAP-active-center conformational state with a straight-bridge helix (Tuske et al., 2005).

Tagetitoxin

Tagetitoxin (Figure 2) produced by *Pseudomonas syringae* pv. *tagetis*, which causes chlorosis of plant leaves attributed to inhibition of the bacterial type chloroplast RNAP (Mathews and Durbin, 1990), has been first isolated in 1981 (Mitchell and Durbin, 1981). After eight years the structure has been defined as a bicyclic phytotoxin based on NMR and mass spectrometry (Mitchell et al., 1989).

Tagetitoxin also inhibits eukaryotic RNAP III from yeasts, insects and vertebrates, while it exhibits no or a very mild effect on single-subunit phage RNAPs and nuclear RNAPs I and II (Mathews and Durbin, 1990, 1994).

Co-crystallization of tagetitoxin with the *Thermus thermophilus* RNAP revealed that tagetitoxin binds within the secondary channel of *Tth* RNAP holoenzyme near the active site of the enzyme and makes contact with several residues in the β and β' subunits of the core RNAP (Vassylyev et al., 2005). Later it was complemented that tagetitoxin interacts with the β' subunit trigger loop, stabilizing it in an inactive conformation by constructing a structural model of tagetitoxin bound to the transcription elongation complex (Artsimovitch et al., 2011). However, the detailed mechanism of inhibition remains a subject of heated debate (Klyuyev and Vassylyev, 2012; Svetlov et al., 2012).

Microcin J25

Microcin J25 (MccJ25, Figure 2) is a 21-residue, ribosomally synthesized peptide (Blond et al., 1999; Salomon and Farias, 1992) produced by strains of *Escherichia coli* (*E. coli*) harboring a plasmidborne synthesis, maturation and export system (Solbiati et al., 1999). It exhibits bacteriocidal activity against a range of Gram-negative bacteria species (Salomon and Farias, 1992).

Genetic and biochemical results suggest that MccJ25 inhibits transcription by binding within and obstructing the RNAP secondary channel also known as the “NTP uptake channel” or “pore”

(Adelman et al., 2004; Mukhopadhyay et al., 2004). Binding of MccJ25 within this channel that branches off from the main channel blocks the nucleotide substrates from entering the enzyme active site to elongation. In detail, it inhibits GreA/GreB-dependent transcript cleavage, impedes unformation of backtracked complexes, and can be crosslinked to the 3'-end of the nascent RNA in elongation complexes.

Myxopyronin, Corallopyronin and Ripostatin

Myxopyronin, the structurally related compound corallopyronin and the macrolactone ripostatin are produced by myxobacteria (Irschik et al., 1995; Irschik et al., 1983; Irschik et al., 1985).

Myxopyronin (Figure 3) is an alpha-pyrone antibiotic, first isolated from *Myxococcus fulvus* Mf50 (Irschik et al., 1983). After a total synthesis of myxopyronin was reported (Hu et al., 1998), some novel analogs of myxopyronin were synthesized (Doundoulakis et al., 2004; Lira et al., 2007). Myxopyronin exhibits broad-spectrum antibacterial activity, with potent antibacterial activity against most Gram-positive and some Gram-negative species. It has no cross-resistance with rifamycins and now is under investigation as a potential lead compound to address the growing problem of drug resistance for broad-spectrum antibacterial therapy (Srivastava et al., 2012).

Corallopyronins (Figure 3) are 2-pyrone-containing molecules, produced by myxobacterium *Corallococcus coralloides* (Irschik et al., 1985). Corallopyronins inhibit the growth of Gram-positive bacteria, but do not affect Gram-negative bacteria, yeast or fungi.

Ripostatins (Figure 3) are macrolides, produced by the myxobacterium *Sorangium cellulosum* (Irschik et al., 1995). Ripostatins A and B are active against Gram-positive bacteria. In *Staphylococcus aureus* (*S. aureus*) they inhibit chain initiation of RNA synthesis (Chang et al., 2003).

With the aim to elucidate that the “Switch Region” of RNAP is a good target for inhibitors, myxopyronin together with the structurally related α -pyrone antibiotic corallopyronin and the structurally unrelated macrocyclic-lactone antibiotic ripostatin have been investigated (Mukhopadhyay et al., 2008). It was revealed that myxopyronin interacts with the RNAP “switch region”-the hinge that mediates opening and closing of the RNAP active center cleft-to prevent interaction of RNAP with promoter DNA. Corallopyronin and ripostatin exhibit function analogously to myxopyronin.

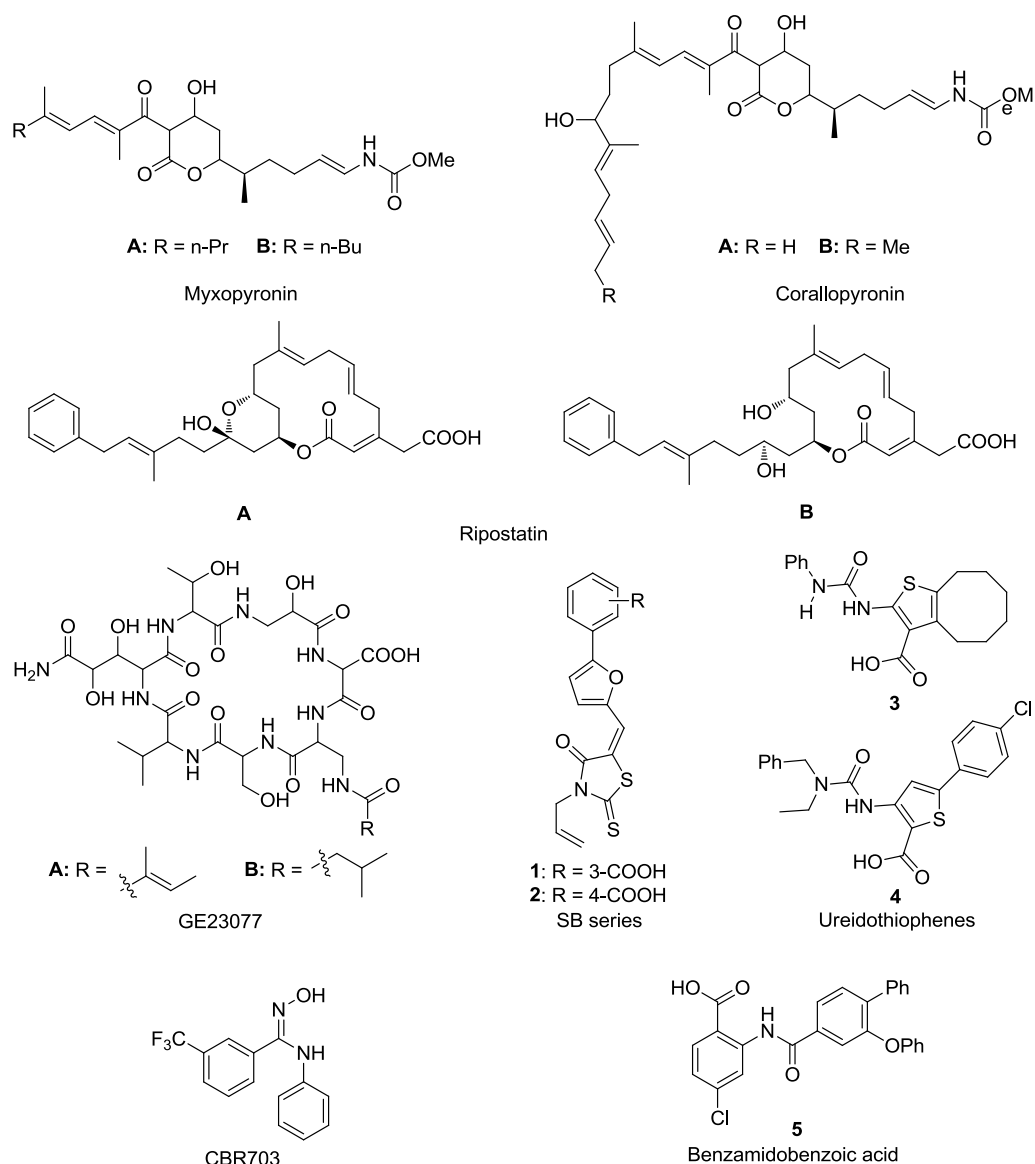


Figure 3 RNAP inhibitors (II)

GE23077

GE23077 (Figure 3) is a cyclic heptapeptide, isolated from the fermentation broth of an *Actinomadura* sp and discovered during the screening of natural products for specific inhibitors of bacterial RNAP (Ciciliato et al., 2004; Marazzi et al., 2005). Although it is a potent inhibitor of *E. coli* and *B. subtilis* RNAPs ($IC_{50} \sim 10$ nM), its antimicrobial activity is weak and restricted only to a few microorganisms (Ciciliato et al., 2004; Sarubbi et al., 2004).

The binding site of GE23077 on RNAP is different from that of rifamycin. In a combination of genetic, biochemical, and structural approaches, it was validated that GE23077 binds directly to the RNAP active center 'i' and 'i+1' sites, preventing the binding of initiating nucleotides and thereby preventing transcription initiation (Zhang et al., 2014).

CBR703

CBR703 (Figure 3) is the first synthetic inhibitor of the RNAP discovered in a HTS searching for small molecule inhibitors of RNAP (Artsimovitch et al., 2003). CBR703 shows only moderate antibacterial activity against *E. coli* TolC (MIC~15 µg/ml). Analogs have been optimized to obtain activity against wild-type strains of *E. coli*. Later, CBR703 has been reported to significantly reduce the *Staphylococcus epidermidis* biofilm mass (Villain-Guillot et al., 2007a). Thus this class of synthetic molecules has been considered to be promising for development of anti-infective agents. However, our very recent results based on systematic investigations of CBR703 have led us to conclude that they are not attractive as antibacterial agents for further development (Zhu et al., 2014).

CBR703 has first been identified to allosterically inhibit transcription by binding to a surface-exposed groove at the junction of the β' bridge helix and the β subunit (Artsimovitch et al., 2003). Very recently the same group has appended that CBR703 binds in a cavity walled by the β' bridge helix, the β' F-loop and the β fork loop (Malinen et al., 2014).

SB series

The phenyl-furanylrhodanines (SB series) of antibiotics is a new class of synthetic bacterial RNAP inhibitors, which have been discovered by screening a library of synthetic compounds using an *E. coli* core RNAP- σ^{70} factor dissociation assay (Andre et al., 2004). Its representative compound **1** (Figure 3) is active against pathogenic Gram-positive bacteria, for example, *S. aureus* and *Bacillus anthracis*, but shows no activity against Gram-negative pathogens like *E. coli* or *Pseudomonas aeruginosa* (*P. aeruginosa*). Compound **2** (Figure 3), an analogue of **1**, shows interesting activity against *S. epidermidis* biofilms. Furthermore, these molecules are not toxic against various eukaryotic cells (Gualtieri et al., 2006a). The structure-activity relationship (SAR) of this series of compounds is also explored (Villain-Guillot et al., 2007b). However, another group concluded that the SB series of compounds are not specific RNAP inhibitors as the representative molecules also exhibit potency to many other enzymes and whole-cell membrane damaging activity, thus they are unattractive for further drug development (Mariner et al., 2010).

Ureidothiophenes

The related ureidocyclooctathiophenes were first identified by screening a library of commercial available compounds targeted against the *S. aureus* RNAP holoenzyme by using a functional assay to measure the incorporation of radiolabeled nucleosides. The core structure of this class of

compounds is based on a 2-ureidothiophene-3-carboxylate scaffold (Arhin et al., 2006), shown as a related compound **3** (Figure 3). They show antibacterial effects against several *S. aureus* strains but not against other Gram-positive or Gram-negative bacteria. Till now their binding site has not been further investigated.

Recently, our group identified a hit bearing a scaffold of 5-aryl-3-ureidothiophene-2-carboxylic acid by virtual screening, based on the flexible alignment of known inhibitors (Sahner et al., 2013b). The representative compound **4** is shown in Figure 3. A systematic SAR study of ureidothiophenes has also been explored by position alternation of aryl substitution and carboxylic acid group (Elgaher et al., 2014; Sahner et al., 2013b). The new compounds displayed good antibacterial activities against Gram-positive bacteria and Gram-negative *E.coli* TolC and a reduced resistance frequency compared to the established antibiotic rifampicin. Interestingly, the 5-aryl-ureidothiophene-2-carboxylic acids exhibit potent inhibition of PqsD, an enzyme essential for *P. aeruginosa* quorum sensing apparatus (Sahner et al., 2013a).

The binding mode of compound **4** was proven by the targeted introduction of a moiety mimicking the enecarbamate side chain of myxopyronin into the hit compound, accompanied by enhanced RNAP inhibitory potency.

Benzamidobenzoic acids

Recently, a series of benzamidobenzoic acids (Figure 3) has been described as potent novel RNAP inhibitors (Hinsberger et al., 2013) derived from a known inhibitor of PqsD (Pistorius et al., 2011). The novel derivatives are active against Gram-positive pathogens and reveal significantly lower resistance frequencies compared to rifampicin.

The molecular mechanism of compound **5** (Figure 3) has been validated and indicates that this series of compounds prevents the protein-protein interaction (PPI) between σ^{70} and the RNAP core enzyme (Hinsberger et al., 2013).

Summarily, thanks to the development of crystallographic and molecular biology tools, more RNAP inhibitors and their binding sites were uncovered. Although most of these molecules are not good enough for clinical application and must be modified, there is no doubt that development of novel bacterial RNAP inhibitors to combat infection, especially in the war against anti-resistance, hold a promising future.

1.3 CYP11B1 and the corresponding inhibitors

1.3.1 CYP11B1: a promising target for cortisol dependent diseases

Steroid hormones are essential for a great number of pivotal physiological processes, however, just like every coin has two sides, their abnormal levels are also associated with life-threatening diseases. Due to the latter, the enzymes in the biosynthetic pathway of the steroid hormones have been proposed as targets for chemical intervention. The application of these enzymes inhibition has been highlighted by azole antifungals, which are inhibitors of fungal lanosterol 14 α -demethylase (CYP51) (de With et al., 2005), and human aromatase (CYP19) inhibitors in clinic for the treatment of breast and ovarian cancer (Brueggemeier et al., 2005; Jonat and Mundhenke, 2007; Simpson and Dowsett, 2002).

Cortisol is a major steroidal hormone produced in the zona fasciculata of the adrenal cortex. The production and release of cortisol is controlled by the hypothalamus-pituitary-adrenal axis. The biosynthesis of cortisol is a complex multi-step reaction (pathway shown in Figure 4), started from cholesterol and catalyzed by many enzymes, such as 3 β -hydroxysteroid dehydrogenase and 11- β -hydroxylase (CYP11B1). It is released in response to stress, and regulates metabolism and immunity but also neuronal survival and neurogenesis (Zunszain et al., 2011). It also decreases bone formation (Chyun et al., 1984). Abnormal levels of cortisol in the bloodstream cause broad functional problems (Mavoungou et al., 2005; Palacios and Sugawara, 1982; Piroli et al., 2007). Higher levels and prolonged exposure of cortisol are associated with well known diseases such as Cushing's syndrome that is characterized by visceral obesity, hypertension and diabetes (Orth, 1995). As reported, elevated cortisol also impairs chronic wound healing (Ebrecht et al., 2004; Marucha et al., 1998).

Cushing's syndrome is also called Itsenko-Cushing syndrome or hyperadrenocorticism or hypercorticism, and was firstly described by Harvey Cushing in 1932. The signs and symptoms are associated with prolonged exposure to inappropriately high levels of the cortisol (Orth, 1995). Since nearly all cases of endogenous Cushing's syndrome are caused by tumors, the surgical removal of the tumor is the first-line treatment. When a tumor recurs or resection is not feasible due to size or location of the tumor, radiotherapy is applied as an alternative. However, the inherent adverse effects and the uncertainty of long time consumption to reach biochemical normalization reduce its efficacy (Fleseriu and Petersenn, 2012; Nieman, 2002). Therefore, there is an urgent need

for a medical therapy that can effectively reduce the serum levels of cortisol. Furthermore, it is reported that the expression of CYP11B1 in epidermis is elevated after injury and thus promotes the levels of cortisol, while application of metyrapone to inhibit CYP11B1 accelerates the wound closure by decreasing cortisol (Vukelic et al., 2011). Knowing that reduced levels of cortisol speed up wound healing (Ebrect et al., 2004), it was proposed that inhibition of cortisol synthesis, such as CYP11B1 inhibitors, is a promising novel therapy strategy.

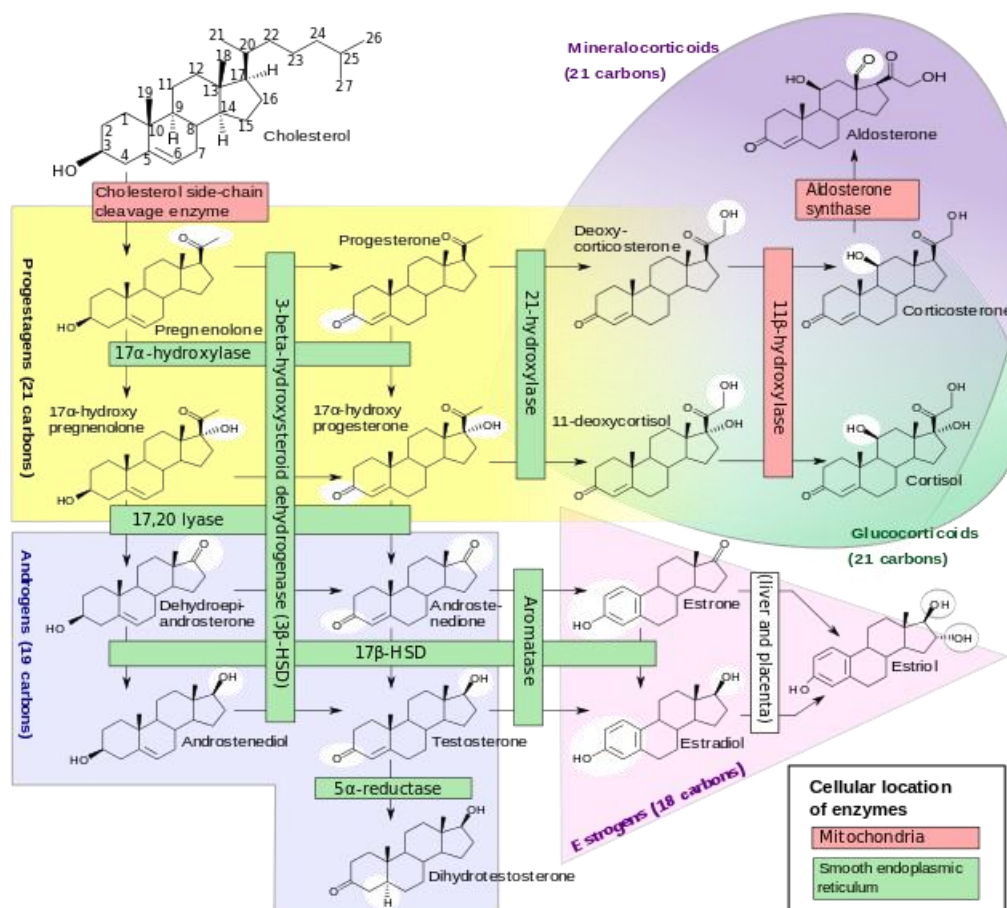


Figure 4. Steroidogenic biosynthetic pathways (adopted from http://www.genome.jp/kegg-bin/show_pathway?ko00140+C02140).

As shown in Figure 4, CYP11B1 is the key enzyme responsible for the last step in the biosynthetic pathway of cortisol, involved in the conversion of 11-deoxycortisol to cortisol (Bureik et al., 2002). There is no doubt that it is an effective strategy employing molecules inhibiting CYP11B1 to block the synthesis of cortisol. Actually, there are already some known non-selective and selective CYP11B1 inhibitors to regulate the levels of cortisol.

1.3.2 CYP11B1 inhibitors

Metyrapone

Metyrapone is a dipyridine-containing compound (Figure 5), a potent CYP11B1 and aldosterone synthase (CYP11B2) inhibitor. In V79 cells, metyrapone shows a half maximal inhibitory concentration (IC_{50}) of 15 nM and is approximately 5-fold less potent inhibition against CYP11B2 (Hille et al., 2011a). Additionally, metyrapone also inhibits CYP11A1 as well as 11 β -hydroxysteroid dehydrogenase (11 β -HSD1) (Raven et al., 1995). Some analogs of metyrapone have been prepared and their activities against CYP11B1 have been evaluated in bovine cells (Hays et al., 1984; Tobes et al., 1985).

Metyrapone is the only CYP11B1 inhibitor with certain selectivity in clinic, mainly used in the diagnosis of adrenal insufficiency and occasionally in the treatment of Cushing's syndrome. Due to its lack of selectivity toward CYP11B2, side effects as hypokalemia, edema and hypertension have been reported (Verhelst et al., 1991).

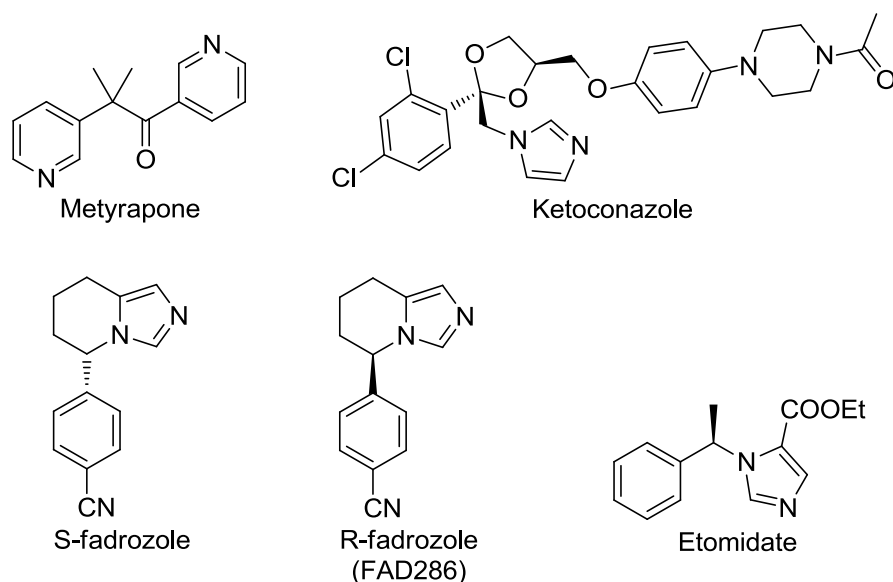


Figure 5 Non-selective CYP11B1 inhibitors

Ketoconazole

Ketoconazole (Figure 5) is a synthetic imidazole derivative. It is in clinic used primarily to treat fungal infections by inhibiting fungal CYP51. It is also used for the treatment of prostate cancer by inhibiting 17 α -hydroxylase-17,20-lyase (CYP17) to block the biosynthesis of androgen (Vasaitis et al., 2011). The inhibiting potency in V79 cellular assay has been reported to show CYP11B1 inhibition with an IC_{50} of 127 nM and CYP11B2 of 67 nM (Hille et al., 2011a). Due to CYP11B1 inhibition, this drug has also been applied for the suppression of cortisol synthesis in the treatment of Cushing's syndrome (Loli et al., 1986).

Fadrozole

Fadrozole (Figure 5) is a tetrahydroimidazopyridinyl type CYP19 inhibitor with a chiral center and thus two enantiomers (Raats et al., 1992). It was marketed as Afema by Novartis in Japan for the treatment of breast cancer (Tominaga et al., 2003). Later it was shown to impact levels of aldosterone and cortisol. The *S*-enantiomer is more potent in inhibiting CYP11B1 ($IC_{50} = 40$ nM) than CYP11B2 ($IC_{50} = 170$ nM) while *R*-fadrozole (FAD286) is a mere selective CYP11B2 inhibitor ($IC_{50} = 6$ nM) with a selectivity factor (SF) about 20 over CYP11B1 (Roumen et al., 2010).

Etomidate

Etomidate (Figure 5) is a carboxylated imidazole derivative showing anesthetic and amnestic effects. It also exhibits adrenostatic side effects, resulting in low levels of plasma cortisol after long-term infusion (Drake et al., 1998; Fellows et al., 1983). The CYP11B1 inhibition has been reported with IC_{50} values of 0.5 nM in V79 cells (Hille et al., 2011b) and 15 nM in H295R cells (Fassnacht et al., 2000) while CYP11B2 inhibition is 0.1 nM in V79 cells (Hille et al., 2011b) and approximately 1 nM in H295R cells (Hahner et al., 2010).

To develop adrenal imaging agents, radical labeled derivatives of etomidate have been prepared and evaluated as inhibitors of adrenal steroid 11β -hydroxylations, displaying high affinity to rat adrenal membranes as well as strong inhibition of cortisol secretion in NCI-H295 cells (Zolle et al., 2008). However, selectivity issues of this series of compounds have not been investigated yet.

Selective CYP11B1 inhibitors

As described above, nowadays all drugs with application as CYP11B1 inhibition are non-specific and non-selective CYP11B1 inhibitors. Not surprisingly, their adverse effects are broad and severe. Therefore, efforts have been undertaken by medicinal chemists to develop more specific and selective inhibitors. In spite of a high sequence identity (93%) between CYP11B1 and CYP11B2, CYP11B1 inhibitors with remarkably improved selectivity are available.

Based on FAD286, a series of N-benzylimidazoles as potent and selective CYP11B2 inhibitors have been prepared and reported by Novartis (Adams et al., 2010). In their report, the most expressive compound **6** (Figure 6) possesses very potent CYP11B2 inhibition ($IC_{50} = 0.3$ nM) and very good selectivity over CYP11B1 (SF = 607). In contrast, a close analogue **7** (Figure 6) turns out to be a conversed CYP11B1 inhibitor ($IC_{50} = 2$ nM), which is 20 more potent compared to CYP11B2.

Nearly at the same time, the first series of highly active and selective inhibitors of CYP11B1 in our group have been developed by outgoing from etomidate (Hille et al., 2011b). The inhibitor **8**

(Figure 6) with an IC_{50} of 152 nM toward human CYP11B1 exhibits selectivity over CYP11B2 ($SF = 18$). Furthermore, it shows negligible activities to the most important steroidogenic CYP enzymes, namely human CYP17 and CYP19 at the concentrations of 2 μ M. Later, further optimizations of these compounds have also been described and divided into three parts.

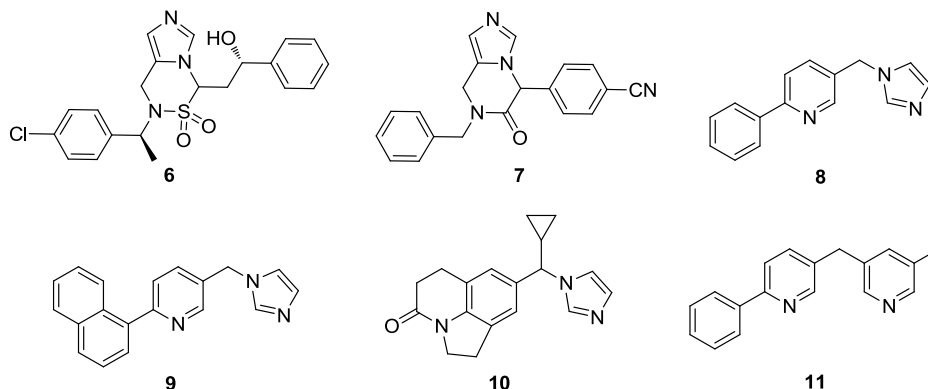


Figure 6 Selective CYP11B1 inhibitors

Firstly, the imidazolylmethyl pyridine core of this series of compounds has been further optimized to obtain compound **9** (Figure 6). The CYP11B1 activity ($IC_{50} = 42$ nM) as well as the selectivity toward CYP11B2 ($SF = 49$) has been improved. Meanwhile, selectivity has been sustained toward CYP17 and CYP19, respectively (Hille et al., 2011a).

In parallel, Yin et al demonstrated an optimization work on imidazolylmethyl quinolinones with focus on the modifications of the methyl bridge, connecting the imidazole and the core. Finally, compound **10** (Figure 6) has been identified as a very potent CYP11B1 inhibitor ($IC_{50} = 2$ nM) and with selectivity over CYP11B2 ($SF = 11$). This compound also shows potent inhibition of rat CYP11B1 but good selectivity over human CYP17 and CYP19 (Yin et al., 2012).

Later, the effect of pyridine as well as imidazole of compound **9** on the activity and selectivity was investigated by replacing of either with other heterocycles. Compound **11** (Figure 6) with two pyridine groups is known to be the most potent CYP11B1 inhibitor ($IC_{50} = 2$ nM) with a SF of 15 over CYP11B2. It is also selective over CYP17 and CYP19. The experimental results of metabolic stability show that **11** is stable in human liver S9 fraction ($t_{1/2} > 150$ min) and plasma ($t_{1/2} > 150$ min), thus it is considered as a promising candidate for Cushing's syndrome (Emmerich et al., 2013).

In summary, selective CYP11B1 inhibitors which are stable in human plasma as well as in live microsomes, have been obtained as promising candidates for the treatment of diseases that are associated with elevated cortisol levels such as Cushing's syndrome. Nevertheless, the metabolic

profiles of CYP11B1 inhibitors for wound healing are expected to be different. To maintain efficacious concentrations, the inhibitors in topical application ought to be stable in wound fluid. Since the components of wound liquid including proteases are similar to that of plasma (Tregrove et al., 1996), they should be stable in plasma. Meanwhile, when these inhibitors diffuse into circulation via wounds, they should be immediately metabolized by liver. Similar strategies that the drugs are designed with shorter metabolic time in liver to achieve more safety have been successfully applied in the inhalant glucocorticoids treating asthma (Derendorf et al., 2006). Therefore, it is necessary to design potent CYP11B1 inhibitors to be stable in plasma while unstable in liver microsomes.

2 Work Strategy

As described above, compounds targeting infections or blocking cortisol synthesis could be promising to promote wound healing. Bacterial RNA polymerase (RNAP) and steroid 11 β -hydroxylase (CYP11B1) are attractive target enzymes on the road to cure chronic wounds. Thus, we aimed to design, synthesize and evaluate novel inhibitors of these enzymes.

2.1 Design of RNAP inhibitors for anti-infection

High-throughput screening (HTS) has become a key tool in the Pharmaceutical Industry as well as in academic centers due to its ability of testing large numbers of compounds quickly and efficiently in order to identify hit compounds (Major, 1998). During our development of novel bacterial RNA polymerase inhibitors for the treatment of infectious diseases, this method was also employed.

In one study, we performed a fragment based screening using a small commercial compound library and intended to identify some small active molecules, which were expected to obtain novel potential RNAP inhibitors by connecting and enlarging the fragments.

In the other study, CBR703, a known RNAP inhibitor discovered by Artsimovitch et al. in a HTS, was used as a starting point. Firstly, we explored the structure activity relationship (SAR) on its core structure with the aim to develop more active or at least similarly active RNAP inhibitors. Afterwards, further modifications were performed to get potential antibacterial agents.

2.2 Design of CYP11B1 inhibitors for wound healing

Elevated cortisol levels induced by stress or other reasons impair wound healing, whereas the reduction of cortisol levels speeds up wound healing (Ebrecht et al., 2004). Recently, CYP11B1, a key enzyme in cortisol biosynthesis, was identified to be expressed in epidermis. The increased expression of CYP11B1 by injury elevates synthesis of cortisol and thus impairs wound healing (Vukelic et al., 2011). Therefore, CYP11B1 inhibitors with specific metabolic profiles are proposed as topical application for wound healing. To maintain efficacy, the inhibitors should be stable in wound fluid. As its composition is similar to that of plasma, the compounds were tested in plasma. To avoid the interference of endogenous steroid production, the inhibitors are expected to be fast metabolized in liver when they diffuse into blood via wound. In our previous work, pyridyl indolines have been discovered as aldosterone synthase (CYP11B2) inhibitors. With the replacement of amido by sulfonyl, the indolines were converted into CYP11B1 inhibitors.

Moreover, the most potent sulfonylation pyridyl indoline derivative exhibited promising metabolic profile. Thus, the compounds were optimized to improve potency and metabolic profiles in three directions. Firstly, different aromatic and alkyl sulfony moieties were employed to investigate the effect on potency. Secondly, the indoline ring was replaced by other rings to get novel types of inhibitors. Finally, the influences of 4-pyridyl and 3-pyridyl as well as the introduction of a bridge connecting the core and pyridyl were also investigated.

2.3 Biological Evaluation of Synthesized RNAP inhibitors

The prepared compounds were tested for *E. coli* RNAP inhibition and their ability to inhibit the growth of *E. coli TolC*. The antibacterial spectrum as well as the toxicity towards mammalian cells of the most potent compounds was then investigated. Additionally, the mode of inhibition will be also explored.

2.4 Biological Evaluation of Synthesized CYP11B1 inhibitors

The synthesized compounds were initially evaluated for CYP11B1 inhibition as well as CYP11B2 inhibition. Only very potent CYP11B1 inhibitors were further tested for selectivity over other steroidogenic CYP enzymes (CYP17 and CYP19). Metabolic stabilities of the most interesting compounds in human plasma and human liver S9 fraction were also investigated. Finally, the mutagenic potential of the most potent compound was assessed.

3 Results and Discussions

This part is composed of 2 papers and 1 chapter.

3.1 Paper I: A Detective Story in Drug Discovery: Elucidation of a Screening Artifact Reveals Polymeric Carboxylic Acids as Potent Inhibitors of RNA Polymerase

This paper has been published in *Chemistry-a European Journal* **2013**, 19:8397–400.

Reprinted with permission from *John Wiley and Sons*.

A Detective Story in Drug Discovery: Elucidation of a Screening Artifact Reveals Polymeric Carboxylic Acids as Potent Inhibitors of RNA Polymerase

Weixing Zhu, Matthias Groh, Jörg Haupenthal, and Rolf W. Hartmann*[a]

Scientific progress is hampered by publications with erroneous results.^[1] An improvement of this nuisance will depend on an enhanced alertness of researchers and reviewers of experimental artifacts. In the field of drug discovery high-throughput screening traditionally performed by the pharmaceutical industry, has found its way into academic research.^[2] The hit compounds are reported to the scientific community as good starting points for drug discovery. However, in many cases these compounds act by unspecific inhibition modes, like aggregation,^[3] or interfere with the bioassay,^[4] meaning that they represent false starts.^[5,6] During our quest for novel bacterial RNA polymerase (RNAP) inhibitors for the treatment of infectious diseases, we recently performed a fragment screening using a small commercial compound library and thereby identified compound **1** as being fairly active. Literature search revealed that three structurally related compounds (**2–4**) have already been described as RNAP inhibitors.^[7,8] Resynthesis of compound **1** resulted in an inactive compound. In the subsequent elucidation of this phenomenon we discovered that a polymeric side product was responsible for RNAP inhibition. During this process it was disclosed that the negatively charged macromolecule interacts with the positively charged protein surface.

Due to the increasing appearance of resistant microbes against clinically used drugs, novel antibiotics are urgently needed.^[9] Since the therapeutic success of rifamycins, bacterial RNA polymerase is regarded as a promising target for broad-spectrum antibacterial therapy. However, their efficiency has been reduced by an upcoming rifampicin resistance.^[10–12] Biological screening using low-molecular-weight fragments has recently become a promising alternative to high-throughput screening using drug-like molecules since the hit rate is much higher. By subsequent fragment growing or fragment linking, the initial hits can be optimized to lead compounds, which ideally fit into the target binding site.^[13,14]

In a recent project we determined the in vitro inhibitory activity of 500 commercially available fragments (molecular weight, MW < 300) towards *E. coli* RNAP. During that process compound **1** was identified, showing 85% *E. coli* RNAP inhibition at a concentration of 200 μM . Its purity was 91%, determined by HPLC-UV. Surprisingly, compound **1** synthesized in our laboratory (>96% HPLC-UV) exhibited no RNAP inhibition. Remarkably, the closely related compounds **2–4** have already been reported as inhibitors of bacterial RNAP (Figure 1).^[7,8] Synthesis of these compounds and subsequent testing in our laboratory revealed no activity (Table 1).

As we had observed that the color of compounds **1–4** turned to red under “bench conditions” (exposed to air at room temperature for several hours), we considered the possibility that they might be unstable and their inhibitory activities are due to the formation of decomposition products. To speed up the degradation process, compound **1** was

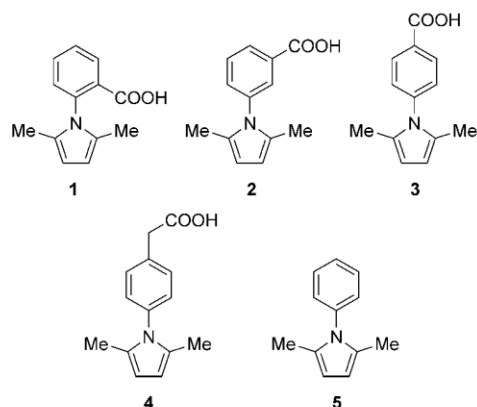


Figure 1. Compounds **1–5**.

[a] W. Zhu,* Dr. M. Groh,* Dr. J. Haupenthal, Prof. Dr. R. W. Hartmann
Helmholtz Institute for Pharmaceutical Research Saarland and
Pharmaceutical and Medicinal Chemistry, Saarland University
Campus C2.3, 66123 Saarbrücken (Germany)
Fax: (+49) 681-302-70308
E-mail: rolf.hartmann@helmholtz-hzi.de

[*] These authors contributed equally to this work.

Supporting information for this article is available on the WWW
under <http://dx.doi.org/10.1002/chem.201301289>.

Table 1. *E. coli* RNAP inhibition of compounds **1–5** and **P1–P5**.

Compound	Inhibition at 200 μM	Compound	IC ₅₀ [$\mu\text{g mL}^{-1}$]
1	n.i. ^[a]	P1	0.6
2	n.i. ^[a]	P2	1.0
3	n.i. ^[a]	P3	0.8
4	n.i. ^[b]	P4	2.5
5	n.i. ^[c]	P5	n.i. ^[d]

[a] 200 μM = 43.0 $\mu\text{g mL}^{-1}$. [b] 200 μM = 45.8 $\mu\text{g mL}^{-1}$. [c] 200 μM = 34.2 $\mu\text{g mL}^{-1}$. [d] 20.0 $\mu\text{g mL}^{-1}$; n.i. = no inhibition (inhibition < 15 %).

heated and analyzed by HPLC-UV. The results revealed that it was decomposed (Figure 2a). The effect of decomposition on RNAP inhibition was determined and an increase of activity was observed with enhanced degradation (Fig-

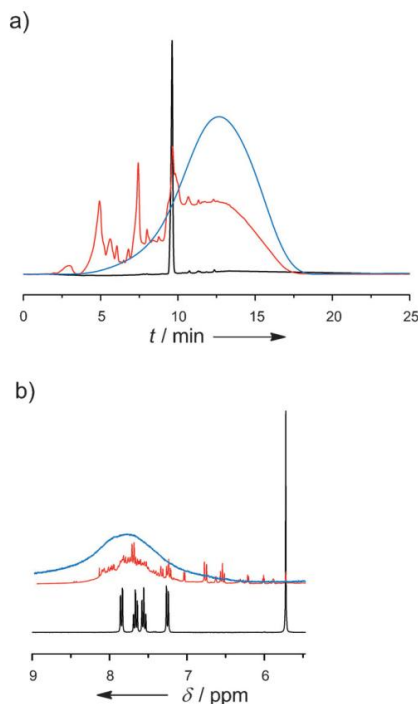


Figure 2. a) HPLC analysis, UV detection at 254 nm, b) ^1H NMR spectra. Black line: **1**; red line: **1** decomposed after 10 days heating at 50°C ; blue line: **P1**.

ure S1 in Supporting Information). From the ^1H NMR spectra it becomes apparent that the signal of the $\beta\text{-C-H}$ on the pyrrole ring ($\delta=5.7$ ppm) of compound **1** disappears whereas in the aromatic range ($\delta=8.5$ to 7.0 ppm) a broad new signal can be observed (Figure 2b). The appearance of a broad peak in the chromatogram and broad signals in the NMR spectra suggests that the decomposed product might be a polymer. Accordingly, a decomposition sample was subjected to ultrafiltration (cut-off 3.5 kDa) and it turned out that the active component was of high MW. Finally the pure polymeric compound derived from **1**, named **P1** was isolated.

By gel permeation chromatography (GPC) it was shown that **P1** exhibits a broad molecular distribution with a weight-average molecular weight (M_w) of around 40 kDa (Figure S3 in the Supporting Information). UV/Vis spectroscopy of **P1** shows an absorption peak at 498 nm (2.49 eV) associated with the $\pi\text{-}\pi^*$ transition, indicating a well conjugated π electron system in the backbone. Absorption at 498 nm could also be observed in the commercial compound **1** (Figure S4 in the Supporting Information). Interestingly, for the related compounds **2–5** polymer formation was also observed. Subsequent isolation resulted in compounds **P2–P5** (Figure S5 in the Supporting Information). In the IR

spectra of **P1–P4** the signal of the carboxylic acid group is still present (Figure S6 and Table S1 in the Supporting Information). This is in accordance to the observation that compounds **P1–P4** can be easily dissolved in water at basic pH in contrast to **P5**. In a gel electrophoresis experiment, the “polyanionic character” of **P1** was confirmed. At pH 7.8 **P1** migrated to the anode. At this pH, **P5** and at pH 3.6, both compounds remained at the starting point (Figure S7 in the Supporting Information). Based on our findings that in the polymeric compounds **P1–P4** the $\beta\text{-C-H}$ on the pyrrole ring signal is missing, the benzoic acid group is still present and a conjugated system of double bonds has been demonstrated, the only plausible structure, to the best of our knowledge, is shown in Figure 3 with **P1** as an example.

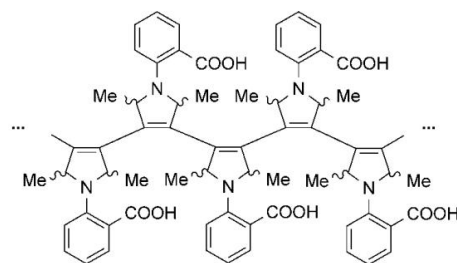


Figure 3. Supposed structure of the polymeric compound **P1**.

The ability of **1–5** and **P1–P5** to inhibit *E. coli* RNAP was determined in an in vitro transcription assay (Table 1). None of the monomeric compounds affected transcription, whereas the polymers bearing a carboxylic acid group (**P1–P4**) inhibited *E. coli* RNAP in a concentration-dependent manner with IC_{50} values between 0.6 and $2.5\ \mu\text{g mL}^{-1}$. **P5** lacking the carboxylic acid group was inactive indicating that the carboxylic acid group is essential for inhibitory activity.

Considering the mode of inhibition of the polymers, it is worth mentioning that there are positively charged amino acid residues on the surface of RNAP, including the DNA binding channel (Figure 4), serving as a counterpart for the negatively charged DNA. Therefore, it can be rationalized that the inhibitory mechanism of **P1** is based on multiple

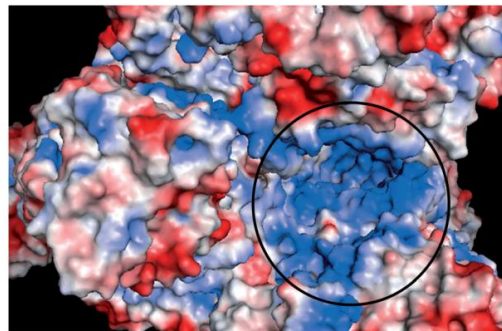


Figure 4. Electrostatic surface of *E. coli* RNAP core enzyme visualized using PyMOL (PDB ID: 3LU0).^[18] The circle highlights the DNA binding channel. Red shows the negatively charged and blue positively charged electrostatic potential surface.

electrostatic interactions between the negatively charged carboxylate groups and the positively charged protein surface. In this context it is of interest that some other polyanions including polysulfated heparins have already been reported to inhibit RNAP.^[15–17]

The electrostatic interaction of **P1** with RNAP was demonstrated by gel electrophoresis. In the presence of RNAP the mobility of **P1** was reduced (Figure S7 in the Supporting Information). Considering the averaged molecular weight of around 40 kDa, the IC_{50} value of **P1** against *E. coli* RNAP can be calculated to be approximately 15 nM. Since the concentration of enzyme in the assay is 36 nM, it can be concluded that **P1** binds to the protein at a molar ratio of about 1:1 and is a very potent inhibitor. Under identical experimental conditions a 70-fold excess of heparin is required to obtain the same inhibitory effect.

On closer examination it is obvious that the bound polymer should sterically block the loading of the DNA template to RNAP and thus inhibit transcription at its earliest step. To corroborate this hypothesis, the influence of **P1** on DNA binding to the RNAP main channel was investigated. We expected that **P1** should be less effective if the DNA template already occupied the main channel. Indeed, our results revealed a significantly reduced RNAP inhibition when the DNA template was added prior to **P1** compared to a vice versa chronology of addition. For rifampicin, which affects the transcription process by binding to an allosteric site close to the active site within the DNA binding channel,^[19] a similar trend was observed (Figure 5). As a negative control, CBR703, was used as it is described to bind to a surface-exposed groove distant from the main channel, which should not influence the binding of the DNA template to its channel.^[20] As expected, CBR703 inhibited RNAP independently of whether the DNA channel was already occupied by the DNA template or not. In summary, this experiment supports our hypothesized mechanism of **P1** RNAP inhibition.

To find out whether these inhibitory profiles can also be observed for RNA polymerases from other species, RNAP from bacteriophage T7 was employed. **P1** showed a strong inhibitory effect ($IC_{50}=0.06 \mu\text{g mL}^{-1}$) whereas compound **1** was inactive at 200 μM ($43.3 \mu\text{g mL}^{-1}$). In contrast to these findings, **P1** showed no or only moderate activity against seven other enzymes (Table S2 in the Supporting Information). In a further experiment, **P1** did not inhibit growth of *E. coli* and *Pseudomonas aeruginosa* (at 20 $\mu\text{g mL}^{-1}$). The lack of in vivo activity was expected as **P1** is too hydrophilic for passive diffusion and too large to permeate the porins and enter the bacterial cell.

Nevertheless, it is feasible that the knowledge gained in this study could be exploited for an antibacterial therapy. Biological in vitro effects of polyanions including inhibition of RNAP have indeed already been described.^[15–17] However, the polymers were devoid of antibacterial activity. It seems viable that in vivo activity could be achieved for our polymers by strongly reducing their size, thus enabling hydrophilic substances to penetrate the porins. On the other hand polyanions of such a molecular weight should not be capable of passing the membranes of mammalian cells, and therefore they could be potential therapeutics for local infections of the skin and lung.

In summary, we could demonstrate that the activity of the hit compound **1** found in an experimental screening approach can be attributed to a highly active polymeric impurity formed by decomposition of **1**. Remarkably, the closely related compound **4** is also described as a RNAP inhibitor.^[7] In our assay “synthesized” **4** was inactive, whereas the polymerized compound strongly inhibited the bacterial enzyme. Furthermore, **2** was also reported to be active against poliovirus RNAP,^[21] which seems doubtful with respect to our findings. It is worth mentioning that compounds **1–4** are reported to inhibit HIV-1 gp41,^[22] anthrax lethal factor^[23] and Eph receptors.^[24] Remarkably around 500 related derivatives of *N*-phenyl-2,5-dimethyl pyrrole are reported in numerous patents and publications as biologically active compounds;^[25] nevertheless, they do not have a clean slate and have been propagated as pan assay interference compounds (PAINS).^[26] However, the molecular mechanism of the false positive results remained “mysterious” until this investigation.

In conclusion, researchers should be cautious with compounds that tend to polymerize, as even traces of polymeric impurities might cause tremendous effects in biological assays.

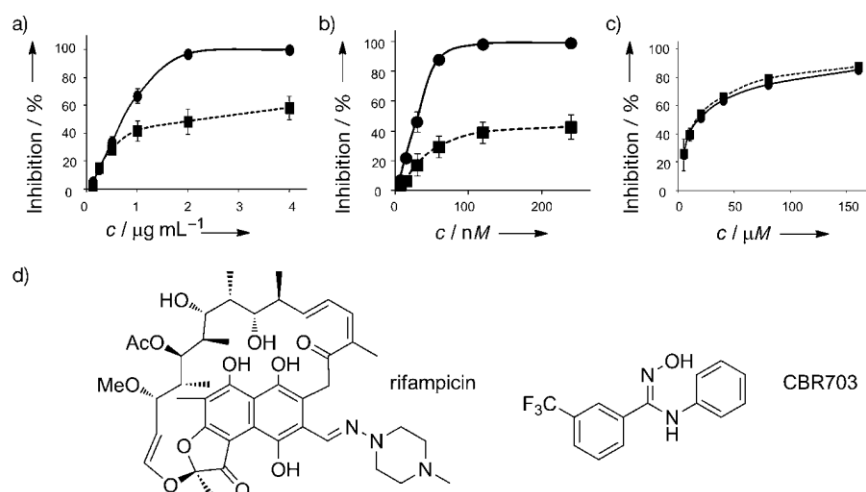


Figure 5. *E. coli* RNAP transcription assay with different chronology of addition of DNA template and inhibitor. Solid line: normal test procedure: inhibitor was added before the DNA template. Dashed line: reversed test procedure: DNA template was added before the inhibitor. Concentration-dependent inhibition of: a) **P1**, b) rifampicin, c) CBR703; d) structures of rifampicin and CBR703.

Acknowledgements

W.Z. thanks the China Scholarship Council for a PhD fellowship. The authors thank Jeannine Jung for technical assistance.

Keywords: biological screening • drug discovery • experimental artifacts • inhibitors • polyanions

- [1] U. Poeschl, *Learn. Publ.* **2004**, *17*, 105–113.
- [2] M. Baker, *Nat. Methods* **2010**, *7*, 787–792.
- [3] a) S. L. McGovern, E. Caselli, N. Grigoieff, B. K. Shoichet, *J. Med. Chem.* **2002**, *45*, 1712–1722; b) K. E. Coan, B. K. Shoichet, *J. Am. Chem. Soc.* **2008**, *130*, 9606–9612.
- [4] a) J. Inglese, R. L. Johnson, A. Simeonov, M. Xia, W. Zheng, C. P. Austin, D. S. Auld, *Nat. Chem. Biol.* **2007**, *3*, 466–479; b) D. S. Auld, N. Thorne, D. T. Nguyen, J. Inglese, *ACS Chem. Biol.* **2008**, *3*, 463–470; c) A. Jadhav, R. S. Ferreira, C. Klumpp, B. T. C. P. Mott, C. P. Austin, J. Inglese, C. J. Thomas, D. J. Maloney, B. K. Shoichet, A. Simeonov, *J. Med. Chem.* **2010**, *53*, 37–51.
- [5] B. K. Shoichet, *Drug Discovery Today* **2006**, *11*, 607–615.
- [6] J. B. Baell, *Future Med. Chem.* **2010**, *2*, 1529–1546.
- [7] E. André, L. Bastide, P. Villain-Guillot, J. Latouche, J. Rouby, J. P. Leonetti, *Assay Drug Dev. Technol.* **2004**, *2*, 629–635.
- [8] B. Pau, J. P. Leonetti, J. Rouby, *PCT Int. Appl.* **2002**, WO 2002044735A1 20020606.
- [9] L. Freire-Moran, B. Aronsson, C. Manz, I. C. Gyssens, A. D. So, D. L. Monnet, O. Cars, *Drug Resist. Updates* **2011**, *14*, 118–124.
- [10] I. Chopra, *Curr. Opin. Investig. Drugs* **2007**, *8*, 600–607.
- [11] S. A. Darst, *Trends Biochem. Sci.* **2004**, *29*, 159–162.
- [12] J. B. P. Villain-Guillot, L. Bastide, M. Gualtieri, J. P. Leonetti, *Drug Discovery Today* **2007**, *12*, 200–208.
- [13] D. C. Rees, M. Congreve, C. W. Murray, R. Carr, *Nat. Rev. Drug Discovery* **2004**, *3*, 660–672.
- [14] D. A. Erlanson, *Curr. Opin. Biotechnol.* **2006**, *17*, 643–652.
- [15] C. T. Warnick, H. M. Zazarus, *Nucleic Acids Res.* **1975**, *2*, 735–744.
- [16] K. Ono, H. Nakane, M. Fukushima, *Eur. J. Biochem.* **1988**, *172*, 349–353.
- [17] F. de M. Dossin, S. Schenkenman, *Eukaryotic Cell* **2005**, *4*, 960–970.
- [18] N. Opalka, J. Brown, W. J. Lane, K. A. F. Twist, R. Landick, F. J. Asturias, S. A. Darst, *PLoS Biol.* **2010**, *8*, e1000483.
- [19] E. A. Campbell, N. Korzhova, A. Mustaev, K. Murakami, S. Nair, A. Goldfarb, S. A. Darst, *Cell* **2001**, *104*, 901–912.
- [20] I. Artsimovitch, C. Chu, A. S. Lynch, R. Landick, *Science* **2003**, *302*, 650–654.
- [21] G. Campagnola, P. Gong, O. B. Peersen, *Antiviral Res.* **2011**, *91*, 241–251.
- [22] K. Liu, H. Lu, L. Hou, Z. Qi, C. Teixeira, F. Barbault, B. Fan, S. Liu, S. Jiang, L. Xie, *J. Med. Chem.* **2008**, *51*, 7843–7854.
- [23] R. Noberini, M. Koolpe, S. Peddibhotla, R. Dahl, Y. Su, N. D. P. Cosford, G. P. Roth, E. B. Pasquale, *J. Biol. Chem.* **2008**, *283*, 29461–29472.
- [24] D. J. Shaw, W. F. Wood, *J. Chem. Educ.* **1992**, *69*, A313.
- [25] Number based on SciFinder literature search for compounds containing the *N*-phenyl-2,5-dimethyl pyrrole core.
- [26] J. B. Baell, G. A. Holloway, *J. Med. Chem.* **2010**, *53*, 2719–2740.

Received: April 5, 2013
Published online: May 16, 2013

3.2 Paper II: New insights into the bacterial RNA polymerase inhibitor CBR703 as a starting point for optimization as an anti-infective agent

This paper has been published in *Antimicrobial Agents and Chemotherapy* **2014**, 58:4242-4245.

Reprinted with permission from *ASM*.

New Insights into the Bacterial RNA Polymerase Inhibitor CBR703 as a Starting Point for Optimization as an Anti-Infective Agent

Weixing Zhu,^a Jörg Haupenthal,^a Matthias Groh,^a Michelle Fountain,^c Rolf W. Hartmann^{a,b}

Helmholtz Institute for Pharmaceutical Research Saarland (HIPS), Department of Drug Design and Optimization,^a and Pharmaceutical and Medicinal Chemistry,^b Saarland University, Saarbrücken, Germany; Helmholtz Centre for Infection Research, Braunschweig, Germany^c

CBR703 was reported to inhibit bacterial RNA polymerase (RNAP) and biofilm formation, considering it to be a good candidate for further optimization. While synthesized derivatives of CBR703 did not result in more-active RNAP inhibitors, we observed promising antibacterial activities. These again correlated with a significant cytotoxicity toward mammalian cells. Furthermore, we suspect the promising effects on biofilm formation to be artifacts. Consequently, this class of compounds can be considered unattractive as antibacterial agents.

Bacterial RNA polymerase (RNAP) is essential for bacterial growth and survival and is thus an attractive target for drug development (1, 2). Along with the recently FDA-approved fidaxomicin (3), the rifamycins, applied as first-line antituberculosis drugs, are the only RNAP inhibitors that are in clinical use (2). However, similarly to other anti-infectives, the use of rifamycins resulted in the occurrence of resistant bacterial strains (1, 4–7), which represents a remarkable threat to public health (8, 9). Consequently, there is a need to focus on novel promising inhibitors. Recently, interesting peptidic and peptidomimetic (10–12) as well as nonpeptidic (13–18) small-molecule RNAP inhibitors have been described. Another example is CBR703 (Fig. 1), whose mechanism of action is reported to be different from that of the rifamycins (19, 20). This compound has been identified in a high-throughput screening searching for small-molecule inhibitors of RNAP (19). Two more-potent analogs in that report reveal the potential of optimizing CBR703 by structural enlargement. Furthermore, pursuing the hypothesis that RNAP is of particular importance for bacterial survival in biofilms, Villain-Guillot et al. showed CBR703 to significantly reduce *Staphylococcus epidermidis* biofilm mass (21). We therefore considered CBR703 to be a promising starting point for drug development. Consequently, we focused on CBR703 to perform systematic modifications on its core structure, aiming to obtain a more appropriate starting point for further structural optimization.

Detailed information concerning the materials and methods used in synthesis and biology can be found in the supplemental material.

In total, 30 final compounds and 24 intermediates were obtained and tested for *Escherichia coli* RNAP inhibition and their ability to inhibit the growth of *E. coli* TolC (see Table S1 to S3 in the supplemental material). According to their structures, the synthesized derivatives can be divided into three structures with modifications in part A, B, or C (Fig. 1). Compounds 1 to 25 (see Scheme S1 in the supplemental material) with introduction of substituents into the aromatic moieties (part A or B) were prepared by condensation of an intermediate amide with hydroxylamine (22, 23). In order to ensure an appropriate coverage of lipophilic and electronic properties, the substituents were chosen rationally from all quadrants of a Craig plot (e.g., Hansch-Fujita π versus σ constant) (24). The results (see Table S1) showed that compounds 1 to 25 display decreased RNAP inhibition compared

to CBR703, with the exception of two compounds (18 and 19) with similar activities (50% inhibitory concentrations [IC₅₀s] in the range of 20 μ M). As previously reported (19), there were two more-potent CBR703 analogs with a larger size, one of which was optimized by replacing the linker amidoxime with a pyrazole system. To investigate this structural modification, compounds 26 to 30 with a different linking part (part C) have been synthesized (see Table S2). Remarkably, in our case, replacement of the amidoxime moiety by other functional groups, including N-heterocycles, led to a decrease in or complete loss of activity. Additionally, all amide intermediates turned out to be inactive against RNAP (see Table S3). Surprisingly, 11 compounds, including intermediates with little or even no RNAP inhibition, showed stronger antibacterial potency in *E. coli* TolC than CBR703. Compound 3a with a MIC of 2 μ g/ml was even more potent than rifampin. The fact that no correlation between RNAP inhibition and antibacterial activity (see Table S1 to S3) could be observed led us to the conclusion that additional mechanisms besides RNAP inhibition must be responsible for the antibacterial activity.

To obtain further information about the antibacterial profiles, four compounds (Fig. 1) were selected based on the results of the previous experiments (see Table S1 to S3 in the supplemental material) and compared with reference compounds. In a first step, the effects of these compounds on the growth of *E. coli* K-12, *Pseudomonas aeruginosa* PAO1, *Bacillus subtilis*, and *Staphylococcus aureus* were investigated (Table 1). Notably, compounds 7 (the best compound against *E. coli* TolC bearing an amidoxime group) and 19 (the most active RNAP inhibitor) showed only moderate activity against *B. subtilis*. Compound 3a (the most active compound against *E. coli* TolC) exhibited rather potent activities against *B. subtilis* and *S. aureus*. For compound 26 (the only com-

Received 19 February 2014 Returned for modification 18 March 2014

Accepted 5 May 2014

Published ahead of print 12 May 2014

Address correspondence to Rolf W. Hartmann, rolf.hartmann@helmholtz-hzi.de.

Supplemental material for this article may be found at <http://dx.doi.org/10.1128/AAC.02600-14>.

Copyright © 2014, American Society for Microbiology. All Rights Reserved.

doi:10.1128/AAC.02600-14

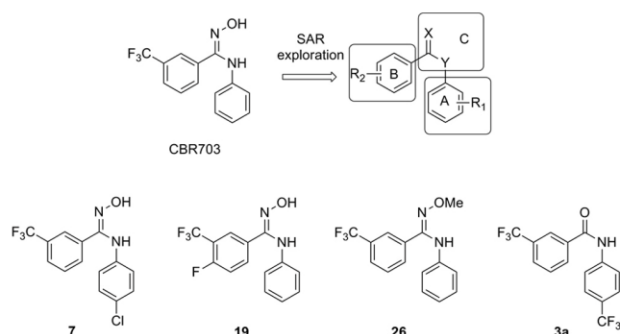


FIG 1 CBR703 and the most potent compounds in different classes: compound 7, best compound against *E. coli* TolC bearing an amidoxime group; compound 19, most RNAP-inhibitory derivative; compound 26, the only RNAP inhibitor after replacement of the amidoxime linker; compound 3a, most active against *E. coli* TolC. SAR, structure activity relationship.

pound with RNAP inhibition after replacement of the amidoxime linker), we observed no detectable activities against Gram-positive species. None of the compounds inhibited the growth of Gram-negative strains K-12 and PAO1. In addition, the toxicity of the inhibitors toward mammalian cells was tested using the human embryonic kidney 293 (HEK293) cell line. Interestingly, the most active compound in the MIC experiment, compound 3a, showed significant cytotoxicity and the other tested compounds were also at least moderately toxic (Table 2). As it is known that lipophilic compounds bind to serum proteins, which were also present in our MTT [3-(4,5-dimethyl-2-thiazolyl)-2,5-diphenyl-2H-tetrazolium bromide] assay as a component of fetal calf serum (FCS), we added the same amount of FCS (10%) to the bacterial growth medium and performed the MIC determinations in *E. coli* TolC. Surprisingly, the antibacterial activity of the tested compounds was abolished or drastically reduced (see Table S4). This finding led to the assumption that the cytotoxicities of our compounds are even more pronounced in the absence of serum.

As it had been shown that CBR703 efficiently eradicated biofilm-embedded bacteria (21), we considered that this effect could be due to Fe(III) chelation (25, 26). The fact that the amidoxime moiety plays a prominent role in the activity in our compounds and the well-known property of amidoxime functional groups to form Fe(III) complexes gave rise to the presumption that the amidoximes display their antibacterial effect due to such a complex-

TABLE 2 Investigation of cytotoxicity in HEK293 cells^a

Compound	LD ₅₀ at 24 h (μM)	LD ₅₀ at 72 h (μM)
CBR703	58	52
7	43	40
19	34	33
26	25	38
3a	15	13
Rifampin	>100	81
Doxorubicin	5	0.3

^a The most potent antibacterial compound, compound 3a, was also the most toxic one. Rifampin, negative control; doxorubicin, positive control; LD₅₀, 50% lethal dose.

ation (27, 28). Consequently, we examined this hypothesis. First, the ability of CBR703 to form Fe(III) complexes was confirmed by a color change reaction (29). After addition of a CBR703 solution, the brown red FeCl₃ solution turned to blue whereas this change was not observed after addition of compound 26 (see Table S5 in the supplemental material). In a following step, the complex stability constants were determined by potentiometric titration. Thereby, it was uncovered that formation of Fe(OH)₃ was observed even under acidic conditions (pH = 4). This means that, under physiological conditions, CBR703 cannot form stable Fe(III) complexes. These results were supported by biological tests which were performed in parallel. Indeed, addition of Fe(III) had an effect on the anti-TolC activity of the positive control deferoxamine mesylate (DFO)—a known iron chelator with antibacterial activity (30)—but not on that of CBR703, leading to our conclusion that the antibacterial effects of CBR703 are not attributable to iron complexation (see Fig. S1). Interestingly, each of the three most antibacterial compounds (compounds 3a, 10a, and 21a) possesses two strong electron-withdrawing (leading to a polarity decrease) and highly lipophilic CF₃ groups which might be the reason for their antibacterial potency. Such properties could facilitate cell penetration and could furthermore result in nonspecific inhibition of a variety of other enzymes.

During the determination of MIC values, we found that CBR703 showed slight precipitation at 100 μg/ml whereas its MIC was determined to be 100 μg/ml in the literature (21). Beyond that, a significant effect on *Staphylococcus epidermidis* biofilm was reported at concentrations between 100 and 400 μg/ml. At these concentrations, we observed strong and concentration-dependent precipitation of CBR703 and selected derivatives in Mueller-

TABLE 1 RNAP inhibition and antibacterial profile of selected compounds^a

Compound	% inhibition of <i>E. coli</i> RNAP (at 50 μM) or IC ₅₀ value	MIC (μg/ml) ^b				
		Gram-negative bacteria			Gram-positive bacteria	
		<i>E. coli</i> TolC	<i>E. coli</i> K-12	<i>P. aeruginosa</i> PAO1	<i>B. subtilis</i>	<i>S. aureus</i>
CBR703	18 μM ^c	14	>25	>25	>25	>25
7	35	9	>25	>25	23	>25
19	19 μM ^c	21	>50	>50	43	>50
26	29	24	>25	>25	>25	>25
3a	n.i.	2	>25	>25	5	11
Rifampin	24 nM ^c	6	7	13	5	0.02

^a No correlation between RNAP inhibition and antibacterial activities was observed, suggesting that the antibacterial activity was due to a mechanism other than RNAP inhibition. The standard deviations (SD) in these experiments were <25% (in most cases, <15%). n.i., no inhibition (<10% inhibition).

^b >25 and >50, MIC determinations were limited due to insufficient solubility of the compound.

^c IC₅₀ value.

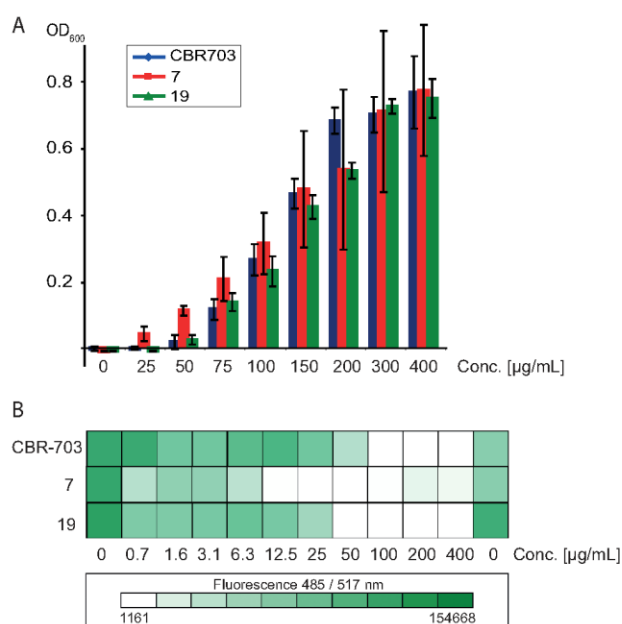


FIG 2 Correlation between precipitation and biofilm mass. (A) Concentration-dependent precipitation of CBR703 and compounds 7 and 19 in MHB. (B) Quantification of the washed biofilm mass. A complete biofilm reduction can be observed only at concentrations at which precipitates have formed. The most prominent effect can be observed for compound 7.

Hinton broth (MHB) (Fig. 2A; see also Fig. S2 in the supplemental material), the medium used in the literature (21). Nevertheless, we evaluated all compounds on *S. aureus* biofilms with concentrations in a soluble range but without observing an effect. At higher concentrations (100 to 400 μg/ml), CBR703 and its derivatives (e.g., compounds 7 and 19) showed a clear reduction in biofilm formation (Fig. 2B), indicating a correlation between antibiofilm activity and precipitation.

In this work, we designed and synthesized derivatives of CBR703 as a follow-up to a published paper (19), aiming to optimize their promising biological effects by modifying the core structure. However, no compound showed enhanced RNAP inhibition. Nevertheless, in some cases we observed promising antibacterial activities. These again turned out to correlate with a significant cytotoxicity toward HEK293 cells. Furthermore, the reported effects on biofilm formation, which were among the main reasons for choosing CBR703 as a starting point, were suspected to be artifacts due to compound precipitation. This finding should be a reminder to the scientific community to be cautious with published data, as they could include such artifacts (31). Consequently, we rank this class of compounds as unattractive for development as antibacterial agents.

ACKNOWLEDGMENTS

W. Zhu thanks China Scholarship Council for her Ph.D. fellowship.

We thank Jeannine Jung and Jannine Ludwig for technical assistance, Kaspar Hegetschweiler and Bernd Morgenstern of the Department of Chemistry, Saarland University, Germany, for the determination of complex stability constants, Werner Tegge of the Helmholtz Centre for Infection Research, Braunschweig, Germany, for supporting M. Fountain's biofilm tests, and Wolfgang Witte of the Robert Koch Institute, Wernigerode, Germany, for kindly providing the MSSA ST30 strain.

REFERENCES

- Chopra I. 2007. Bacterial RNA polymerase: a promising target for the discovery of new antimicrobial agents. *Curr. Opin. Investig. Drugs* 8:600–607.
- Mariani R, Maffioli SI. 2009. Bacterial RNA polymerase inhibitors: an organized overview of their structure, derivatives, biological activity and current clinical development status. *Curr. Med. Chem.* 16:430–454. <http://dx.doi.org/10.2174/092986709787315559>.
- Talpaert M, Campagnari F, Clerici L. 1975. Lipiarmycin: an antibiotic inhibiting nucleic acid polymerases. *Biochem. Biophys. Res. Commun.* 63:328–334. [http://dx.doi.org/10.1016/S0006-291X\(75\)80047-7](http://dx.doi.org/10.1016/S0006-291X(75)80047-7).
- Darst SA. 2004. New inhibitors targeting bacterial RNA polymerase. *Trends Biochem. Sci.* 29:159–162. <http://dx.doi.org/10.1016/j.tibs.2004.02.005>.
- Villain-Guillot P, Bastide L, Gualtieri M, Leonetti JP. 2007. Progress in targeting bacterial transcription. *Drug Discov. Today* 12:200–208. <http://dx.doi.org/10.1016/j.drudis.2007.01.005>.
- Bryskier A. 2005. Anti-MRSA agents: under investigation, in the exploratory phase and clinically available. *Expert Rev. Anti Infect. Ther.* 3:505–553. <http://dx.doi.org/10.1586/14787210.3.4.505>.
- Floss HG, Yu TW. 2005. Rifamycin—mode of action, resistance, and biosynthesis. *Chem. Rev.* 105:621–632. <http://dx.doi.org/10.1021/cr030112j>.
- Coates ARM, Halls G, Hu Y. 2011. Novel classes of antibiotics or more of the same? *Br. J. Pharmacol.* 163:184–194. <http://dx.doi.org/10.1111/j.1476-5381.2011.01250.x>.
- Walsh C. 2003. Where will new antibiotics come from? *Nat. Rev. Microbiol.* 1:65–70. <http://dx.doi.org/10.1038/nrmicro727>.
- Hüßeken K, Negri M, Fruth M, Boettcher S, Hartmann RW, Hauptenthal J. 2013. Peptide-based investigation of the *Escherichia coli* RNA polymerase $\sigma(70)$:core interface as target site. *ACS Chem. Biol.* 8:758–766. <http://dx.doi.org/10.1021/cb3005758>.
- Kuznedelov K, Semenova E, Knappe TA, Mukhamedyarov D, Srivastava A, Chatterjee S, Ebright RH, Marahiel MA, Severinov K. 2011. The antibacterial threaded-lasso peptide capistrin inhibits bacterial RNA polymerase. *J. Mol. Biol.* 412:842–848. <http://dx.doi.org/10.1016/j.jmb.2011.02.060>.
- Ma C, Yang X, Kandemir H, Mielczarek M, Johnston EB, Griffith R, Kumar N, Lewis PJ. 2013. Inhibitors of bacterial transcription initiation complex formation. *ACS Chem. Biol.* 8:1972–1980. <http://dx.doi.org/10.1021/cb400231p>.
- Sahner JH, Groh M, Negri M, Hauptenthal J, Hartmann RW. 2013. Novel small molecule inhibitors targeting the “switch region” of bacterial RNAP: structure-based optimization of a virtual screening hit. *Eur. J. Med. Chem.* 65:223–231. <http://dx.doi.org/10.1016/j.ejmech.2013.04.060>.
- Hinsberger S, Hüßeken K, Groh M, Negri M, Hauptenthal J, Hartmann RW. 2013. Discovery of novel bacterial RNA polymerase inhibitors: pharmacophore-based virtual screening and hit optimization. *J. Med. Chem.* 56:8332–8338. <http://dx.doi.org/10.1021/jm400485e>.
- André E, Bastide L, Michaux-Charachon S, Gouby A, Villain-Guillot P, Latouche J, Bouchet A, Gualtieri M, Leonetti JP. 2006. Novel synthetic molecules targeting the bacterial RNA polymerase assembly. *J. Antimicrob. Chemother.* 57:245–251. <http://dx.doi.org/10.1093/jac/dki426>.
- Arhin F, Belanger O, Ciblat S, Dehbi M, Delorme D, Dietrich E, Dixit D, Lafontaine Y, Lehoux D, Liu J, McKay GA, Moock G, Reddy R, Rose Y, Srikumar R, Tanaka KS, Williams DM, Gros P, Pelletier J, Parr TRJ, Far AR. 2006. A new class of small molecule RNA polymerase inhibitors with activity against rifampicin-resistant *Staphylococcus aureus*. *Bioorg. Med. Chem.* 14:5812–5832. <http://dx.doi.org/10.1016/j.bmc.2006.05.035>.
- Buurman EdT, Foulk MA, Gao N, Laganas VA, McKinney DC, Moustakas DT, Rose JA, Shapiro AB, Fleming PR. 2012. Novel rapidly diversifiable antimicrobial RNA polymerase switch region inhibitors with confirmed mode of action in *Haemophilus influenzae*. *J. Bacteriol.* 194:5504–5512. <http://dx.doi.org/10.1128/JB.01103-12>.
- Elgaher WAM, Fruth M, Groh M, Hauptenthal J, Hartmann RW. 2014. Expanding the scaffold for bacterial RNA polymerase inhibitors: design, synthesis and structure activity relationships of ureido-heterocyclic-carboxylic acids. *RSC Adv.* 4:2177–2194. <http://dx.doi.org/10.1039/c3ra45820b>.
- Artsimovitch I, Chu C, Lynch AS, Landick R. 2003. A new class of bacterial RNA polymerase inhibitor affects nucleotide addition. *Science* 302:650–654. <http://dx.doi.org/10.1126/science.1087526>.
- Malinen AM, Nandymazumdar M, Turtola M, Malmi H, Grocholski T,

- Artsimovitch I, Belogurov GA. 2014. CBR antimicrobials alter coupling between the bridge helix and the β subunit in RNA polymerase. *Nat. Commun.* 5:3408. <http://dx.doi.org/10.1038/ncomms4408>.
21. Villain-Guillot P, Gualtieri M, Bastide L, Leonetti JP. 2007. In vitro activities of different inhibitors of bacterial transcription against *Staphylococcus epidermidis* biofilm. *Antimicrob. Agents Chemother.* 51:3117–3121. <http://dx.doi.org/10.1128/AAC.00343-07>.
 22. Li L, Chen X, Fan P, Mihalic JT, Cutler ST. 2001. Synthesis, antibacterial activity and RNA polymerase inhibition of phenylamidine derivatives. *PCT Int. Appl. WO 2001051456 A2 20010719*.
 23. Krajete A, Steiner G, Kopacka H, Ongania KH, Wurst K, Kristen MO, Preishuber-Pflugl P, Bildstein B. 2004. Iminohydroxamate early and late transition metal halide complexes—new precatalysts for aluminoxane-cocatalyzed olefin insertion polymerization. *Eur. J. Inorg. Chem.* 8:1740–1752. <http://dx.doi.org/10.1002/ejic.200300405>.
 24. Patrick GL. 1995. Chapter 9.5, the Craig plot, p 143. *In* An introduction to medicinal chemistry, 1st ed. Oxford University Press, New York, NY.
 25. Singh PK, Parsek MR, Greenberg EP, Welsh MJ. 2002. A component of innate immunity prevents bacterial biofilm development. *Nature* 417: 552–555. <http://dx.doi.org/10.1038/417552a>.
 26. Ardehali R, Shi L, Janatova J, Mohammad SF, Burns GL. 2002. The effect of apo-transferrin on bacterial adhesion to biomaterials. *Artif. Organs* 26:512–520. <http://dx.doi.org/10.1046/j.1525-1594.2002.06923.x>.
 27. Thompson MG, Corey BW, Si Y, Craft DW, Zurawski DV. 2012. Antibacterial activities of iron chelators against common nosocomial pathogens. *Antimicrob. Agents Chemother.* 56:5419–5421. <http://dx.doi.org/10.1128/AAC.01197-12>.
 28. de Léséleuc L, Harris G, Kuo LR, Chen W. 2012. In vitro and in vivo biological activities of iron chelators and gallium nitrate against *Acinetobacter baumannii*. *Antimicrob. Agents Chemother.* 56:5397–5400. <http://dx.doi.org/10.1128/AAC.00778-12>.
 29. Smith PAS. 1966. The chemistry of open-chain organic nitrogen compounds, vol 2, p 73–76. Benjamin Publishers, New York, NY.
 30. Flournoy DJ. 1991. In vitro antimicrobial properties of deferoxamine mesylate. *Eur. J. Clin. Microbiol. Infect. Dis.* 10:597–598. <http://dx.doi.org/10.1007/BF01967285>.
 31. Zhu W, Groh M, Haupenthal J, Hartmann RW. 2013. A detective story in drug discovery: elucidation of a screening artifact reveals polymeric carboxylic acids as potent inhibitors of RNA polymerase. *Chem. Eur. J.* 19:8397–8400. <http://dx.doi.org/10.1002/chem.201301289>.

3.3 Chapter III: Potent 11 β -Hydroxylase Inhibitors with Inverse Metabolic Stability in Human Plasma and Hepatic S9 fraction to Promote Wound Healing

This chapter has been submitted as a brief article to *J. Med. Chem.*

Potent 11 β -Hydroxylase Inhibitors with Inverse Metabolic Stability in Human Plasma and Hepatic S9 Fractions to Promote Wound Healing

ABSTRACT: Topical application of CYP11B1 inhibitors to reduce cutaneous cortisol is a novel strategy to promote healing of chronic wounds. Pyridyl substituted arylsulfonyltetrahydroquinolines were designed and synthesized resulting in a strong inhibitor **34** (IC_{50} = 5 nM). It showed no inhibition of CYP17 and CYP19 and no mutagenic effects. It exhibited inverse metabolic stability in plasma ($t_{1/2}$ >> 150 min), which is similar to wound fluid in composition, and in liver S9 fractions ($t_{1/2}$ = 16 min).

INTRODUCTION

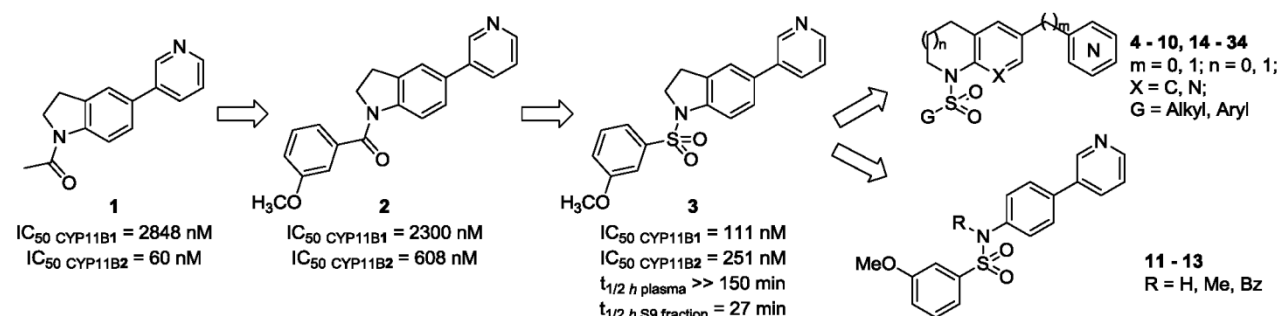
It has been reported that around 2% (6.5 million) of the general population in the United States are suffering from chronic wound healing,¹ which frequently appears as a comorbid condition with diabetes and/or obesity.² Actually, 15% of diabetic patients develop chronic non-healing diabetic foot ulcers that significantly impair their lives and compose a major cause of hospitalization.³ Despite of the facts that a standard care guideline was recommended⁴ and new treatments, such as skin substitutes and stem cell applications, were explored,⁵ the outcomes of managing healing of chronic wounds are still not satisfying, whereas the costs (exceeding \$50 billion per year) rapidly grow into a burden for society.¹ Therefore, novel therapeutic strategies are in urgent need. The wound healing process comprises four phases, namely hemostasis, inflammation, proliferation, and tissue remodeling,⁶ which are strictly controlled regarding sequence, initiating and terminating timings, as well as intensity. Cortisol, as a major glucocorticoid, blocks inflammation, fibroblast proliferation and collagen synthesis,² and thus probably contributes to the formation of chronic wounds and ulcers when cutaneously over-expressed. This hypothesis was supported by numerous observations that elevated cortisol levels induced by stress or other reasons impair wound healing.⁷ Recently, steroid 11 β -hydroxylase (CYP11B1), which is the key enzyme in cortisol biosynthesis, was identified to be expressed in epidermis.⁸ More important is that biosynthesis of this enzyme is up-regulated when tissues are injured and more cortisol impairing wound healing is produced in keratinocytes.⁸ In vivo studies also revealed that topical application of metyrapone (Table 1, IC_{50} = 15 nM) to inhibit CYP11B1 accelerated wound closure.⁸ These findings suggest that the inhibition of CYP11B1 could be a novel therapy to promote wound healing. Moreover, locally expressed estrogens have been shown to keep skin moisture, prevent skin

aging and, in particular, accelerate wound healing.⁹ Since the cutaneous production of estrogens involve two important steroidogenic enzymes that are also expressed in epidermis, namely 17 α -hydroxylase-17,20-lyase (CYP17) and aromatase (CYP19),¹⁰ inhibitors of CYP11B1 aiming at promoting wound healing should not inhibit these two enzymes. In contrast, to our best knowledge, aldosterone synthase (CYP11B2) is not detected in skin cells.¹⁰ The selectivity over CYP11B2 is therefore not important for this indication. Furthermore, the applied compounds ought to be stable in wound fluid to maintain efficacious concentrations. Since the components of wound liquid including proteases are similar to that of plasma,¹¹ plasma stability is an important parameter to be considered for the development of compounds for cutaneous application. In fact, it is inevitable that minor amount of topically administered CYP11B1 inhibitors diffuse into circulation. To avoid that such compounds interfere with adrenal steroid biosynthesis and thus lead to severe side effects, they should be fast metabolized by the liver. Similar strategies have been successfully applied for inhaled glucocorticoids in the treatment of asthma in order to achieve better safety profiles.¹² Accordingly, a suitable drug candidate to promote wound healing should not only show potent CYP11B1 inhibition and selectivity over CYP17 and CYP19, but also a high metabolic stability in plasma, whereas a short half-life ($t_{1/2}$) regarding hepatic S9 fraction, which contains microsomes and cytosol and thus is a good indicator of both phase I and II metabolism in liver, is also required.

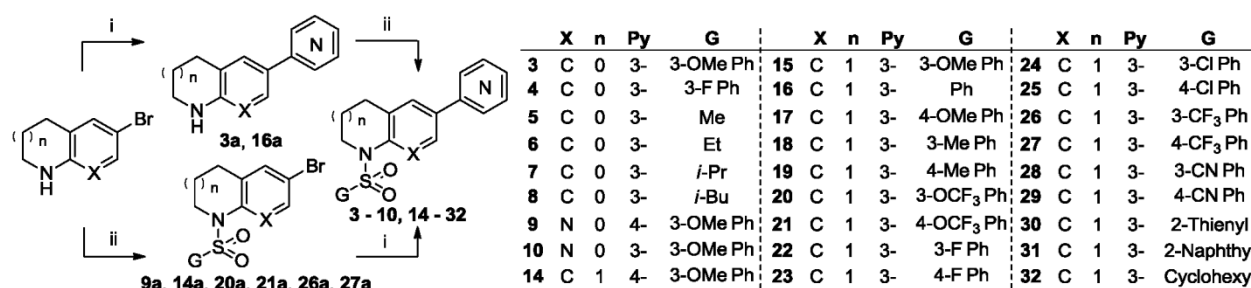
Metyrapone, which is a clinically used CYP11B1 inhibitor to reduce circulating cortisol levels for patients with Cushing syndrome, meets the criteria of potency, selectivity and plasma stability ($t_{1/2 \text{ plasma}}$ > 150 min). However, it exhibits a half-life of 49 min in human liver S9 fractions, which is most likely too

long for this indication. Similarly, although some of our previously identified CYP11B1

Chart 1. Design concept and title compounds.

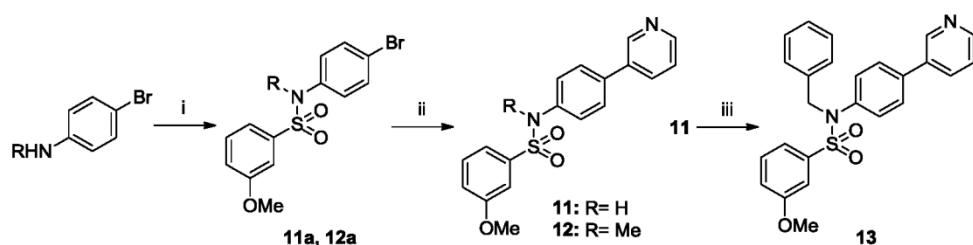


Scheme 1^a



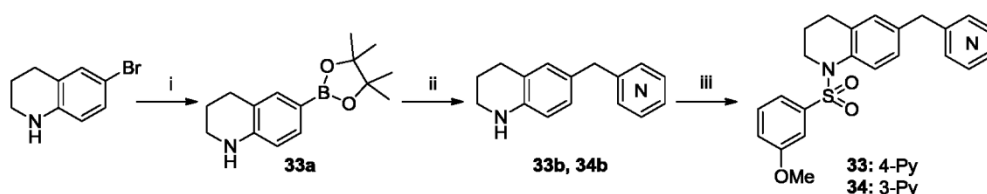
^a Reagents and conditions: (i) Method A: corresponding boronic acid, Pd(PPh₃)₄, Na₂CO₃, DME / H₂O, 95 °C. (ii) Method B: corresponding sulfonyl chloride, pyridine, DMAP, dry THF, RT to 60 °C or Method C: corresponding sulfonyl chloride, NaH, dry THF, 60 °C.

Scheme 2^a



^a Reagents and conditions: (i) Method B: corresponding sulfonyl chloride, pyridine, DMAP, dry THF, RT to 60 °C; (ii) Method A: corresponding boronic acid, Pd(PPh₃)₄, Na₂CO₃, DME / H₂O, 95 °C; (iii) Benzyl bromide, NaH, dry DMF, 0 to 80 °C.

Scheme 3^a



^a Reagents and conditions: (i) Bis(pinacolato)diboron, Pd(dppf)Cl₂, CH₃COOK, dry 1,4-dioxane, 80 °C; (ii) Method A: corresponding bromomethyl pyridine, Pd(PPh₃)₄, Na₂CO₃, DME / H₂O, 95 °C; (iii) Method B: corresponding sulfonyl chloride, pyridine, DMAP, dry THF, RT to 60 °C.

inhibitors¹³ fulfill most of the requirements, their hepatic metabolism is not rapid enough. In this study, we report a novel series of CYP11B1 inhibitors exhibiting the desired inverse metabolic stability profile. The design of novel CYP11B1

inhibitors was inspired by an observation in the pyridyl indoline class¹⁴ of CYP11B2 inhibitors (Chart 1). Compound **1**, bearing an acetyl group at the indoline core, is a potent CYP11B2 inhibitor (IC₅₀ CYP11B2 = 60 nM) showing only weak

inhibition of CYP11B1 with an IC_{50} value of 2848 nM. Replacing the small acetyl group by a bulky 3-methoxybenzoyl moiety (**2**),¹⁴ reduced CYP11B2 inhibition by 10-fold to 608 nM, whereas inhibition of CYP11B1 was slightly increased (IC_{50} = 2300 nM). Surprisingly, in preliminary studies we found out that further exchange of the amido group by the corresponding sulfonamide moiety (**3**) resulted in a significant elevation of CYP11B1 inhibition by 20-fold to 111 nM. More important is the fact that compound **3** exhibits the desired inverse metabolic stability profile: the half life in plasma was far longer than 150 min whereas the one in hepatic S9 fractions was 27 min. The latter is about half of that of metyrapone, which makes compound **3** more attractive as a lead compound than metyrapone. This encouraged us to modify the structure to further improve CYP11B1 inhibition as well as the metabolic profile. Various groups (alkyl or aryl) were introduced at the sulfonamide moiety; the pyrrolidine ring of the indoline core was expanded or opened; a methylene bridge was inserted between the core and the pyridyl substituent; furthermore the position of the pyridyl N (3- or 4-pyridyl) was also investigated (Chart 1). To improve selectivity, the addition of an N atom in the core was attempted as well. These efforts led to compounds **4** – **34** which were subsequently biologically evaluated: the inhibition of CYP11B1 and CYP11B2 was determined and the most potent CYP11B1 inhibitors were further tested for inhibition of CYP17 and CYP19, metabolic stability in human plasma and hepatic S9 fractions as well as mutagenicity.

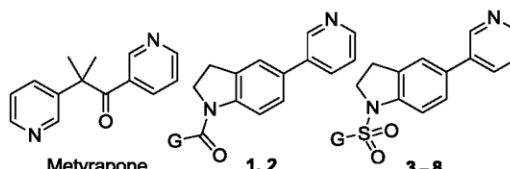
RESULTS AND DISCUSSION

Chemistry. The synthesis of the final compounds **3** – **12** and **14** – **32** (Schemes 1 and 2) was achieved in two steps. For compounds **3** – **8**, **16** – **19**, **22** – **25** and **28** – **32**, the route started from commercially available 5-bromoindoline or 6-bromo-1,2,3,4-tetrahydroquinoline using a Suzuki coupling reaction to introduce the pyridyl moiety. Subsequently, a sulfonylation reaction was employed to insert the corresponding sulfonamide group resulting in the desired products. For compounds **9** – **12**, **14**, **15**, **20**, **21**, **26** and **27**, the same reactions were applied in reversed order. In some sulfonylations NaH was employed as a stronger base instead of pyridine to ensure satisfying yields. Compound **11** was further substituted with a benzyl group by reacting with benzyl bromide leading to compound **13** (Scheme 2). To introduce the methylene bridge into compounds **33** and **34**, 6-bromo-1,2,3,4-tetrahydroquinoline was first converted into the borate before coupling with the corresponding bromomethyl pyridine under conventional Suzuki coupling conditions (Scheme 3). 3-Methoxyphenyl sulfonyl was subsequently inserted to give the final compounds.

Inhibition of Human CYP11B1. To assess the inhibitory activities, the synthesized compounds were tested in an assay using V79 MZh cells expressing human CYP11B1 with 11-deoxycorticosterone (100 nM) as the substrate.¹⁵ The results are presented in Tables 1 – 3 in comparison to metyrapone. As mentioned above, the replacement of the small acetyl group (**1**) by a bulky aromatic 3-methoxybenzoyl moiety (**2**) increased CYP11B1 inhibition by 20% (Table 1), while exchange of the carbonyl group by a sulfone moiety leading to the corresponding sulfonamide **3** boosted CYP11B1 inhibition by a factor of around 20 to 111 nM. This dramatic elevation

led to the speculation that the sulfonamide moiety could form more favorable interactions like H-bonds than the carboxamide group. Another explanation was that the different geometry of the sulfonamide was more appropriate to stretch the aromatic ring into a nearby hydrophobic pocket. In any cases pyridyl substituted sulfonylindolines could be considered as promising starting points for the design of potent CYP11B1 inhibitors. The influence of alkyl and phenyl substitution at the sulfonyl moiety was first explored. As expected, methylsulfonyl compound **5** (IC_{50} = 1674 nM) is more potent than the corresponding acetyl analogue **1** (IC_{50} = 2848 nM). With increasing bulkiness of the sulfonyl substituents, namely Me (**5**) to Et (**6**) and *i*-Pr (**7**), the inhibition was promoted by around 2-fold. However, the *i*-Bu compound **8** only showed a weak inhibition of around 2 μ M. This observation might be due to the length of the group, which might result in clashes to the pocket wall, rather than bulkiness because the large 3-OMe Ph (**3**) and 3-F Ph (**4**) groups lead to potent CYP11B1 inhibitors with IC_{50} values of 111 nM and 327 nM, respectively. Of course, the aromaticity of these phenylsulfonyl moieties providing the possibility of π - π interactions could be a significant contributor of affinity.

Table 1. Inhibition of CYP11B1 by compounds 3 – 8.




Compd.	G	IC_{50} (nM) ^a	Compd.	G	IC_{50} (nM) ^a
1	Me	2848	5	Me	1674
2	3-OMe Ph	2300	6	Et	690
3	3-OMe Ph	111	7	<i>i</i> -Pr	499
4	3-F Ph	327	8	<i>i</i> -Bu	2003
Metyrapone		15			

^a Mean value of at least three independent tests, standard deviation less than 25%. Hamster fibroblasts expressing human CYP11B1; substrate 11-deoxycorticosterone, 100 nM.

After having observed that the aromatic sulfonyl moiety was important for CYP11B1 inhibition, the 3-OMe phenyl substituent was kept constant and modifications on the indoline core were performed (Table 2). Also the influence of a 3- or 4-pyridyl group was investigated. Since an N atom inside the central ring was demonstrated to improve the selectivity over CYP17 and CYP19,^{13c} it was inserted into the benzene nucleus of the indoline core. However, in this series of compounds, this structural modification reduced the potency by a factor of 5 (**10**). The exchange of the 3-pyridyl substituent by a 4-pyridyl ring further decreased inhibition to 1750 nM (**9**). Upon opening of the pyrrolidine nucleus of the indoline core to provide more flexibility to the aryl sulfonyl moiety, a 2-fold improvement of CYP11B1 inhibition was observed for the *N*-Me analogue **12** (IC_{50} = 68 nM) compared to the parent compound **3** (IC_{50} = 111 nM). In contrast, the *N*-H compound **11** was less potent (IC_{50} = 188 nM) compared to the *N*-Me analogue **12** indicating that the hydrogen is unfavorable. Substitu-

tion on the N with a benzyl moiety reduced CYP11B1 inhibition to 2 μ M probably due to a steric clash. The pyrrolidine nucleus was also expanded leading to 1,2,3,4-tetrahydroquinoline as a new core. In contrast to the total loss of inhibitory potency induced by 4-pyridyl (**14**), the 3-pyridyl substituted 1,2,3,4-tetrahydroquinoline analogue **15** exhibited a 4-fold elevation of CYP11B1 inhibition compared to lead compound **3** almost reaching the potency of metyrapone (IC_{50} values of 28 nM and 15 nM, respectively).

Table 2. Inhibition of CYP11B1 by compounds 9 – 15.

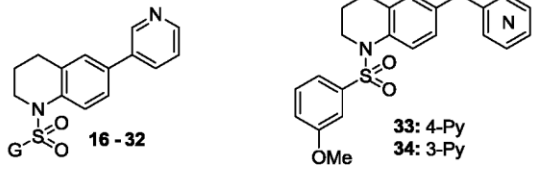


Compd.	IC_{50} (nM) ^a	Compd.	IC_{50} (nM) ^a
Metyrapone	15	12	68
3	111	13	2001
9	1750	14	>5000
10	587	15	28
11	188		

^a Mean value of at least three independent tests, standard deviation less than 25%. Hamster fibroblasts expressing human CYP11B1; substrate 11-deoxycorticosterone, 100 nM.

After optimization of the core resulting in 1,2,3,4-tetrahydroquinoline, the substituents on the phenyl sulfonyl moiety were further scrutinized (Table 3). Various groups with different bulkiness, electrostatic properties and potential of forming hydrogen or halogen bonds were introduced into the *m*- or *p*-position of the phenyl sulfonyl moiety. With the exception of the F substituted compounds **22** and **23**, all *m*-substituted analogues were 2- to 10-fold more potent than the corresponding *p*-substituted ones (see compound pairs **15**, **17**

Table 3. Inhibition of CYP11B1 by compounds 16 – 34.



Compd.	G	IC_{50} (nM) ^a	Compd.	G	IC_{50} (nM) ^a	Compd.	G	IC_{50} (nM) ^a
Metyrapone		15	21	<i>p</i> -OCF ₃ Ph	929	28	<i>m</i> -CN Ph	65
16	Ph	65	22	<i>m</i> -F Ph	71	29	<i>p</i> -CN Ph	114
15	<i>m</i> -OMe Ph	28	23	<i>p</i> -F Ph	49	30	2-Thienyl	60
17	<i>p</i> -OMe Ph	334	24	<i>m</i> -Cl Ph	62	31	2-Naphthyl	663
18	<i>m</i> -Me Ph	26	25	<i>p</i> -Cl Ph	137	32	<i>c</i> -hexyl	1167
19	<i>p</i> -Me Ph	278	26	<i>m</i> -CF ₃ Ph	309	33		6
20	<i>m</i> -OCF ₃ Ph	382	27	<i>p</i> -CF ₃ Ph	1224	34		5

^a Mean value of at least three independent tests, standard deviation less than 25%. Hamster fibroblasts expressing human CYP11B1; substrate 11-deoxycorticosterone, 100 nM.

– **21** and **24** – **29**). This finding together with the observation that the long *i*-Bu sulfonyl substituent strongly decreased potency might indicate that the hydrophobic pocket occupied by these moieties is rather shallow. The non-substituted phenyl sulfonyl compound **16** showed a strong inhibition of CYP11B1 with an IC_{50} of 65 nM. *m*-Substitution with electron donating groups OMe (**15**) and Me (**18**) increased the potency by 2-fold to less than 30 nM. In contrast, electron withdrawing groups F (**22**), Cl (**24**) and CN (**28**) did not show much impact on CYP11B1 inhibition compared to the non-substituted compound **16**. Interestingly, although exhibiting different electrostatic potentials, the OCF₃ (**20**) and CF₃ (**26**) groups reduced inhibitory potencies by a factor of about 5, which might indicate multi F substitution is not tolerated. The replacement of the phenyl moiety by other rings was also attempted. In contrast to the similar potency rendered by a 2-thienyl group (**30**, IC_{50} = 60 nM), substitution with the more bulky naphthyl ring (**31**) led to a 10-fold decrease of CYP11B1 inhibition compared to the phenyl sulfonyl compound **16**. In accordance to the observation that alkyl compounds are less potent than aryl analogues (Table 1), substitution with a *c*-hexyl ring (**32**) reduced potency by a factor of nearly 20 compared to the phenyl compound **16**. As a result of this investigation, *m*-OMe- and *m*-Me-phenyl sulfonyl substitution was identified as most suitable for CYP11B1 inhibition.

Introduction of a methylene bridge¹⁶ disrupts the conjugation between core and heme-binding heterocycle, provides the molecule more flexibility and changes orientation of the compound with regard to the co-ordination of its *sp*² hybrid N with the heme iron. These changes in molecular shape and conformational flexibility consequently lead to alterations in binding affinity and inhibitory profiles toward the CYP enzyme targets.¹⁷ To exploit these opportunities, a methylene bridge was inserted accompanied with a 3- or 4-pyridyl substituent (compounds **34** and **33**, respectively). Surprisingly, both compounds showed a 10-fold improvement of CYP11B1 inhibition compared to the parent compound **16** resulting in IC_{50} values of around 5 nM. Thus, the compounds were more potent than metyrapone (IC_{50} = 15 nM).

Metabolic Stabilities in Human Plasma and Hepatic S9 Fractions. As discussed above, a CYP11B1 inhibitor for the promotion of wound healing should be stable in plasma but metabolically labile in liver to achieve both efficacy and safety. Compound **3** as lead had exhibited the desired inverse metabolic stabilities. As a result from optimization, compound **34**, showed not only a very long half-life in human plasma ($t_{1/2 \text{ plasma}} \gg 150 \text{ min}$), but also instability in human liver S9 fraction ($t_{1/2 \text{ S9}} = 16 \text{ min}$), being much better than metyrapone ($t_{1/2 \text{ S9}} = 49 \text{ min}$).

Inhibition of Human CYP17 and CYP19. Because of their crucial roles in the biosynthesis of sex hormones, inhibition of CYP17¹⁸ and CYP19¹⁹ has been exploited in the treatment of hormone sensitive prostate and breast cancers, respectively. These two enzymes are also expressed in the skin and are involved in the cutaneous production of estrogens, which are known to accelerate wound healing. The selectivity over CYP17 and CYP19 was therefore considered as safety criteria, and four of the most potent CYP11B1 inhibitors, namely compounds **15**, **18**, **33** and **34**, were tested for inhibition of these two enzymes. Since these compounds had shown IC_{50} values below 30 nM toward human CYP11B1, a more than 60-fold higher concentration (2 μM) was selected for these selectivity assays. All tested compounds exhibited less than 15% inhibition of CYP17 (Table 4). As for CYP19, only the 4-pyridyl analogue **33** showed strong inhibition (88%), whereas the other compounds exhibited inhibition values of around 30%. Accordingly, these compounds were considered to be selective enough for a safe application.

Table 4. Inhibition of CYP17 and CYP19 by selected compounds.

Compd.	%Inhibition ^a	
	CYP17 ^b	CYP19 ^c
Metyrapone	3	0
15	11	32
18	9	29
33	14	88
34	9	26

^a Mean value of at least three independent tests, standard deviation less than 25%. ^b *E. coli* expressing human CYP17; substrate progesterone, 25 μM ; inhibitor concentration, 2.0 μM ; ^c Human placental CYP19; substrate androstenedione, 500 nM; inhibitor concentration, 2.0 μM .

Inhibition of Human CYP11B2. CYP11B2 is the pivotal enzyme responsible for the biosynthesis of aldosterone and its inhibition was therefore proposed as a novel therapy for related cardiovascular and renal diseases.²⁰ Despite of the challenges in achieving selectivity between CYP11B1 and CYP11B2, which is due to the high homology between these two enzymes (> 93%), selective inhibitors of CYP11B1¹³ and CYP11B2²¹ have been developed. Although the selectivity over CYP11B2 is not that important for cutaneous application required in wound healing, this series of CYP11B1 inhibitors were still tested for inhibition of CYP11B2 because the compounds originated from pyridyl substituted indoline type of CYP11B2 inhibitors and the information obtained on inhibitory profiles could facilitate future design of selective inhibitors

of both enzymes. In spite of the fact that all compounds exhibited preference for CYP11B1 inhibition, the selectivity over CYP11B2 was not strong (Table S1, see supporting information). The tested compounds showed potent to modest inhibition of CYP11B2 with IC_{50} values ranging from 5 to around 2000 nM. However, the compounds are expected to be rapidly metabolized and excreted after diffusion into circulation and thus have no chance to interfere with either CYP11B1 or CYP11B2 in the adrenals.

Mutagenicity Evaluation. The Ames II mutagenicity assay was employed to assess the mutagenic potential of compound **34** using the genotypes of the TA98 and TAMix *Salmonella typhimurium* strains. No positive signal was observed in both strains with or without S9 mix at a compound concentration up to 100 μM indicating that compound **34** was non-mutagenic.

CONCLUSION

Topical application of CYP11B1 inhibitors to reduce the cutaneous production of cortisol is a novel strategy to promote healing of chronic wounds. A suitable drug candidate for this indication should be selective over CYP17 and CYP19 that are also expressed in epidermis. Stability in wound fluid, which shows a very similar composition as plasma, is a must to maintain therapeutic concentrations. On the other hand the inhibitor is expected to be rapidly metabolized in the liver as it cannot be excluded that minor amounts of the compound diffuse into circulation and interfere with adrenal steroid biosynthesis. In this study, pyridyl substituted arylsulfonyl tetrahydroquinolines were designed and synthesized for this aim. As the best compound from this series, compound **34** is a highly potent CYP11B1 inhibitor ($\text{IC}_{50} = 5 \text{ nM}$) being stronger than the lead compound **3** and metyrapone (the latter is being used clinically for the treatment of Cushing syndrome). It showed no mutagenic effects and no significant inhibition of CYP17 and CYP19 providing a wide enough therapeutic window at the treatment doses. In contrast to its long half-life ($t_{1/2 \text{ plasma}} \gg 150 \text{ min}$) in human plasma, compound **34** is fast metabolized in human liver S9 fractions ($t_{1/2 \text{ S9}} = 16 \text{ min}$, being clearly superior to metyrapone). Therefore, it is considered for further *in vivo* evaluation.

EXPERIMENTAL SECTION

Biology. (see supporting information for details)

Chemistry. The purities of the final compounds were higher than 95% as determined by HPLC.

Method A: Suzuki Coupling.

To the solution of the corresponding bromide (0.5 mmol, 1.0 equiv) in 1,2-dimethoxyethane (12 mL) and water (4 mL) were added 3- or 4-pyridyl boronic acid (1.0 – 2.0 eq.) and Na_2CO_3 (3.0 – 5.0 eq.). The mixture was degassed under reduced pressure and flushed with N_2 for three times before $\text{Pd(PPh}_3)_4$ (5 – 10 mol%) was added. The resulting suspension was then heated to 95 $^\circ\text{C}$ for 4 – 8 h. After cooling down to room temperature, water (20 mL) and EtOAc (40 mL) were added. The phases were separated, and the aqueous phase was extracted twice with EtOAc (40 mL). The combined organic extracts were washed with brine, dried over MgSO_4 and concentrated under reduced pressure to give the crude product, which was purified with flash chromatography on silica gel.

Method B: Sulfonylation Reaction.

To the solution of the corresponding amine (1 mmol, 1.0 eq.), 4-dimethylaminopyridine (DMAP, 0.2 eq.) and pyridine (3.0 –

5.0 eq.) in dry THF (8 mL) was added dropwise the corresponding sulfonyl chloride (1.0 – 2.0 eq.) in an ice bath. Subsequently, the resulting mixture was stirred at room temperature or heated to 60 °C for 1 – 6 h and the reaction was monitored with TLC until the starting materials were consumed. The mixture was then cooled to ambient temperature and quenched by the addition of saturated Na₂CO₃ aqueous solution (20 mL). It was extracted with EtOAc (3 x 30 mL). The combined organic extracts were washed with brine, dried over MgSO₄ and concentrated under reduced pressure to give the crude product, which was further purified with flash chromatography on silica gel.

6-(4,4,5,5-tetramethyl-1,3,2-dioxaborolan-2-yl)-1,2,3,4-tetrahydroquinoline (33a). To the solution of 6-bromo-1,2,3,4-tetrahydroquinoline (530 mg, 2.5 mmol) and bis(pinacolato)diboron (1.27 g, 5 mmol) in dry 1,4-dioxane (12 mL) was added potassium acetate (1.22 g, 12.5 mmol). The mixture was degassed under reduced pressure and flushed with N₂ for three times before Pd(dppf)Cl₂ (92 mg, 5 mol%) was added. The resulting suspension was then heated to 80 °C for 2 h. After cooling down, water (20 mL) and EtOAc (40 mL) were added. The phases were separated, and the aqueous phase was extracted twice with EtOAc (40 mL). The combined organic extracts were washed with brine, dried over MgSO₄ and concentrated under reduced pressure to give the crude product, which was purified with flash chromatography on silica gel (*n*-hexane/EtOAc, 20:1 to 5:1) to yield a white solid (440 mg, 68%). ¹H-NMR (300 MHz, CDCl₃): δ 7.41 (m, 2H), 6.43 (d, *J* = 8.2 Hz, 1H), 4.06 (s, br, 1H), 3.30 (m, 2H), 2.75 (t, *J* = 6.3 Hz, 2H), 1.92 (m, 2H), 1.31 (s, 12H).

6-(pyridin-3-ylmethyl)-1,2,3,4-tetrahydroquinoline (34b). The title compound was synthesized according to Method A using **33a** (194 mg, 0.75 mmol), 3-(bromomethyl)pyridine hydrobromide (190 mg, 0.75 mmol), Na₂CO₃ (380 mg, 3.6 mmol), Pd(PPh₃)₄ (65 mg, 7.5 mol %) and 1,2-dimethoxyethane (18 mL) / water (6 mL) to yield the crude product, which was purified by flash chromatography on silica gel (CH₂Cl₂/MeOH, 500:1 to 62.5:1) to yield a reddish solid (86 mg, 51%). ¹H-NMR (300 MHz, CDCl₃): δ 8.48 (d, *J* = 2.0 Hz, 1H), 8.42 (dd, *J* = 4.8, 1.5 Hz, 1H), 7.47 (m, 1H), 7.18 (m, 1H), 6.75 (m, 2H), 6.41 (d, *J* = 8.3 Hz, 1H), 3.82 (s, 2H), 3.27 (m, 2H), 2.71 (t, *J* = 6.3 Hz, 2H), 1.91 (m, 2H).

1-(3-methoxyphenyl)sulfonyl-6-(pyridin-3-ylmethyl)-1,2,3,4-tetrahydroquinoline (34). The title compound was synthesized according to Method B using **34b** (56 mg, 0.25 mmol), 3-methoxybenzene-1-sulfonyl chloride (103 mg, 0.5 mmol), DMAP (6 mg, 0.05 mmol), pyridine (100 mg, 1.2 mmol) and dry THF (4 mL) to yield the crude product, which was purified by flash chromatography on silica gel (*n*-hexane/EtOAc, 20:1 to 4:1) to yield a light brown oil (70 mg, 72%). HPLC: 97% pure; MS (ESI) *m/z* = 395 [M⁺+H]; ¹H-NMR (500 MHz, CDCl₃): δ 8.46 (m, 2H), 7.72 (d, *J* = 8.2 Hz, 1H), 7.45 (m, 1H), 7.30 (dd, *J* = 8.4, 7.7 Hz, 1H), 7.20 (m, 2H), 7.02 (m, 2H), 6.97 (m, 1H), 6.80 (m, 1H), 3.90 (s, 2H), 3.77 (m, 2H), 3.61 (s, 3H), 2.37 (t, *J* = 6.6 Hz, 2H), 1.60 (m, 2H); ¹³C-NMR (125 MHz, CDCl₃): δ 159.6, 150.1, 147.7, 140.6, 136.7, 136.3, 136.2, 135.3, 131.2, 130.0, 129.3, 127.0, 125.3, 123.4, 119.4, 119.2, 111.4, 55.4, 46.6, 38.4, 26.6, 21.4.

ASSOCIATED CONTENT

Supporting Information.

Experimental procedures and characterization of the not mentioned intermediates and final compounds, HPLC purities and retention time of all final compounds, inhibition of CYP11B2 by compounds **3** – **34** and descriptions of biological tests are supplied as supporting information. This material is available free of charge via the Internet at <http://pubs.acs.org>.

AUTHOR INFORMATION

Corresponding Author

* R.W.H.: phone, +(49) 681 302 70300; fax, +(49) 681 302 70308; e-mail, rolf.hartmann@helmholtz-hzi.de; home page, <http://www.helmholtz-hzi.de/?id=3897>.

Author Contribution

± W. Z and Q. H. contributed equally to this paper.

Notes

The authors declare no competing financial interest.

ACKNOWLEDGMENT

W. Zhu thanks China Scholarship Council for her PhD fellowship. The authors appreciate the help from Dr. Stefan Boettcher with LC-MS/MS determination.

ABBREVIATIONS

CYP11B1, 11β-hydroxylase; CYP11B2, aldosterone synthase; CYP17, 17α-hydroxylase-17,20-lyase; CYP19, aromatase; t_{1/2}, biological half-life; eq., equivalent; DMAP, 4-dimethylaminopyridine.

REFERENCES

- (1) Sen, C. K.; Gordillo, G. M.; Roy, S.; Kirsner, R.; Lambert, L.; Hunt, T. K.; Gottrup, F.; Gurtner, G. C.; Longaker, M. T. Human skin wounds: a major and snowballing threat to public health and the economy. *Wound Repair Regen.* **2009**, *17*, 763–771.
- (2) Guo, S.; DiPietro, L. A. Factors affecting wound healing. *J. Dent Res.* **2010**, *89*, 219–229.
- (3) Brem, H.; Tomic-Canic, M. Cellular and molecular basis of wound healing in diabetes. *J. Clin. Invest.* **2007**, *117*, 1219–1222.
- (4) Chronic wound care guidelines. <http://www.woundheal.org/assets/documents/final%20pocket%20guide%20treatment.pdf> (accessed on Jun. 12, 2014)
- (5) Montfrans, C. V.; Stok, M.; Geerkens, M. Biology of chronic wounds and new treatment strategies. *Phlebology* **2014**, *19*, 165–167.
- (6) Gosain, A.; DiPietro, L. A. Aging and wound healing. *World J. Surg.* **2004**, *28*, 321–326.
- (7) Ebrecht, M.; Hextall, J.; Kirtley, L.; Taylor, A.; Dyson, M.; Weinman, J. Perceived stress and cortisol levels predict speed of wound healing in healthy male adults. *Psychoneuroendocrinology* **2004**, *29*, 798–809.
- (8) Vukelic, S.; Stojadinovic, O.; Pastar, I.; Rabach, M.; Krzyzanowska, A.; Lebrun, E.; Davis, S. C.; Resnik, S.; Brem, H.; Tomic-Canic, M. Cortisol synthesis in epidermis is induced by IL-1 and tissue injury. *J. Biol. Chem.* **2011**, *286*, 10265–10275.
- (9) Shah, M. G.; Maibach, H. I. Estrogen and skin. An overview. *Am. J. Clin. Dermatol.* **2001**, *2*, 143–150.
- (10) Slominski, A.; Zbytek, B.; Nikolakis, G.; Manna, P. R.; Skobowiat, C.; Zmijewski, M.; Li, W.; Janjetovic, Z.; Postlethwaite, A.; Zouboulis, C. C.; Tuckey, R. C. Steroidogenesis in the skin: implications for local immune functions. *J. Steroid. Biochem. Mol. Biol.* **2013**, *137*, 107–123.
- (11) Trengove, N. J.; Langton, S. R.; Stacey, M. C. Biochemical analysis of wound fluid from nonhealing and healing chronic leg ulcers. *Wound Repair Regen.* **1996**, *4*, 234–239.

- (12) Derendorf, H.; Nave, R.; Drollmann, A.; Cerasoli, F.; Wurst, W. Relevance of pharmacokinetics and pharmacodynamics of inhaled corticosteroids to asthma. *Eur. Respir. J.* **2006**, *28*, 1042–1050.
- (13) (a) Yin, L.; Lucas, S.; Maurer, F.; Kazmaier, U.; Hu, Q.; Hartmann, R. W. Novel imidazol-1-ylmethyl substituted 1,2,5,6-tetrahydro-pyrrolo[3,2,1-ij]quinolin-4-ones as potent and selective CYP11B1 inhibitors for the treatment of Cushing's syndrome. *J. Med. Chem.* **2012**, *55*, 6629–6633. (b) Emmerich, J.; Hu, Q.; Hanke, N.; Hartmann, R. W. Cushing's syndrome: development of highly potent and selective CYP11B1 inhibitors of the (pyridylmethyl)pyridine type. *J. Med. Chem.* **2013**, *56*, 6022–32.
- (14) Yin, L.; Hu, Q.; Emmerich, J.; Lo, M. M.; Metzger, E.; Ali, A.; Hartmann, R. W. Novel pyridyl- or isoquinolyl- substituted indolines and indoles as potent and selective aldosterone synthase inhibitors. *J. Med. Chem.* **2014**, *57*, 5179–5189.
- (15) Ehmer, P. B.; Bureik, M.; Bernhardt, R.; Müller, U.; Hartmann, R. W. Development of a test system for inhibitors of human aldosterone synthase (CYP11B2): Screening in fission yeast and evaluation of selectivity in V79 cells. *J. Steroid Biochem. Mol. Biol.* **2002**, *81*, 173–179.
- (16) (a) Hu, Q.; Yin, L.; Jagusch, C.; Hille, U. E.; Hartmann, R. W. Isopropylidene substitution increases activity and selectivity of biphenyl methylene 4-pyridine type CYP17 inhibitors. *J. Med. Chem.* **2010**, *53*, 5049–5053. (b) Hille, U. E.; Hu, Q.; Vock, C.; Negri, M.; Bartels, M.; Mueller-Vieira, U.; Lauterbach, T.; Hartmann, R. W. Novel CYP17 inhibitors: Synthesis, biological evaluation, structure-activity relationships and modeling of methoxy- and hydroxy-substituted methyleneimidazolyl biphenyls. *Eur. J. Med. Chem.* **2009**, *44*, 2765–2775. (c) Pinto-Bazurco Mendieta, M. A. E.; Negri, M.; Hu, Q.; Hille, U. E.; Jagusch, C.; Jahn-Hoffmann, K.; Müller-Vieira, U.; Schmidt, D.; Lauterbach, T.; Hartmann, R. W. CYP17 inhibitors. Annulations of additional rings in methylene imidazole substituted biphenyls: synthesis, biological evaluation and molecular modeling. *Arch. Pharm. (Weinheim)* **2008**, *341*, 597–609.
- (17) (a) Hu, Q.; Negri, M.; Jahn-Hoffmann, K.; Zhuang, Y.; Olgen, S.; Bartels, M.; Müller-Vieira, U.; Lauterbach, T.; Hartmann, R. W. Synthesis, biological evaluation, and molecular modeling studies of methylene imidazole substituted biaryls as inhibitors of human 17 α -hydroxylase-17,20-lyase (CYP17)-Part II: Core rigidification and influence of substituents at the methylene bridge. *Bioorg. Med. Chem.* **2008**, *16*, 7715–7727. (b) Hu, Q.; Jagusch, C.; Hille, U. E.; Hauptenthal, J.; Hartmann, R. W. Replacement of imidazolyl by pyridyl in biphenyl methylenes results in selective CYP17 and dual CYP17 / CYP11B1 inhibitors for the treatment of prostate cancer. *J. Med. Chem.* **2010**, *53*, 5749–5758. (c) Krug, S. J.; Hu, Q.; Hartmann, R. W. Hits identified in library screening demonstrate selective CYP17A1 lyase inhibition. *J. Steroid Biochem. Mol. Biol.* **2013**, *134*, 75–79.
- (18) (a) Hu, Q.; Negri, M.; Olgen, S.; Hartmann, R. W. The role of fluorine substitution in biphenyl methylene imidazole type CYP17 inhibitors for the treatment of prostate carcinoma. *ChemMedChem*. **2010**, *5*, 899–910. (b) Hille, U. E.; Hu, Q.; Pinto-Bazurco Mendieta, M. A. E.; Bartels, M.; Vock, C. A.; Lauterbach, T.; Hartmann, R. W. Steroidogenic cytochrome P450 (CYP) enzymes as drug targets: Combining substructures of known CYP inhibitors leads to compounds with different inhibitory profile. *C. R. Chim.* **2009**, *12*, 1117–1126. (c) Jagusch, C.; Negri, M.; Hille, U. E.; Hu, Q.; Bartels, M.; Jahn-Hoffmann, K.; Pinto-Bazurco Mendieta, M. A. E.; Rodenwaldt, B.; Müller-Vieira, U.; Schmidt, D.; Lauterbach, T.; Recanatini, M.; Cavalli, A.; Hartmann, R. W. Synthesis, biological evaluation and molecular modeling studies of methyleneimidazole substituted biaryls as inhibitors of human 17 α -hydroxylase-17,20-lyase (CYP17) – Part I: heterocyclic modifications of the core structure. *Bioorg. Med. Chem.* **2008**, *16*, 1992–2010. (d) Pinto-Bazurco Mendieta, M. A. E.; Negri, M.; Jagusch, C.; Müller-Vieira, U.; Lauterbach, T.; Hartmann, R. W. Synthesis, Biological Evaluation, and Molecular Modeling of Abiraterone Analogues: Novel CYP17 Inhibitors for the Treatment of Prostate Cancer. *J. Med. Chem.* **2008**, *51*, 5009–5018. (e) Yin, L.; Hu, Q.; Hartmann, R. W. Recent progress in pharmaceutical therapy for castration-resistant prostate cancer. *Int. J. Mol. Sci.* **2013**, *14*, 13958–13978.
- (19) (a) Lézé, M.-P.; Le Borgne, M.; Pinson, P.; Paluszczak, A.; Duflos, M.; Le Bauta, G.; Hartmann, R. W. Synthesis and biological evaluation of 5-[(aryl)(1H-imidazol-1-yl)methyl]-1H-indoles: potent and selective aromatase inhibitors. *Bioorg. Med. Chem. Lett.* **2006**, *16*, 1134–1137. (b) Gobbi, S.; Cavalli, A.; Negri, M.; Schewe, K. E.; Belluti, F.; Piazza, L.; Hartmann, R. W.; Recanatini, M.; Bisi, A. Imidazolylmethylbenzophenones as highly potent aromatase inhibitors. *J. Med. Chem.* **2007**, *50*, 3420–3422. (c) Hartmann, R. W.; Frotscher, M.; Ledergerber, D.; Wächter, G. A.; Grün, G. L.; Sergejew, T. F. Synthesis and evaluation of azole-substituted tetrahydronaphthalenes as inhibitors of P450 arom, P450 17, and P450 TxA2. *Arch. Pharm. (Weinheim)* **1996**, *329*, 251–261. (d) Gobbi, S.; Hu, Q.; Negri, M.; Zimmer, C.; Belluti, F.; Rampa, A.; Hartmann, R. W.; Bisi, A. Modulation of cytochromes P450 with xanthone-based molecules: from aromatase to aldosterone synthase and steroid 11 β hydroxylase inhibition. *J. Med. Chem.* **2013**, *56*, 1723–1729. (e) Abadi, A. H.; Abou-Seri, S. M.; Hu, Q.; Negri, M.; Hartmann, R. W. Synthesis and biological evaluation of imidazolylmethylacridones as cytochrome P-450 enzymes inhibitors. *MedChemComm.* **2012**, *3*, 663–666.
- (20) (a) Hu, Q.; Yin, L.; Hartmann, R. W. Aldosterone synthase inhibitors as promising treatments for mineralocorticoid dependent cardiovascular and renal diseases. *J. Med. Chem.* **2014**, *57*, 5011–5022. (b) Hu, Q.; Yin, L.; Hartmann, R. W. Selective dual inhibitors of CYP19 and CYP11B2: targeting cardiovascular diseases hiding in the shadow of breast cancer. *J. Med. Chem.* **2012**, *55*, 7080–7089. (c) Yin, L.; Hu, Q.; Hartmann, R. W. Tetrahydropyrroloquinolinone type dual inhibitors of aromatase / aldosterone synthase as a novel strategy for breast cancer patients with elevated cardiovascular risks. *J. Med. Chem.* **2013**, *56*, 460–470. (d) Pinto-Bazurco Mendieta, M. A. E.; Hu, Q.; Engel, M.; Hartmann, R. W. Highly potent and selective non-steroidal dual inhibitors of CYP17 / CYP11B2 for the treatment of prostate cancer to reduce risks of cardiovascular diseases. *J. Med. Chem.* **2013**, *56*, 6101–6107.
- (21) (a) Roumen, L.; Peeters, J. W.; Emmen, J. M. A.; Beugels, I. P. E.; Custers, E. M. G.; de Gooyer, M.; Plate, R.; Pieterse, K.; Hilbers, P. A. J.; Smits, J. F. M.; Vekemans, J. A. J.; Leysen, D.; Ottenheijm, H. C. J.; Janssen, H. M.; Hermans, J. J. R. Synthesis, biological evaluation, and molecular modeling of 1-benzyl-1H-imidazoles as selective inhibitors of aldosterone synthase (CYP11B2). *J. Med. Chem.* **2010**, *53*, 1712–1725. (b) Yin, L.; Hu, Q.; Hartmann, R. W. 3-Pyridinyl substituted aliphatic cycles as CYP11B2 inhibitors: aromaticity abolishment of the core significantly increased selectivity over CYP1A2. *PLoS One* **2012**, *7*(11), e48048. (c) Lucas, S.; Heim, R.; Ries, C.; Schewe, K. E.; Birk, B.; Hartmann, R. W. In vivo active aldosterone synthase inhibitors with improved selectivity: lead optimization providing a series of pyridine substituted 3,4-dihydro-1H-quinolin-2-one derivatives. *J. Med. Chem.* **2008**, *51*, 8077–8087. (d) Lucas, S.; Heim, R.; Negri, M.; Antes, I.; Ries, C.; Schewe, K. E.; Bisi, A.; Gobbi, S.; Hartmann, R. W. Novel aldosterone synthase inhibitors with extended carbocyclic skeleton by a combined ligand-based and structure-based drug design approach. *J. Med. Chem.* **2008**, *51*, 6138–6149. (e) Heim, R.; Lucas, S.; Grombein, C. M.; Ries, C.; Schewe, K. E.; Negri, M.; Müller-Vieira, U.; Birk, B.; Hartmann, R. W. Overcoming undesirable CYP1A2 inhibition of pyridyl-naphthalene-type aldosterone synthase inhibitors: influence of heteroaryl derivatization on potency and selectivity. *J. Med. Chem.* **2008**, *51*, 5064–5074. (f) Voets, M.; Antes, I.; Scherer, C.; Müller-Vieira, U.; Biemel, K.; Marchais-Oberwinkler, S.; Hartmann, R. W. Synthesis and evaluation of heteroaryl-substituted dihydronaphthalenes and indenes: potent and selective inhibitors of aldosterone synthase (CYP11B2) for the treatment of congestive heart failure and myocardial fibrosis. *J. Med. Chem.* **2006**, *49*, 2222–2231.

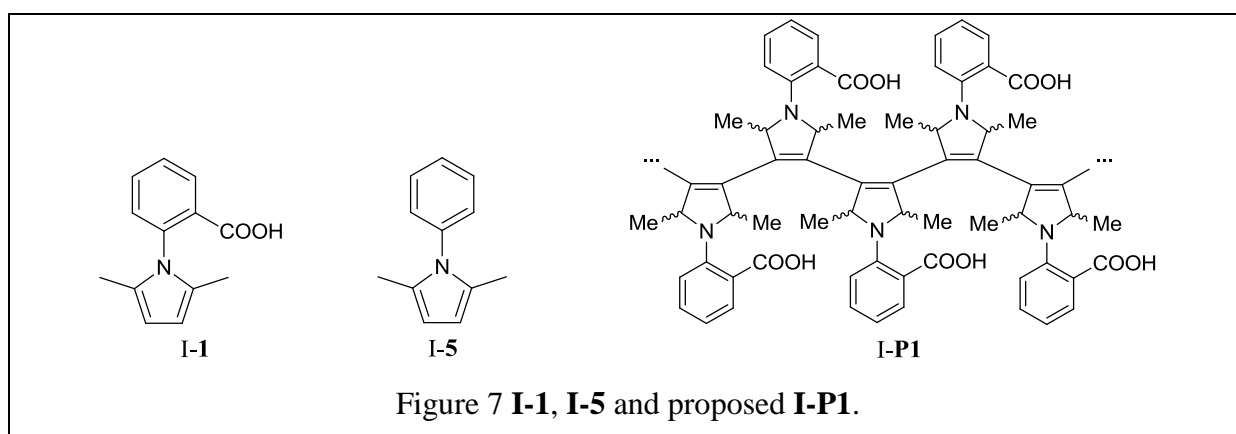
4 Summary and Conclusions

Anti-infection and blockade of cortisol synthesis are favorable strategies for wound healing. As enzymes are considered to be the most attractive targets in drug discovery and drug development, this dissertation describes our work regarding the developments of bacterial RNAP inhibitors as antibacterial agents and steroidal CYP11B1 inhibitors as strategies for the treatment of wound healing.

4.1 RNAP inhibitors

In our search to discover novel bacterial RNA polymerase (RNAP) inhibitors for the treatment of infectious diseases, two hit compounds, compound **I-1** and CBR703, were chosen based on experimental screening results.

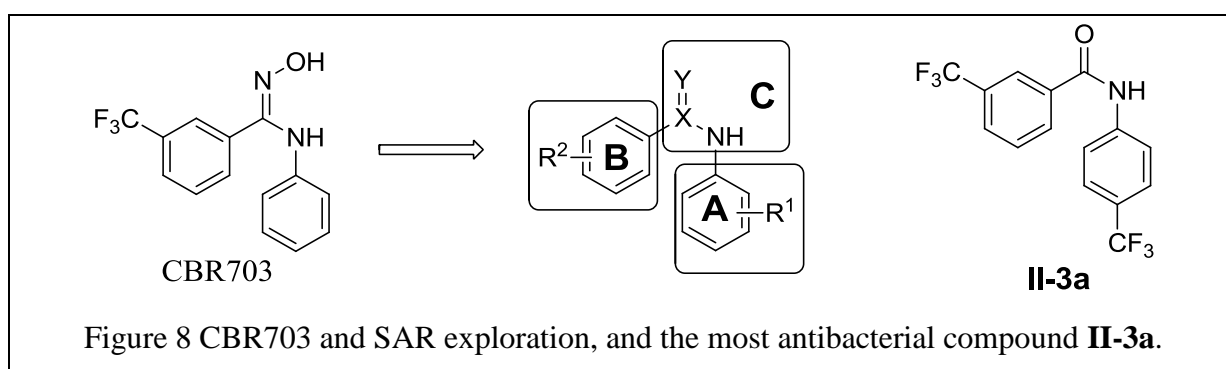
I-1 was identified as a fairly active RNAP inhibitor in our experimental screening by using a small library of commercial compounds. However, resynthesis of **I-1** resulted in an inactive compound. In the subsequent elucidation of this phenomenon we discovered that a polymeric side product was responsible for RNAP inhibition. After the purity of the polymer was confirmed by HPLC, it was analyzed by gel permeation chromatography (GPC), UV-Vis, NMR and IR, and the structure was proposed as **I-P1**. Some structure related inactive derivatives were also revealed to form polymers. Interestingly, the polymers with carboxylic acid groups were active against bacterial RNAP while the polymer without carboxylic acid groups formed from **I-5** showed no activity.



This fact led to the design of a gel electrophoresis experiment, which confirmed the “polyanionic character” of **I-P1** and the electrostatic interaction of **P1** with RNAP. Knowing that there are positively charged amino acid residues on the surface of RNAP, mainly in the DNA binding channel, the influence of **P1** on DNA binding to the RNAP main channel was investigated. Accordingly, the results revealed that the polymer could sterically block the loading of the DNA

template to RNAP and thus inhibit transcription. Although **P1** showed no antibacterial activity, we believed that *in vivo* activity could be achieved for our polymers by strongly reducing their size and they could be potential therapeutics for local infections of the skin and the lung.

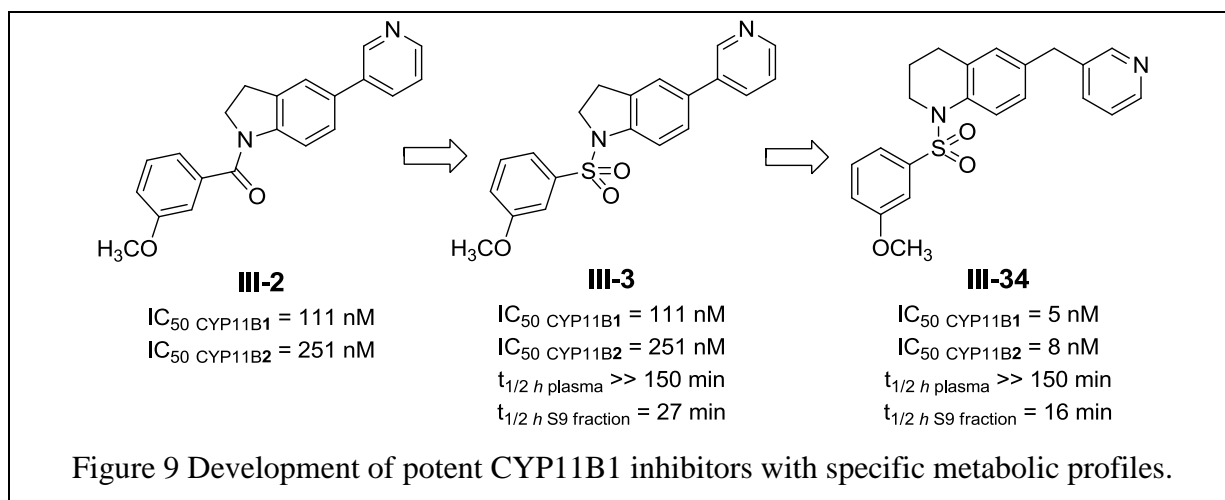
CBR703 was identified to be an RNAP inhibitor ($IC_{50} = 10 \mu M$) by HTS (Artsimovitch et al., 2003) and reported to be able to significantly reduce the *Staphylococcus epidermidis* biofilm mass (Villain-Guillot et al., 2007a). Systematic modifications divided into three parts were performed on its core structure, aiming to obtain a more appropriate starting point for further structural optimization. However, no compound showed an enhanced RNAP inhibition. Nevertheless, in some cases we observed promising anti-*E. coli TolC* activity. Then the antibacterial spectrum as well as cytotoxicity towards HEK 293 cells of the most potent compounds was investigated. None of the compounds inhibited the growth of the Gram-negative strains *K12* and *PAO1*, while **II-3a** exhibited rather potent activities against *B. subtilis* and *S. aureus*. However, this compound again turned out to correlate with a significant cytotoxicity towards HEK 293 cells. As no correlation between RNAP inhibition and antibacterial activity could be observed, it led us to the conclusion that additional mechanisms besides RNAP inhibition must be responsible for the antibacterial activity. The well-known property of amidoxime functional groups to complex Fe(III), which has been reported to correlate with biofilm formation, gave rise to the presumption that the amidoximes display their antibacterial effect due to a complexation reaction. Unfortunately, the antibacterial effects of CBR703 were not attributed to iron complexation. Furthermore, the reported effects on biofilm formation, which were one of the main reasons for choosing CBR703 as a starting point, were suspected to be artifacts due to compound precipitation. Consequently, we rank this class of compounds as unattractive for the development as antibacterial agents.



In summary, both of these two studies for development of RNAP inhibitors were involved in the discovery of experimental artifacts, which is why we alerted the scientific community to be cautious with published data.

4.2 CYP11B1 inhibitors

To develop a novel strategy for the treatment of chronic wounds, topical application of CYP11B1 inhibitors to reduce cutaneous cortisol was proposed. The CYP11B1 inhibitors should maintain effective potency and guarantee safety by possessing specific metabolic profiles-stable in wound fluid and unstable in liver. In an initial work, it was observed that compound **III-2** was converted from CYP11B2 inhibitor to CYP11B1 inhibitor **III-3** by replacing amide with sulfonamide.



Subsequently, **III-3** exhibiting the desired inversed metabolic stability in human plasma ($t_{1/2}$ plasma >> 150 min) and in human liver S9 fraction ($t_{1/2}$ S9 fraction = 27 min), was used as the lead compound to perform a series of optimizations. Firstly various groups (alkyl or aryl) were introduced onto the sulfonamide moiety. Then the pyrrolidine rest of the indoline core was expanded or opened. Afterwards, a methylene bridge was inserted between the core and pyridyl moiety. Finally, the influence of 3- or 4-pyridyl was also investigated. As the best compound from this series, compound **III-34** was a highly potent CYP11B1 inhibitor (IC_{50} = 5 nM) being stronger than the lead compound **III-3**. In contrast, it did not inhibit two other important steroidogenic enzymes, namely 17 α -hydroxylase-17,20-lyase (CYP17) and aromatase (CYP19), which are also expressed in epidermis and involved in the biosynthesis of cutaneous estrogens. These estrogens are important for keeping skin moisture, preventing skin aging and, in particular, accelerating wound healing (Shah and Maibach, 2001; Thiboutot et al., 2003). Compound **III-34** showed a long half-life ($t_{1/2}$ >> 150 min) in human plasma, which is similar to the wound fluid in composition, whereas it was fast metabolized in human liver S9 fractions ($t_{1/2}$ = 16 min). Furthermore, it showed no mutagenic effects. Therefore compound **III-34** was considered as a good candidate for further *in vivo* evaluations.

5 References

- Adams, C.M., Hu, C.W., Jeng, A.Y., Karki, R., Ksander, G., LaSala, D., Leung-Chu, J., Liang, G.Q., Liu, Q.A., Meredith, E., *et al.* (2010). The discovery of potent inhibitors of aldosterone synthase that exhibit selectivity over 11-beta-hydroxylase. *Bioorg Med Chem Lett* 20, 4324-4327.
- Adelman, K., Yuzenkova, J., La Porta, A., Zenkin, N., Lee, J., Lis, J.T., Borukhov, S., Wang, M.D., and Severinov, K. (2004). Molecular mechanism of transcription inhibition by peptide antibiotic microcin J25. *Mol Cell* 14, 753-762.
- Andre, E., Bastide, L., Vullian-Guillot, P., Latouche, J., Rouby, J., and Leonetti, J.P. (2004). A multiwell assay to isolate compounds inhibiting the assembly of the prokaryotic RNA polymerase. *Assay Drug Dev Techn* 2, 629-635.
- Arhin, F., Belanger, O., Ciblat, S., Dehbi, M., Delorme, D., Dietrich, E., Dixit, D., Lafontaine, Y., Lehoux, D., Liu, J., *et al.* (2006). A new class of small molecule RNA polymerase inhibitors with activity against Rifampicin-resistant *Staphylococcus aureus*. *Bioorgan Med Chem* 14, 5812-5832.
- Artsimovitch, I., Chu, C., Lynch, A.S., and Landick, R. (2003). A new class of bacterial RNA polymerase inhibitor affects nucleotide addition. *Science* 302, 650-654.
- Artsimovitch, I., Svetlov, V., Nemetski, S.M., Epshtein, V., Cardozo, T., and Nudler, E. (2011). Tagetitoxin Inhibits RNA Polymerase through Trapping of the Trigger Loop. *Journal of Biological Chemistry* 286, 40395-40400.
- Artsimovitch, I., Vassilyeva, M.N., Svetlov, D., Svetlov, V., Perederina, A., Igarashi, N., Matsugaki, N., Wakatsuki, S., Tahirov, T.H., and Vassilyev, D.G. (2005). Allosteric modulation of the RNA polymerase catalytic reaction is an essential component of transcription control by rifamycins. *Cell* 122, 351-363.
- Auld, D.S., Thorne, N., Nguyen, D.T., and Inglese, J. (2008). A specific mechanism for nonspecific activation in reporter-gene assays. *ACS Chem Biol* 3, 463-470.
- Baell, J.B. (2010). Observations on screening-based research and some concerning trends in the literature. *Future Med Chem* 2, 1529-1546.
- Baker, M. (2010). Academic screening goes high-throughput. *Nat Methods* 7, 787-792.
- Balerna, M., Keller-Schierlein, W., Martius, C., Wolf, H., and Zahner, H. (1969). [Metabolic products of microorganisms. 72. Naphthomycin, an antimetabolite of vitamin K]. *Arch Mikrobiol* 65, 303-317.
- Blond, A., Peduzzi, J., Goulard, C., Chiuchiolo, M.J., Barthelemy, M., Prigent, Y., Salomon, R.A., Farias, R.N., Moreno, F., and Rebuffat, S. (1999). The cyclic structure of microcin J25, a 21-residue peptide antibiotic from *Escherichia coli*. *Eur J Biochem* 259, 747-755.
- Brueggemeier, R.W., Hackett, J.C., and Diaz-Cruz, E.S. (2005). Aromatase inhibitors in the treatment of breast cancer. *Endocr Rev* 26, 331-345.
- Bureik, M., Lisurek, M., and Bernhardt, R. (2002). The human steroid hydroxylases CYP1B1 and CYP11B2. *Biol Chem* 383, 1537-1551.
- Campbell, E.A., Korzheva, N., Mustaev, A., Murakami, K., Nair, S., Goldfarb, A., and Darst, S.A. (2001a). Structural mechanism for rifampicin inhibition of bacterial rna polymerase. *Cell* 104, 901-912.
- Campbell, E.A., Korzheva, N., Mustaev, A., Murakami, K., Nair, S., Goldfarb, A., and Darst, S.A. (2001b). Structural mechanism for rifampicin inhibition of bacterial RNA polymerase. *Cell* 104, 901-912.
- Campbell, E.A., Pavlova, O., Zenkin, N., Leon, F., Irschik, H., Jansen, R., Severinov, K., and Darst, S.A. (2005). Structural, functional, and genetic analysis of sorangicin inhibition of bacterial RNA polymerase. *Embo J* 24, 674-682.
- Cassani, G., Burgess, R.R., Goodman, H.M., and Gold, L. (1971). Inhibition of RNA polymerase by streptolydigin. *Nat New Biol* 230, 197-200.

- Chang, S., Sievert, D.M., Hageman, J.C., Boulton, M.L., Tenover, F.C., Downes, F.P., Shah, S., Rudrik, J.T., Pupp, G.R., Brown, W.J., *et al.* (2003). Infection with vancomycin-resistant *Staphylococcus aureus* containing the vanA resistance gene. *N Engl J Med* 348, 1342-1347.
- Chopra, I. (2007). Bacterial RNA polymerase: a promising target for the discovery of new antimicrobial agents. *Curr Opin Investig Drugs* 8, 600-607.
- Chyun, Y.S., Kream, B.E., and Raisz, L.G. (1984). Cortisol decreases bone formation by inhibiting periosteal cell proliferation. *Endocrinology* 114, 477-480.
- Ciciliato, I., Corti, E., Sarubbia, E., Stefanelli, S., Gastaldo, L., Montanini, N., Kurz, M., Losi, D., Marinelli, F., and Selva, E. (2004). Antibiotics GE23077, novel inhibitors of bacterial RNA polymerase I. Taxonomy, isolation and characterization. *J Antibiot* 57, 210-217.
- Coan, K.E., and Shoichet, B.K. (2008). Stoichiometry and physical chemistry of promiscuous aggregate-based inhibitors. *J Am Chem Soc* 130, 9606-9612.
- Copeland, R.A. (2005). Evaluation of enzyme inhibitors in drug discovery. A guide for medicinal chemists and pharmacologists. *Methods Biochem Anal* 46, 1-265.
- Coronelli, C., White, R.J., Lancini, G.C., and Parenti, F. (1975). Lipiarmycin, a new antibiotic from *Actinoplanes*. II. Isolation, chemical, biological and biochemical characterization. *J Antibiot (Tokyo)* 28, 253-259.
- Cramer, P. (2002). Multisubunit RNA polymerases. *Curr Opin Struc Biol* 12, 89-97.
- Cramer, P., Bushnell, D.A., and Kornberg, R.D. (2001). Structural basis of transcription: RNA polymerase II at 2.8 angstrom resolution. *Science* 292, 1863-1876.
- Darst, S.A. (2001). Bacterial RNA polymerase. *Curr Opin Struct Biol* 11, 155-162.
- Darst, S.A. (2004). New inhibitors targeting bacterial RNA polymerase. *Trends Biochem Sci* 29, 159-160.
- de With, K., Steib-Bauert, M., Knoth, H., Dorje, F., Strehl, E., Rothe, U., Maier, L., and Kern, W.V. (2005). Hospital use of systemic antifungal drugs. *BMC Clin Pharmacol* 5, 1.
- Derendorf, H., Nave, R., Drollmann, A., Cerasoli, F., and Wurst, W. (2006). Relevance of pharmacokinetics and pharmacodynamics of inhaled corticosteroids to asthma. *Eur Respir J* 28, 1042-1050.
- Doundoulakis, T., Xiang, A.X., Lira, R., Agrios, K.A., Webber, S.E., Sisson, W., Aust, R.M., Shah, A.M., Showalter, R.E., Appleman, J.R., *et al.* (2004). Myxopyronin B analogs as inhibitors of RNA polymerase, synthesis and biological evaluation. *Bioorg Med Chem Lett* 14, 5667-5672.
- Drake, W.M., Perry, L.A., Hinds, C.J., Lowe, D.G., Reznick, R.H., and Besser, G.M. (1998). Emergency and prolonged use of intravenous etomidate to control hypercortisolemia in a patient with Cushing's syndrome and peritonitis. *J Clin Endocr Metab* 83, 3542-3544.
- Ebrecht, M., Hextall, J., Kirtley, L.G., Taylor, A., Dyson, M., and Weinman, J. (2004). Perceived stress and cortisol levels predict speed of wound healing in healthy male adults. *Psychoneuroendocrinology* 29, 798-809.
- Ebright, R.H. (2000). RNA polymerase: Structural similarities between bacterial RNA polymerase and eukaryotic RNA polymerase II. *Journal of Molecular Biology* 304, 687-698.
- Edwards, R., and Harding, K.G. (2004). Bacteria and wound healing. *Curr Opin Infect Dis* 17, 91-96.
- Elgaher, W.A.M., Fruth, M., Groh, M., Haupenthal, J., and Hartmann, R.W. (2014). Expanding the scaffold for bacterial RNA polymerase inhibitors: design, synthesis and structure-activity relationships of ureido-heterocyclic-carboxylic acids. *Rsc Adv* 4, 2177-2194.
- Emmerich, J., Hu, Q., Hanke, N., and Hartmann, R.W. (2013). Cushing's syndrome: development of highly potent and selective CYP11B1 inhibitors of the (pyridylmethyl)pyridine type. *J Med Chem* 56, 6022-6032.
- Fassnacht, M., Hahner, S., Beuschlein, F., Klink, A., Reinecke, M., and Allolio, B. (2000). New mechanisms of adrenostatic compounds in a human adrenocortical cancer cell line. *Eur J Clin Invest* 30, 76-82.
- Fellows, I.W., Bastow, M.D., Byrne, A.J., and Allison, S.P. (1983). Adrenocortical Suppression in Multiply Injured Patients - a Complication of Etomidate Treatment. *Brit Med J* 287, 1835-1837.

- Fleseriu, M., and Petersenn, S. (2012). Medical management of Cushing's disease: what is the future? *Pituitary* 15, 330-341.
- Gnatt, A.L., Cramer, P., Fu, J.H., Bushnell, D.A., and Kornberg, R.D. (2001). Structural basis of transcription: An RNA polymerase II elongation complex at 3.3 angstrom resolution. *Science* 292, 1876-1882.
- Gualtieri, M., Bastide, L., Villain-Guillot, P., Michaux-Charachon, S., Latouche, J., and Leonetti, J.P. (2006a). In vitro activity of a new antibacterial rhodanine derivative against *Staphylococcus epidermidis* biofilms. *J Antimicrob Chemoth* 58, 778-783.
- Gualtieri, M., Villain-Guillot, P., Latouche, J., Leonetti, J.P., and Bastide, L. (2006b). Mutation in the *Bacillus subtilis* RNA polymerase beta' subunit confers resistance to lipiarmycin. *Antimicrob Agents Chemother* 50, 401-402.
- Hahner, S., Sturmer, A., Fassnacht, M., Hartmann, R.W., Schewe, K., Cochran, S., Zink, M., Schirbel, A., and Allolio, B. (2010). Etomidate Unmasks Intraadrenal Regulation of Steroidogenesis and Proliferation in Adrenal Cortical Cell Lines. *Hormone and Metabolic Research* 42, 528-534.
- Hays, S.J., Tobes, M.C., Gildersleeve, D.L., Wieland, D.M., and Beierwaltes, W.H. (1984). Structure-activity relationship study of the inhibition of adrenal cortical 11 beta-hydroxylase by new metyrapone analogues. *J Med Chem* 27, 15-19.
- Hille, U.E., Zimmer, C., Haupenthal, J., and Hartmann, R.W. (2011a). Optimization of the First Selective Steroid-11beta-hydroxylase (CYP11B1) Inhibitors for the Treatment of Cortisol Dependent Diseases. *ACS Med Chem Lett* 2, 559-564.
- Hille, U.E., Zimmer, C., Vock, C.A., and Hartmann, R.W. (2011b). First Selective CYP11B1 Inhibitors for the Treatment of Cortisol-Dependent Diseases. *ACS Med Chem Lett* 2, 2-6.
- Hinsberger, S., Husecken, K., Groh, M., Negri, M., Haupenthal, J., and Hartmann, R.W. (2013). Discovery of Novel Bacterial RNA Polymerase Inhibitors: Pharmacophore-Based Virtual Screening and Hit Optimization. *Journal of Medicinal Chemistry* 56, 8332-8338.
- Hopkins, A.L., and Groom, C.R. (2002). The druggable genome. *Nat Rev Drug Discov* 1, 727-730.
- Howe, D., Costanzo, M., Fey, P., Gojobori, T., Hannick, L., Hide, W., Hill, D.P., Kania, R., Schaeffer, M., St Pierre, S., *et al.* (2008). Big data: The future of biocuration. *Nature* 455, 47-50.
- Hu, T., Schaus, J.V., Lam, K., Palfreyman, M.G., Wuonola, M., Gustafson, G., and Panek, J.S. (1998). Total synthesis and preliminary antibacterial evaluation of the RNA polymerase inhibitors (+/-)-myxopyronin A and B. *J Org Chem* 63, 2401-2406.
- Inglese, J., Johnson, R.L., Simeonov, A., Xia, M., Zheng, W., Austin, C.P., and Auld, D.S. (2007). High-throughput screening assays for the identification of chemical probes. *Nat Chem Biol* 3, 466-479.
- Irschik, H., Augustiniak, H., Gerth, K., Hofle, G., and Reichenbach, H. (1995). The Ripostatins, Novel Inhibitors of Eubacterial Rna-Polymerase Isolated from Myxobacteria. *J Antibiot* 48, 787-792.
- Irschik, H., Gerth, K., Hofle, G., Kohl, W., and Reichenbach, H. (1983). The Myxopyronins, New Inhibitors of Bacterial Rna-Synthesis from *Myxococcus-Fulvus* (Myxobacterales). *J Antibiot* 36, 1651-1658.
- Irschik, H., Jansen, R., Gerth, K., Hofle, G., and Reichenbach, H. (1987). Antibiotics from Gliding Bacteria .32. The Sorangicins, Novel and Powerful Inhibitors of Eubacterial Rna-Polymerase Isolated from Myxobacteria. *J Antibiot* 40, 7-13.
- Irschik, H., Jansen, R., Hofle, G., Gerth, K., and Reichenbach, H. (1985). On Antibiotics from Gliding Bacteria .25. The Corallopyronins, New Inhibitors of Bacterial Rna-Synthesis from Myxobacteria. *J Antibiot* 38, 145-152.
- Jadhav, A., Ferreira, R.S., Klumpp, C., Mott, B.T., Austin, C.P., Inglese, J., Thomas, C.J., Maloney, D.J., Shoichet, B.K., and Simeonov, A. (2010). Quantitative analyses of aggregation, autofluorescence, and reactivity artifacts in a screen for inhibitors of a thiol protease. *J Med Chem* 53, 37-51.

- Jansen, R., Wray, V., Irschik, H., Reichenbach, H., and Hofle, G. (1985). Isolation and Spectroscopic Structure Elucidation of Sorangicin-a, a New Type of Macrolide-Polyether Antibiotic from Gliding Bacteria .30. *Tetrahedron Lett* 26, 6031-6034.
- Jonat, W., and Mundhenke, C. (2007). The FACE trial: Letrozole or anastrozole as initial adjuvant therapy? *Cancer Investigation* 25, 14-18.
- Klyuyev, S., and Vassilyev, D.G. (2012). The binding site and mechanism of the RNA polymerase inhibitor tagetitoxin: an issue open to debate. *Transcription* 3, 46-50.
- Lira, R., Xiang, A.X., Doundoulakis, T., Biller, W.T., Agrios, K.A., Simonsen, K.B., Webber, S.E., Sisson, W., Aust, R.M., Shah, A.M., *et al.* (2007). Syntheses of novel myxopyronin B analogs as potential inhibitors of bacterial RNA polymerase. *Bioorg Med Chem Lett* 17, 6797-6800.
- Loli, P., Berselli, M.E., and Tagliaferri, M. (1986). Use of Ketoconazole in the Treatment of Cushings-Syndrome. *J Clin Endocr Metab* 63, 1365-1371.
- Major, J. (1998). Challenges and opportunities in high throughput screening: Implications for new technologies. *J Biomol Screen* 3, 13-17.
- Malinen, A.M., NandyMazumdar, M., Turtola, M., Malmi, H., Grocholski, T., Artsimovitch, I., and Belogurov, G.A. (2014). CBR antimicrobials alter coupling between the bridge helix and the beta subunit in RNA polymerase. *Nature Communications* 5.
- Marazzi, A., Kurz, M., Stefanelli, S., and Colombo, L. (2005). Antibiotics GE23077, novel inhibitors of bacterial RNA polymerase II. Structure elucidation. *J Antibiot* 58, 260-267.
- Mariner, K.R., Trowbridge, R., Agarwal, A.K., Miller, K., O'Neill, A.J., Fishwick, C.W.G., and Chopra, I. (2010). Furanyl-Rhodanines Are Unattractive Drug Candidates for Development as Inhibitors of Bacterial RNA Polymerase. *Antimicrob Agents Ch* 54, 4506-4509.
- Marucha, P.T., Kiecolt-Glaser, J.K., and Favagehi, M. (1998). Mucosal wound healing is impaired by examination stress. *Psychosom Med* 60, 362-365.
- Mathews, D.E., and Durbin, R.D. (1990). Tagetitoxin Inhibits Rna-Synthesis Directed by Rna-Polymerases from Chloroplasts and Escherichia-Coli. *Journal of Biological Chemistry* 265, 493-498.
- Mathews, D.E., and Durbin, R.D. (1994). Mechanistic Aspects of Tagetitoxin Inhibition of Rna-Polymerase from Escherichia-Coli. *Biochemistry-US* 33, 11987-11992.
- Mavoungou, E., Bouyou-Akotet, M.K., and Kremsner, P.G. (2005). Effects of prolactin and cortisol on natural killer (NK) cell surface expression and function of human natural cytotoxicity receptors (NKp46, NKp44 and NKp30). *Clin Exp Immunol* 139, 287-296.
- McClure, W.R. (1980). On the mechanism of streptolydigin inhibition of Escherichia coli RNA polymerase. *J Biol Chem* 255, 1610-1616.
- McGovern, S.L., Caselli, E., Grigorieff, N., and Shoichet, B.K. (2002). A common mechanism underlying promiscuous inhibitors from virtual and high-throughput screening. *Journal of Medicinal Chemistry* 45, 1712-1722.
- Mitchell, R.E., Coddington, J.M., and Young, H. (1989). A Revised Structure for Tagetitoxin. *Tetrahedron Lett* 30, 501-504.
- Mitchell, R.E., and Durbin, R.D. (1981). Tagetitoxin, a Toxin Produced by Pseudomonas-Syringae Pv Tagetis - Purification and Partial Characterization. *Physiol Plant Pathol* 18, 157-168.
- Mukhopadhyay, J., Das, K., Ismail, S., Koppstein, D., Jang, M.Y., Hudson, B., Sarafianos, S., Tuske, S., Patel, J., Jansen, R., *et al.* (2008). The RNA Polymerase "Switch Region" Is a Target for Inhibitors. *Cell* 135, 295-307.
- Mukhopadhyay, J., Sineva, E., Knight, J., Levy, R.M., and Ebright, R.H. (2004). Antibacterial peptide microcin J25 inhibits transcription by binding within and obstructing the RNA polymerase secondary channel. *Mol Cell* 14, 739-751.
- Murakami, K.S., and Darst, S.A. (2003). Bacterial RNA polymerases: the whole story. *Curr Opin Struct Biol* 13, 31-39.

- Murakami, K.S., Masuda, S., Campbell, E.A., Muzzin, O., and Darst, S.A. (2002a). Structural basis of transcription initiation: an RNA polymerase holoenzyme-DNA complex. *Science* 296, 1285-1290.
- Murakami, K.S., Masuda, S., and Darst, S.A. (2002b). Structural basis of transcription initiation: RNA polymerase holoenzyme at 4 Å resolution. *Science* 296, 1280-1284.
- Nieman, L.K. (2002). Medical therapy of Cushing's disease. *Pituitary* 5, 77-82.
- Orth, D.N. (1995). Cushing's syndrome. *N Engl J Med* 332, 791-803.
- Osburne, M.S., and Sonenshein, A.L. (1980). Inhibition by lipiarmycin of bacteriophage growth in *Bacillus subtilis*. *J Virol* 33, 945-953.
- Palacios, R., and Sugawara, I. (1982). Hydrocortisone abrogates proliferation of T cells in autologous mixed lymphocyte reaction by rendering the interleukin-2 Producer T cells unresponsive to interleukin-1 and unable to synthesize the T-cell growth factor. *Scand J Immunol* 15, 25-31.
- Piroli, G.G., Grillo, C.A., Reznikov, L.R., Adams, S., McEwen, B.S., Charron, M.J., and Reagan, L.P. (2007). Corticosterone impairs insulin-stimulated translocation of GLUT4 in the rat hippocampus. *Neuroendocrinology* 85, 71-80.
- Pistorius, D., Ullrich, A., Lucas, S., Hartmann, R.W., Kazmaier, U., and Muller, R. (2011). Biosynthesis of 2-Alkyl-4(1H)-Quinolones in *Pseudomonas aeruginosa*: Potential for Therapeutic Interference with Pathogenicity. *Chembiochem* 12, 850-853.
- Prelog, V., and Oppolzer, W. (1973). [Ansamycins, a novel class of microbial metabolites]. *Helv Chim Acta* 56, 1179-1187.
- Pyta, K., Przybylski, P., Klich, K., and Stefanska, J. (2012). A new model of binding of rifampicin and its amino analogues as zwitterions to bacterial RNA polymerase. *Org Biomol Chem* 10, 8283-8297.
- Raats, J.I., Falkson, G., and Falkson, H.C. (1992). A Study of Fadrozole, a New Aromatase Inhibitor, in Postmenopausal Women with Advanced Metastatic Breast-Cancer. *J Clin Oncol* 10, 111-116.
- Raven, P.W., Checkley, S.A., and Taylor, N.F. (1995). Extra-adrenal effects of metyrapone include inhibition of the 11-oxoreductase activity of 11 beta-hydroxysteroid dehydrogenase: a model for 11-HSD I deficiency. *Clin Endocrinol (Oxf)* 43, 637-644.
- Roumen, L., Peeters, J.W., Emmen, J.M.A., Beugels, I.P.E., Custers, E.M.G., de Gooyer, M., Plate, R., Pieterse, K., Hilbers, P.A.J., Smits, J.F.M., *et al.* (2010). Synthesis, Biological Evaluation, and Molecular Modeling of 1-Benzyl-1H-imidazoles as Selective Inhibitors of Aldosterone Synthase (CYP11B2). *Journal of Medicinal Chemistry* 53, 1712-1725.
- Sahner, J.H., Brengel, C., Storz, M.P., Groh, M., Plaza, A., Muller, R., and Hartmann, R.W. (2013a). Combining in Silico and Biophysical Methods for the Development of *Pseudomonas aeruginosa* Quorum Sensing Inhibitors: An Alternative Approach for Structure-Based Drug Design. *Journal of Medicinal Chemistry* 56, 8656-8664.
- Sahner, J.H., Groh, M., Negri, M., Haupenthal, J., and Hartmann, R.W. (2013b). Novel small molecule inhibitors targeting the "switch region" of bacterial RNAP: structure-based optimization of a virtual screening hit. *Eur J Med Chem* 65, 223-231.
- Salomon, R.A., and Farias, R.N. (1992). Microcin-25, a Novel Antimicrobial Peptide Produced by *Escherichia-Coli*. *Journal of Bacteriology* 174, 7428-7435.
- Sarubbi, E., Monti, F., Corti, E., Miele, A., and Selva, E. (2004). Mode of action of the microbial metabolite GE23077, a novel potent and selective inhibitor of bacterial RNA polymerase. *Eur J Biochem* 271, 3146-3154.
- Schulz, W., and Zillig, W. (1981). Rifampicin inhibition of RNA synthesis by destabilisation of DNA-RNA polymerase-oligonucleotide-complexes. *Nucleic Acids Res* 9, 6889-6906.
- Sen, C.K., Gordillo, G.M., Roy, S., Kirsner, R., Lambert, L., Hunt, T.K., Gottrup, F., Gurtner, G.C., and Longaker, M.T. (2009). Human skin wounds: a major and snowballing threat to public health and the economy. *Wound Repair Regen* 17, 763-771.

- Sensi, P., Margalith, P., and Timbal, M.T. (1959). Rifomycin, a new antibiotic; preliminary report. *Farmaco Sci* 14, 146-147.
- Shah, M.G., and Maibach, H.I. (2001). Estrogen and skin. An overview. *Am J Clin Dermatol* 2, 143-150.
- Shoichet, B.K. (2006). Screening in a spirit haunted world. *Drug Discov Today* 11, 607-615.
- Siddhikol, C., Erbstoesser, J.W., and Weisblum, B. (1969). Mode of action of streptolydigin. *J Bacteriol* 99, 151-155.
- Simpson, E.R., and Dowsett, M. (2002). Aromatase and its inhibitors: significance for breast cancer therapy. *Recent Prog Horm Res* 57, 317-338.
- Solbiati, J.O., Ciaccio, M., Farias, R.N., Gonzalez-Pastor, J.E., Moreno, F., and Salomon, R.A. (1999). Sequence analysis of the four plasmid genes required to produce the circular peptide antibiotic microcin J25. *J Bacteriol* 181, 2659-2662.
- Srivastava, A., Degen, D., Ebright, Y.W., and Ebright, R.H. (2012). Frequency, Spectrum, and Nonzero Fitness Costs of Resistance to Myxopyronin in *Staphylococcus aureus*. *Antimicrob Agents Ch* 56, 6250-6255.
- Svetlov, V., Artsimovitch, I., and Nudler, E. (2012). Response to Klyuyev and Vassilyev: on the mechanism of tagetitoxin inhibition of transcription. *Transcription* 3, 51-55.
- Swanson, R.N., Hardy, D.J., Shipkowitz, N.L., Hanson, C.W., Ramer, N.C., Fernandes, P.B., and Clement, J.J. (1991). In vitro and in vivo evaluation of tiacumicins B and C against *Clostridium difficile*. *Antimicrob Agents Chemother* 35, 1108-1111.
- Thiboutot, D., Jabara, S., McAllister, J.M., Sivarajah, A., Gilliland, K., Cong, Z.Y., and Clawson, G. (2003). Human skin is a steroidogenic tissue: Steroidogenic enzymes and cofactors are expressed in epidermis, normal sebocytes, and an immortalized sebocyte cell line (SEB-1). *J Invest Dermatol* 120, 905-914.
- Tobes, M.C., Hays, S.J., Gildersleeve, D.L., Wieland, D.M., and Beierwaltes, W.H. (1985). Adrenal-Cortical 11-Beta-Hydroxylase and Side-Chain Cleavage Enzymes - Requirement for the α -Pyridyl or β -Pyridyl Ring in Metyrapone for Inhibition. *J Steroid Biochem* 22, 103-110.
- Tominaga, T., Adachi, I., Sasaki, Y., Tabei, T., Ikeda, T., Takatsuka, Y., Toi, M., Suwa, T., and Ohashi, Y. (2003). Double-blind randomised trial comparing the non-steroidal aromatase inhibitors letrozole and fadrozole in postmenopausal women with advanced breast cancer. *Annals of Oncology* 14, 62-70.
- Trengove, N.J., Langton, S.R., and Stacey, M.C. (1996). Biochemical analysis of wound fluid from nonhealing and healing chronic leg ulcers. *Wound Repair Regen* 4, 234-239.
- Tupin, A., Gualtieri, M., Leonetti, J.P., and Brodolin, K. (2010). The transcription inhibitor lipiarmycin blocks DNA fitting into the RNA polymerase catalytic site. *Embo J* 29, 2527-2537.
- Tuske, S., Sarafianos, S.G., Wang, X.Y., Hudson, B., Sineva, E., Mukhopadhyay, J., Birktoft, J.J., Leroy, O., Ismail, S., Clark, A.D., *et al.* (2005). Inhibition of bacterial RNA polymerase by streptolydigin: Stabilization of a straight-bridge-helix active-center conformation. *Cell* 122, 541-552.
- Vasaitis, T.S., Bruno, R.D., and Njar, V.C.O. (2011). CYP17 inhibitors for prostate cancer therapy. *J Steroid Biochem* 125, 23-31.
- Vassilyev, D.G., Svetlov, V., Vassilyeva, M.N., Perederina, A., Igarashi, N., Matsugaki, N., Wakatsuki, S., and Artsimovitch, I. (2005). Structural basis for transcription inhibition by tagetitoxin. *Nat Struct Mol Biol* 12, 1086-1093.
- Verhelst, J.A., Trainer, P.J., Howlett, T.A., Perry, L., Rees, L.H., Grossman, A.B., Wass, J.A., and Besser, G.M. (1991). Short and long-term responses to metyrapone in the medical management of 91 patients with Cushing's syndrome. *Clin Endocrinol (Oxf)* 35, 169-178.
- Villain-Guillot, P., Gualtieri, M., Bastide, L., and Leonetti, J.P. (2007a). In vitro activities of different inhibitors of bacterial transcription against *Staphylococcus epidermidis* biofilm. *Antimicrob Agents Chemother* 51, 3117-3121.

- Villain-Guillot, P., Gualtieri, M., Bastide, L., Roquet, F., Martinez, J., Amblard, M., Pugniere, M., and Leonetti, J.P. (2007b). Structure-activity relationships of phenyl-furanyl-rhodanines as inhibitors of RNA polymerase with antibacterial activity on biofilms. *Journal of Medicinal Chemistry* 50, 4195-4204.
- Vukelic, S., Stojadinovic, O., Pastar, I., Rabach, M., Krzyzanowska, A., Lebrun, E., Davis, S.C., Resnik, S., Brem, H., and Tomic-Canic, M. (2011). Cortisol Synthesis in Epidermis Is Induced by IL-1 and Tissue Injury. *Journal of Biological Chemistry* 286, 10265-10275.
- Wigneshweraraj, S., Bose, D., Burrows, P.C., Joly, N., Schumacher, J., Rappas, M., Pape, T., Zhang, X., Stockley, P., Severinov, K., *et al.* (2008). Modus operandi of the bacterial RNA polymerase containing the sigma54 promoter-specificity factor. *Mol Microbiol* 68, 538-546.
- Wigneshweraraj, S.R., Savalia, D., Severinov, K., and Buck, M. (2006). Interplay between the beta' clamp and the beta' jaw domains during DNA opening by the bacterial RNA polymerase at sigma54-dependent promoters. *J Mol Biol* 359, 1182-1195.
- Wright, G.D., and Sutherland, A.D. (2007). New strategies for combating multidrug-resistant bacteria. *Trends Mol Med* 13, 260-267.
- Yin, L.N., Lucas, S., Maurer, F., Kazmaier, U., Hu, Q.Z., and Hartmann, R.W. (2012). Novel Imidazol-1-ylmethyl Substituted 1,2,5,6-Tetrahydropyrrolo[3,2,1-ij]quinolin-4-ones as Potent and Selective CYP11B1 Inhibitors for the Treatment of Cushing's Syndrome. *Journal of Medicinal Chemistry* 55, 6629-6633.
- Yuzenkova, J., Delgado, M., Nechaev, S., Savalia, D., Epshtein, V., Artsimovitch, I., Mooney, R.A., Landick, R., Farias, R.N., Salomon, R., *et al.* (2002). Mutations of bacterial RNA polymerase leading to resistance to microcin J25. *Journal of Biological Chemistry* 277, 50867-50875.
- Zhang, G., Campbell, E.A., Minakhin, L., Richter, C., Severinov, K., and Darst, S.A. (1999). Crystal structure of *Thermus aquaticus* core RNA polymerase at 3.3 Å resolution. *Cell* 98, 811-824.
- Zhang, Y., Degen, D., Ho, M.X., Sineva, E., Ebright, K.Y., Ebright, Y.W., Mekler, V., Vahedian-Movahed, H., Feng, Y., Yin, R.H., *et al.* (2014). GE23077 binds to the RNA polymerase 'i' and 'i+1' sites and prevents the binding of initiating nucleotides. *Elife* 3.
- Zhu, W., Hauptenthal, J., Groh, M., Fountain, M., and Hartmann, R.W. (2014). New Insights into the Bacterial RNA Polymerase Inhibitor CBR703 as a Starting Point for Optimization as an Anti-Infective Agent. *Antimicrob Agents Chemother* 58, 4242-4245.
- Zolle, I.M., Berger, M.L., Hammerschmidt, F., Hahner, S., Schirbel, A., and Peric-Simov, B. (2008). New selective inhibitors of steroid 11beta-hydroxylation in the adrenal cortex. Synthesis and structure-activity relationship of potent etomidate analogues. *J Med Chem* 51, 2244-2253.
- Zunszain, P.A., Anacker, C., Cattaneo, A., Carvalho, L.A., and Pariante, C.M. (2011). Glucocorticoids, cytokines and brain abnormalities in depression. *Prog Neuro-Psychoph* 35, 722-729.

6 Appendix

6.1 Supplemental Information for Paper I

**A Detective Story in Drug Discovery: Elucidation of a Screening Artifact
Reveals Polymeric Carboxylic Acids as Potent Inhibitors of RNA Polymerase**

Supplementary Figures and Tables

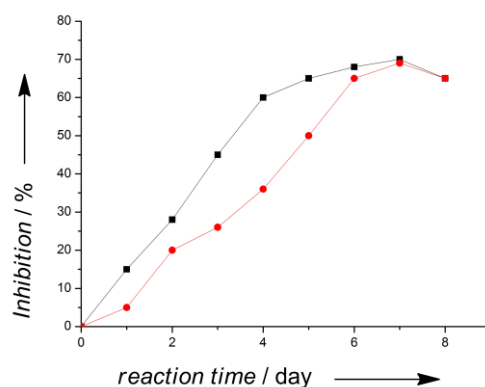


Figure S1. Inhibition of *E. coli* RNAP as a function of decomposition of compound **1**. In red: **1** (10 μ M in MeOH) at 50 $^{\circ}$ C, in black: **1** (10 μ M in DMSO) at 50 $^{\circ}$ C.

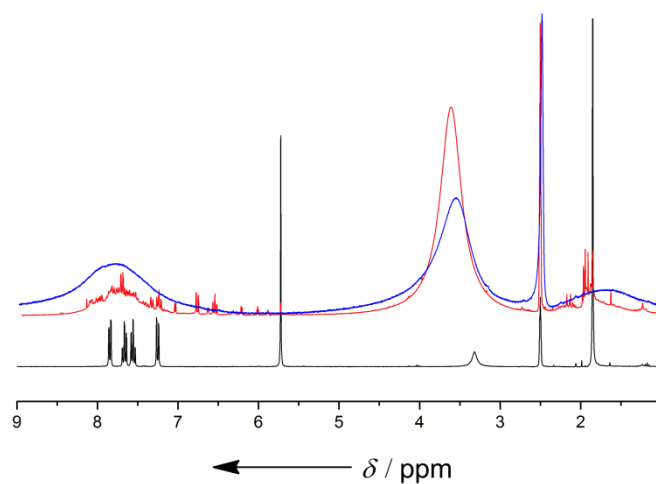


Figure S2. ^1H NMR spectra. In black: **1**, in red: **1** decomposed after 10 days heating at 50 $^{\circ}$ C, in blue: **P1**. Broad peaks in the aromatic range from 8.5 to 7.0 ppm and the protons of methyl group in the range of 2.0 to 1.5 ppm can be observed whereas the signal of the β -C-H on the pyrrole ring (5.7 ppm) is missing. The large peak from 4.1 to 2.7 ppm can be assigned for water and the α -C-H on the pyrrole ring.

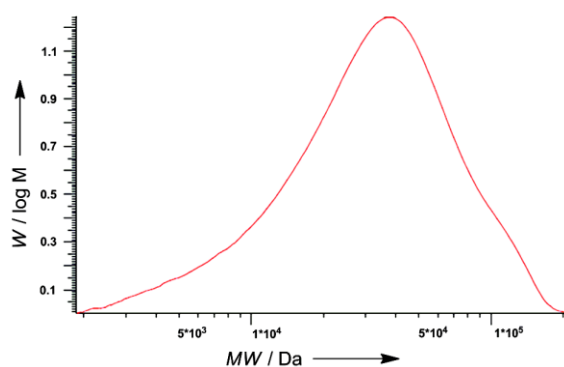


Figure S3. Molecular weight distribution elugram of **P1** by GPC analysis. The averaged molecular weight and distribution of the sample was calculated using the strip method based on the PMMA calibration.

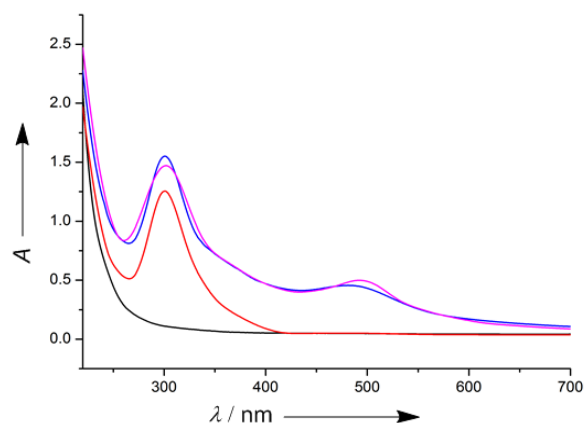


Figure S4. UV-Vis spectroscopy. In black: solvent (0.1 M NaOH), in red: synthetic **1** (200 $\mu\text{g/mL}$ in 0.1 M NaOH), in blue: **P1** of (10 $\mu\text{g/mL}$ in 0.1 M NaOH), in magenta: commercial **1** (200 $\mu\text{g/mL}$ in 0.1 M NaOH).

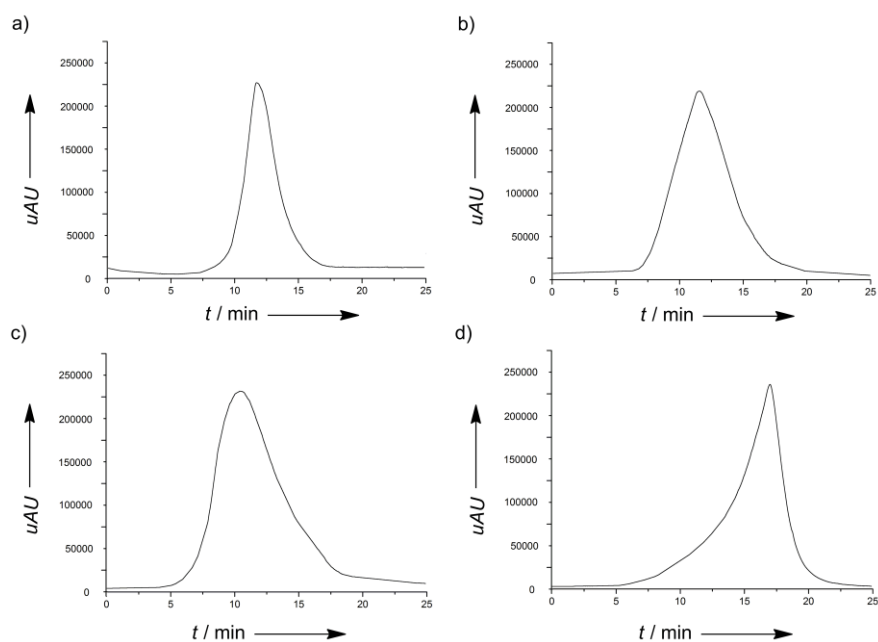


Figure S5. HPLC analysis of **P2** (a), **P3** (b), **P4** (c) and **P5** (d). Analytical conditions: eluent: gradient acetonitrile- H_2O ; concentration: 2.0 mg/mL ; UV detection at 254 nm.

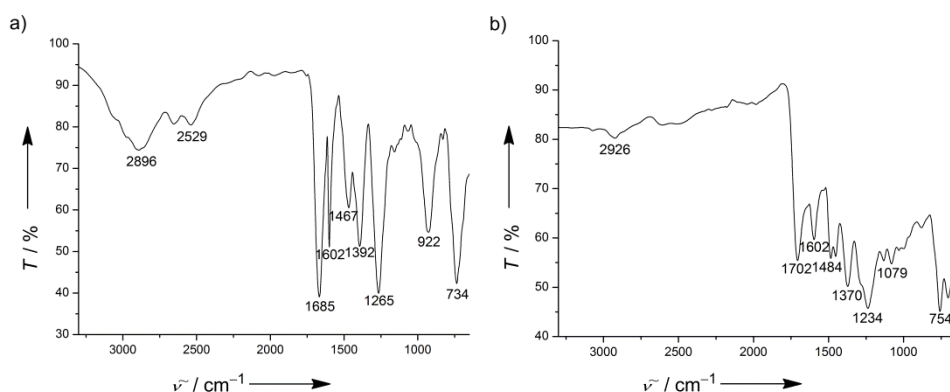


Figure S6. IR spectra of **1** (a) and **P1** (b).

Comparison of **P1–P5** with **1** indicates the carboxylic acid group is still present in **P1–4** in contrast to **P5** (Table S1).

Table S1. IR signals for $\tilde{\nu} \text{C=O}$ of **P1–P5**.

Compound	$\tilde{\nu}$ C=O (cm ⁻¹)
1	1685
P1	1702
P2	1698
P3	1698
P4	1704
P5	—

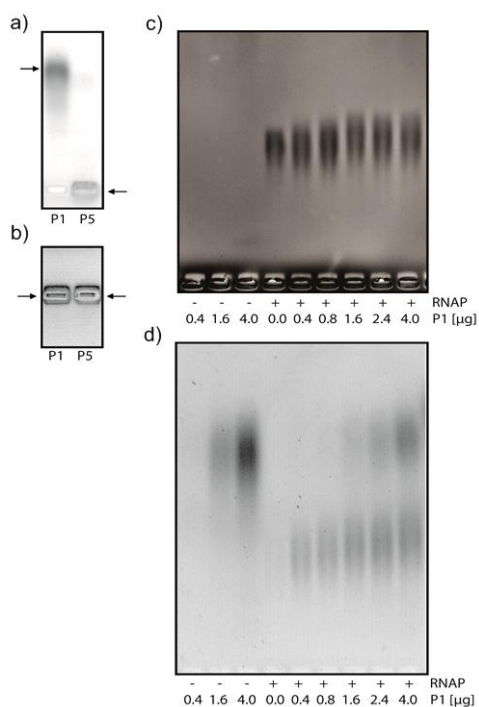


Figure S7. Non-denaturing agarose gel electrophoresis. a) 1.0 μ g of **P1** and **P5** were run at pH 7.8 and b) pH 3.6. c) Different concentrations of **P1** were run in absence or presence of 4.5 μ g RNAP holo enzyme at pH 7.8 (0.4 μ g of **P1** represents a 1:1 ratio of **P1**: RNAP). The protein was visualized by coomassie staining. d) The same samples as in c) were run, **P1** was visualized. Top: positive pole, bottom: negative pole. 1% agarose; the running time (at 100 V) was identical (50 min) for each gel. **P1** was visualized by UV.

Table S2. Inhibition of different proteins by **1** and **P1**.

Proteins	Inhibition	
	1	P1
CYP11B1	n.i.	n.i.
CYP11B2	n.i.	n.i.
CYP17	n.i. ^[a]	65% ^[b]
CYP19	n.i. ^[a]	65% ^[b]
17 β -HSD1	n.i.	50%
17 β -HSD2	30%	80%
PqsD	35%	n.i.

1 was tested at 50 μ M (=10.8 μ g/mL), **P1** was tested at 10 μ g/mL; [a] 100 μ M (= 21.5 μ g/mL), [b] 20.0 μ g/mL. n.i. = no inhibition (inhibition <15%).

Experimental Section

Chemistry.

Commercial reagents were purchased from Sigma-Aldrich or ABCR and used without further purification. Proton nuclear magnetic resonance (^1H NMR) and carbon NMR (^{13}C NMR) spectra were recorded on a Bruker Fourier spectrometer (500 or 125 MHz) at ambient temperature with the chemical shifts recorded as δ values in ppm units by reference to the hydrogenated residues of deuterated solvent as internal standard. Coupling constants (J) are given in Hz and signal patterns are indicated as follows: s, singlet; d, doublet; t, triplet; m, multiplet, br, broad signal. The melting points (m.p.) were determined on a Stuart Scientific SMP3 apparatus and are uncorrected. The SpectraSystems-LC-system consisted of a pump, an autosampler, and a UV detector. Mass spectrometry was performed on a MSQ electro spray mass spectrometer (Thermo Fisher, Dreieich, Germany). The system was operated by the standard software Xcalibur. A RP C18 NUCLEODUR 100-5 (125 x 3 mm) column (Macherey-Nagel GmbH, Dueren, Germany) was used as stationary phase. Solvent system: In a gradient run the percentage of acetonitrile (containing 0.1% trifluoroacetic acid) in 0.1% trifluoroacetic acid was increased from an initial concentration of 0% at 0 min to 100% at 15 min or 20 min and kept at 100% for 5 min. The injection volume was 10 μL and flow rate was set to 0.8 $\mu\text{L}/\text{min}$. MS analysis was carried out at a spray voltage of 3800 V, a capillary temperature of 350 $^\circ\text{C}$ and a source CID of 10 V. Spectra were acquired in positive mode from 100 to 1000 m/z and at 254 nm for the UV trace.

Experiments by microwave heating were performed with a Multi Synth (MLS GmbH) apparatus. UV-Vis spectroscopy was performed using a Nano Drop 2000c spectrophotometer (Thermo Scientific).

General Procedure for the Synthesis of 2,5-dimethyl-1-phenyl-1H-pyrroles. To a solution of the appropriate aniline (2.00 mmol) in glacial acetic acid (3 mL) was added 2,5-hexanedione (2.20 mmol). The reaction mixture was microwave-irradiated for 10 min at 150 $^\circ\text{C}$. The mixture was poured into ice-water (40 mL) and kept without stirring for 4 hours. The precipitate was filtered, washed with water (10 mL) and purified by column chromatography (silica gel, *n*-hexane/EtOAc).

2-(2,5-dimethyl-1H-pyrrol-1-yl)benzoic acid (1). White solid, m.p. 119–120 $^\circ\text{C}$; 55% yield; ^1H NMR (500 MHz, $[\text{D}_6]\text{DMSO}$): δ = 12.79 (br s, 1H; COOH), 7.84 (dd, $^3,^4J$ = 7.6, 1.6 Hz, 1H; Ar-H), 7.66 (ddd, $^3,^3,^4J$ = 7.9, 7.6, 1.6 Hz, 1H; Ar-H), 7.56 (ddd, $^3,^3,^4J$ = 7.6, 7.6, 1.1 Hz, 1H; Ar-H), 7.25 (dd, $^3,^4J$ = 7.9, 1.1 Hz, 1H; Ar-H), 5.72 (s, 2H; C=CH), 1.85 (s, 6H; CH_3) ppm; ^{13}C NMR (125 MHz, $[\text{D}_6]\text{DMSO}$): δ = 167.1, 137.0, 132.3, 132.1, 130.2, 129.9, 128.4, 127.8, 105.3, 12.5 ppm; LC/MS: m/z (%): $[\text{M}+\text{H}]^+$ 216.3 (100%), t_{R} = 9.63 min, 96.5% pure (UV).

3-(2,5-dimethyl-1H-pyrrol-1-yl)benzoic acid (2). White solid, m.p. 148–150 $^\circ\text{C}$; 61% yield; ^1H NMR (500 MHz, $[\text{D}_6]\text{DMSO}$): δ = 13.17 (br s, 1H; COOH), 8.00 (ddd, $^3,^4,^4J$ = 7.6, 1.6, 1.3 Hz, 1H; Ar-H), 7.69 (dd, $^4,^4J$ = 1.9, 1.3 Hz, 1H; Ar-H), 7.65 (dd, $^3,^3J$ = 7.9, 7.6 Hz, 1H; Ar-H), 7.54 (m, 1H; Ar-H), 5.82 (s, 2H; C=CH), 1.96 (s, 6H; CH_3) ppm; ^{13}C NMR (125 MHz, $[\text{D}_6]\text{DMSO}$): δ = 166.6, 138.5, 132.4, 132.0, 129.7, 128.4, 128.3, 127.5, 106.2, 12.8 ppm; LC/MS: m/z (%): $[\text{M}+\text{H}]^+$ 216.3 (100%), t_{R} = 10.27 min, 100% pure (UV).

4-(2,5-dimethyl-1H-pyrrol-1-yl)benzoic acid (3). White solid, m.p. 195–198 °C; 68% yield; ^1H NMR (500 MHz, $[\text{D}_6]\text{DMSO}$): δ = 13.07 (br s, 1H; COOH), 8.05 (d, 3J = 8.5 Hz, 2H; Ar-H), 7.38 (d, 3J = 8.5 Hz, 2H; Ar-H), 5.83 (s, 2H; C=CH), 1.99 (s, 6H; CH_3) ppm; ^{13}C NMR (125 MHz, $[\text{D}_6]\text{DMSO}$): δ = 166.7, 142.1, 130.2, 129.8, 128.0, 127.5, 106.6, 12.8 ppm; LC/MS: m/z (%): $[\text{M}+\text{H}]^+$ 216.3 (100%), t_R = 10.24 min, 100% pure (UV).

2-(4-(2,5-dimethyl-1H-pyrrol-1-yl)phenyl)acetic acid (4). White solid, m.p. 116–118 °C; 67% yield; ^1H NMR (500 MHz, $[\text{D}_6]\text{DMSO}$): δ = 12.40 (br s, 1H; COOH), 7.38 (d, 3J = 8.2 Hz, 2H; Ar-H), 7.18 (d, 3J = 8.2 Hz, 2H; Ar-H), 5.78 (s, 2H; C=CH), 3.66 (s, 2H; CH_2), 1.95 (s, 6H; CH_3) ppm; ^{13}C NMR (125 MHz, $[\text{D}_6]\text{DMSO}$): δ = 172.5, 136.8, 134.4, 130.2, 127.7, 127.5, 105.8, 40.0, 12.9 ppm. LC/MS: m/z (%): $[\text{M}+\text{H}]^+$ 230.1 (100%), t_R = 10.03 min, 97.6% pure (UV).

2,5-dimethyl-1-phenyl-1H-pyrrole (5). White solid, m.p. 50–52 °C; 73% yield; ^1H NMR (500 MHz, CDCl_3): δ = 7.46 (m, 2H; Ar-H), 7.40 (tt, $^{3,4}J$ = 7.4, 1.3 Hz, 1H; Ar-H), 7.22 (m, 2H; Ar-H), 5.91 (s, 2H; C=CH), 2.04 (s, 6H; CH_3) ppm; ^{13}C NMR (125 MHz, CDCl_3): δ = 139.0, 129.0, 128.8, 128.2, 127.6, 105.6, 13.0 ppm; LC/MS: m/z (%): $[\text{M}+\text{H}]^+$ 172.0 (100%), t_R = 12.67 min, 95.7% pure (UV).

General Procedure for the Polymerization of 1–5 to prepare P1–P5.

A solution of the 2,5-dimethyl-1-phenyl-1H-pyrrole derivative (10 μM) was kept for 10 days at 50 °C. The solvent was removed and the crude product was obtained as a black solid. For further purification the crude material was washed with an appropriate solvent. For **P1–P4** acetonitrile and MeOH was used. For **P5** a mixture of *n*-hexane/EtOAc (1:1) was used. **P1–P5** were obtained as dark red powders.

P1: 10% yield. $[\text{D}_6]\text{DMSO}$ was used as solvent for ^1H NMR spectroscopy. The broad peak between 2.7 to 4.1 ppm was assigned for water, which cannot be removed from the amorphous material.

GPC analysis. The selected sample was prepared at concentration of 3 mg/mL in DMSO and was filtrated through a disposable filter (size: 1 μm). First, a calibration curve with commercial polymethyl methacrylate (PMMA) in the separating region of the column (molecular weight range between 1.1 kDa and 100 kDa) was performed. The molecular weight distribution was calculated using the strip method based on the PMMA calibration. M_n = 20.7 kDa, M_w = 40.6 kDa, M_z = 63.7 kDa, PDI (M_w / M_n) = 1.96. Analytical conditions: eluent: DMSO (0.1 M LiCl); column: PSS GRAM, 10 μm , 100 Å, ID 8.0 mm x 300 mm; pump: TSP P1000 HPLC; flow rate: 1.0 mL/min; injection system: TSP AS3000 with 50 μL ; detector: Shodex differential refractometer RI 71; evaluation: PSS WinGPC UnChrom Version 8.0.

Agarose gel electrophoresis. Different amounts of polymeric substance were run on a non-denaturing 1% agarose gel and visualized in a E-BOX VX2 (peqlab, Erlangen, Germany). For protein visualization the gel was incubated for 30 min in fixing solution (10% acetic acid, 40% ethanol) following coloration in a freshly prepared staining solution (0.1% Coomassie Brilliant blue G, 45% ethanol, 10% acetic acid) for 20 min. For decoloration the gel was firstly incubated in fixing solution for 30 min, afterwards for 1 h in a decoloration solution (10% acetic acid, 20% ethanol). Finally the gel was washed twice with water.

Biology.

Transcription assays. *T7* RNAP was purchased from Promega (Madison, WI). *E. coli* RNAP holo enzyme was purchased from Epicentre Biotechnologies (Madison, WI). Final concentrations in a total volume of 30 μ L were 5 units of *T7* RNAP or one unit of *E. coli* RNAP (0.5 μ g) that were used along with reaction buffer provided by the manufacturer for *T7* RNAP or for *E. coli* RNAP, with 40 mM Tris-HCl (pH 7.5), 150 mM KCl, 10 mM MgCl₂ and 0.1% CHAPS. Furthermore to all reactions we added 60 nCi of [5,6-³H]-UTP, 400 μ M of ATP, CTP and GTP, 100 μ M of UTP, 20 units of RNase inhibitor (RiboLock, Fermentas) and 10 mM DTT. As a DNA template we used 3.5 mg of the plasmid pcDNA3.1^[1] per reaction. Prior to starting the experiment, the compounds were dissolved in DMSO (final concentration during experiments: 2%). In case of heparin we used a variant with an average mass of 18.0 kDa (range between 8.0 and 25.0 kDa) (AppliChem, Darmstadt, Germany). The components described above (including the inhibitors) were preincubated in absence of NTPs and DNA for 10 min at 25 °C. Transcription reactions were started by the addition of a mixture containing DNA template and NTPs and incubated for 10 min at 37 °C. In the “reversed” transcription assay the order of compound and DNA template addition was reversed. The reactions were stopped by addition of 10% TCA followed by purification and quantification of the transcripts as described previously.^[1] To obtain inhibition values for each sample, their counts were related to DMSO controls. The determination of IC₅₀ values was performed as described earlier.^[1]

In vitro assays with other enzymes. *In vitro* assays with a set of different other enzymes were performed as described in literature (CYP11B1,^[2] CYP11B2,^[3] CYP17,^[4] CYP19,^[5] 17 β -HSD1,^[6] 17 β -HSD2^[6] and PqsD^[7]).

References

- [1] J. Haupenthal, K. Hüsecken, M. Negri, C. K. Maurer, R. W. Hartmann, *Antimicrob. Agents Ch.* **2012**, *56*, 4536–4539.
- [2] U. E. Hille, C. Zimmer, C. A. Vock, R.W. Hartmann, *Med. Chem. Lett.* **2011**, *2*, 2–6.
- [3] S. Lucas, M. Negri, R. Heim, C. Zimmer, R.W. Hartmann, *J. Med. Chem.* **2011**, *54*, 2307–2319.
- [4] Q. Hu, M. Negri, S. Olgen, R. W. Hartmann, *ChemMedChem.* **2010**, *5*, 899–910.
- [5] A. Cavalli, A. Bisi, C. Bertucci, C. Rosini, A. Paluszczak, S. Gobbi, E. Giorgio, A. Rampa, F. Belluti, L. Piazza, P. Valenti, R. W. Hartmann, M. Recanatini, *J. Med. Chem.* **2005**, *48*, 7282–7289.
- [6] E. Bey, S. Marchais-Oberwinkler, M. Negri, P. Kruchten, A. Oster, T. Klein, A. Spadaro, R. Werth, M. Frotscher, B. Birk, R. W. Hartmann, *J. Med. Chem.* **2009**, *52*, 6724–6743.
- [7] M. P. Storz, C. K. Maurer, C. Zimmer, N. Wagner, C. Brengel, J. C. de Jong, S. Lucas, M. Müsken, S. Häussler, A. Steinbach, R. W. Hartmann, *J. Am. Chem. Soc.* **2012**, *134*, 16143–16146.

6.2 Supplemental Information for Paper II

New insights into the bacterial RNA polymerase inhibitor CBR703 as a starting point for optimization as an anti-infective agent

Experimental Section

Chemistry.

Commercial reagents were purchased and used without further purification. If the acyl chloride was not available it was obtained from the carboxylic acid by refluxing in SOCl_2 for 4 h and removal of the volatiles. Proton nuclear magnetic resonance (^1H NMR) and carbon NMR (^{13}C NMR) spectra were recorded on a Bruker Fourier spectrometer (500 or 300 MHz) at ambient temperature with the chemical shifts recorded as δ values in ppm units by reference to the hydrogenated residues of deuterated solvent as internal standard. Coupling constants (J) are given in Hz and signal patterns are indicated as follows: s, singlet; d, doublet; t, triplet; m, multiplet, br, broad signal. The melting points (m.p.) were determined on a Stuart Scientific SMP3 apparatus and are uncorrected. The SpectraSystems-LC-system consisted of a pump, an autosampler, and a UV detector. Mass spectrometry was performed on a MSQ electro spray mass spectrometer (Thermo Fisher, Dreieich, Germany). The system was operated by the standard software Xcalibur. A RP C18 NUCLEODUR 100-5 (125 x 3 mm) column (Macherey-Nagel GmbH, Duehren, Germany) was used as stationary phase. Solvent system: In a gradient run the percentage of acetonitrile (containing 0.1 % trifluoroacetic acid) in 0.1 % trifluoroacetic acid was increased from an initial concentration of 0% at 0 min to 100 % at 15 min and kept at 100 % for 5 min. The injection volume was 10 μL and flow rate was set to 800 $\mu\text{L}/\text{min}$. MS analysis was carried out at a spray voltage of 3800 V, a capillary temperature of 350 $^\circ\text{C}$ and a source CID of 10 V. Spectra were acquired in positive mode from 100 to 1000 m/z and at 254 nm for the UV trace.

General Procedure for the Preparation of compound 1 – 27 (1, 2).

To a stirred solution of the aniline (2.20 mmol) and triethylamine (404mg, 4.00 mmol) in CH_2Cl_2 (4 mL) at 0 $^\circ\text{C}$ (ice bath) was added drop wise a solution of acyl chloride (2.00 mmol) in CH_2Cl_2 (4 mL). The ice bath was removed and the reaction mixture was stirred for 2 h at room temperature. The solution was washed with 1N HCl and the organic layer was concentrated to give the crude product, which was purified by column chromatography (SiO_2 , *n*-hexane/EtOAc) to yield the amides **1a** – **26a**.

The amide (1.00 mmol) and phosphorous pentachloride (260mg, 1.25 mmol) in 1, 2-dichloroethane (6 mL) was heated at 70 $^\circ\text{C}$ for 5 h. After cooling to room temperature, the solvent was evaporated under reduced pressure, toluene (2 mL) was added and the mixture was

concentrated. The residual material was dissolved in acetonitrile (4 mL) and added at 0 °C to a solution of hydroxylamine (**1** – **25**) or O-methylhydroxylamine (**26**) or hydrazine (**27**) prepared by stirring the appropriate hydrochloride salt (2.50 mmol) and triethylamine (5.00 mmol) in acetonitrile (4 mL) at 0 °C for 1 h. After stirring at room temperature for 16 h, the solvent was removed *in vacuo*. The residue was dissolved partitioned between EtOAc and 0.5 N HCl. The organic layer was concentrated and purified by column chromatography (SiO₂, *n*-hexane/EtOAc).

Procedure for the Preparation of compound **6**, **13** (**3**).

A mixture of the nitro compound **1** or **8** (1.00 mmol) and stannous chloride hydrate (1.13 g, 5.00 mmol) in absolute EtOH (4 mL) was stirred at 70 °C under a nitrogen atmosphere. After 30 min the solid material disappeared indicating a complete reaction. The solution was cooled and poured into ice water. The pH was carefully adjusted to pH=7 – 8 by addition of 5% aqueous Na₂CO₃ solution and the mixture was extracted with EtOAc (x mL). The organic layer was washed with saturated brine, dried (MgSO₄) and concentrated under reduced pressure. The crude material was purified by column chromatography (SiO₂, *n*-hexane/EtOAc).

N'-hydroxy-N-phenyl-3-(trifluoromethyl)benzimidamide (CBR703) white solid, m.p. 118 – 120 °C; 73 % yield; Calc. for C₁₄H₁₁F₃N₂O (*MW* = 280.25): C, 60.00; H, 3.96; N, 10.00; found: C, 59.73; H, 3.82; N, 10.39; ¹H NMR (500 MHz, DMSO-*d*₆): δ= 10.78 (br s, 1H), 8.46 (br s, 1H), 7.71 (d, 1H, *J* = 7.6 Hz), 7.66 (s, 1H), 7.62 (d, 1H, *J* = 7.9 Hz), 7.55 (dd, 1H, *J* = 7.9, 7.6 Hz), 7.08 (dd, 2H, *J* = 8.3, 7.5 Hz), 6.82 (t, 1H, *J* = 7.5 Hz), 6.66 (d, 2H, *J* = 8.3 Hz) ppm; ¹³C NMR (125 MHz, DMSO-*d*₆): δ= 147.9, 141.0, 133.9, 131.6, 129.4, 128.9 (q, *J*_{C-F} = 31.2 Hz), 128.4, 125.4 (q, *J*_{C-F} = 3.7 Hz), 123.9 (q, *J*_{C-F} = 272.2 Hz), 123.8 (q, *J*_{C-F} = 3.7 Hz), 121.0, 120.0 ppm; LC/MS: *m/z* (%): [M+H]⁺ 281.01 (100 %), *t*_R = 11.15 min, 99.2 % pure (UV).

N-(4-nitrophenyl)-3-(trifluoromethyl)benzamide (1a) slight yellow solid, m.p. 181 – 183 °C; 65 % yield; ¹H NMR (500 MHz, CDCl₃): δ= 8.29 (d, 2H, *J* = 9.1 Hz), 8.13 (m, 2H), 8.09 (d, 1H, *J* = 7.9 Hz), 7.87 (m, 3H), 7.69 (dd, 1H, *J* = 7.9, 7.9 Hz) ppm; LC/MS: *m/z* (%): [M+MeCN]⁺ 351.67 (100 %), *t*_R = 12.17 min, 98.6 % pure (UV).

N'-hydroxy-N-(4-nitrophenyl)-3-(trifluoromethyl)benzimidamide (1) slight yellow solid, m.p. 195 – 197 °C; 43 % yield; ¹H NMR (500 MHz, DMSO-*d*₆): δ= 11.46 (br s, 1H), 9.42 (br s, 1H), 8.01 (d, 2H, *J* = 9.3 Hz), 7.80 (m, 2H), 7.74 (d, 1H, *J* = 7.6 Hz), 7.64 (dd, 1H, *J* = 7.9, 7.6 Hz), 6.75 (d, 2H, *J* = 9.3 Hz) ppm; ¹³C NMR (125 MHz, DMSO-*d*₆): δ= 148.3, 145.4, 139.4, 133.5, 131.1, 129.9, 129.3 (q, *J*_{C-F} = 32.1 Hz), 126.1 (q, *J*_{C-F} = 3.7 Hz), 124.9, 123.9 (q, *J*_{C-F} = 272.2 Hz), 123.3 (q, *J*_{C-F} = 3.7 Hz), 122.8, 117.0 ppm; LC/MS: *m/z* (%): [M+H]⁺ 325.80 (100 %), *t*_R = 10.96 min, 98.1 % pure (UV).

N-(p-tolyl)-3-(trifluoromethyl)benzamide (2a) white solid, m.p. 128 – 130 °C; 79 % yield; ^1H NMR (500 MHz, DMSO- d_6): δ = 10.39 (br s, 1H), 8.28 (s, 1H), 8.25 (d, 1H, J = 7.9 Hz), 7.95 (d, 1H, J = 8.1 Hz), 7.78 (dd, 1H, J = 8.1, 7.9 Hz), 7.65 (d, 2H, J = 8.5 Hz), 7.18 (d, 2H, J = 8.5 Hz), 2.29 (s, 3H) ppm; LC/MS: m/z (%): $[\text{M}+\text{MeCN}]^+$ 351.67 (100 %), t_R = 12.17 min, 98.6 % pure (UV).

N'-hydroxy-N-(p-tolyl)-3-(trifluoromethyl)benzimidamide (2) white solid, m.p. 170 – 172 °C; 48 % yield; ^1H NMR (500 MHz, DMSO- d_6): δ = 10.68 (br s, 1H), 8.31 (s, 1H), 7.69 (d, 1H, J = 7.6 Hz), 7.66 (s, 1H), 7.57 (d, 1H, J = 7.9 Hz), 7.53 (dd, 1H, J = 7.9, 7.6 Hz), 6.89 (d, 2H, J = 8.2 Hz), 6.56 (d, 2H, J = 8.2 Hz), 2.14 (s, 3H) ppm; ^{13}C NMR (125 MHz, DMSO- d_6): δ = 148.3, 138.4, 134.0, 131.6, 130.1, 129.3, 128.9, 128.8 (q, $J_{\text{C-F}}$ = 32.1 Hz), 125.3 (q, $J_{\text{C-F}}$ = 3.7 Hz), 123.9 (q, $J_{\text{C-F}}$ = 272.2 Hz), 123.8 (q, $J_{\text{C-F}}$ = 3.7 Hz), 120.5, 20.1 ppm; LC/MS: m/z (%): $[\text{M}+\text{H}]^+$ 294.88 (100 %), t_R = 11.82 min, 100 % pure (UV).

3-(trifluoromethyl)-N-(4-(trifluoromethyl)phenyl)benzamide (3a) white solid, m.p. 145 – 147 °C; 81 % yield; ^1H NMR (500 MHz, DMSO- d_6): δ = 10.78 (br s, 1H), 8.31 (s, 1H), 8.28 (d, 1H, J = 7.9 Hz), 8.00 (m, 3H), 7.81 (dd, 1H, J = 8.1, 7.9 Hz), 7.75 (d, 2H, J = 8.5 Hz) ppm; LC/MS: m/z (%): $[\text{M}+\text{MeCN}]^+$ 374.63 (100 %), t_R = 13.61 min, 99.3 % pure (UV).

N'-hydroxy-3-(trifluoromethyl)-N-(4-(trifluoromethyl)phenyl)benzimidamide (3) white solid, m.p. 173 – 175 °C; 56 % yield; ^1H NMR (500 MHz, DMSO- d_6): δ = 11.15 (br s, 1H), 8.97 (br s, 1H), 7.76 (d, 1H, J = 7.6 Hz), 7.74 (s, 1H), 7.68 (d, 1H, J = 7.9 Hz), 7.60 (dd, 1H, J = 7.9, 7.6 Hz), 7.43 (d, 2H, J = 8.5 Hz), 6.77 (d, 2H, J = 8.5 Hz) ppm; ^{13}C NMR (125 MHz, DMSO- d_6): δ = 146.5, 145.0, 133.6, 131.3, 129.7, 129.2 (q, $J_{\text{C-F}}$ = 32.1 Hz), 125.8 (q, $J_{\text{C-F}}$ = 2.8 Hz), 125.6 (q, $J_{\text{C-F}}$ = 3.7 Hz), 123.9 (q, $J_{\text{C-F}}$ = 272.2 Hz), 123.6 (q, $J_{\text{C-F}}$ = 3.7 Hz), 120.2 (q, $J_{\text{C-F}}$ = 32.1 Hz), 118.4 ppm; LC/MS: m/z (%): $[\text{M}+\text{H}]^+$ 348.69 (100 %), t_R = 12.56 min, 94.9 % pure (UV).

N-(4-cyanophenyl)-3-(trifluoromethyl)benzamide (4a) white solid, m.p. 182 – 184 °C; 70 % yield; ^1H NMR (500 MHz, DMSO- d_6): δ = 10.83 (br s, 1H), 8.29 (s, 1H), 8.26 (d, 1H, J = 7.9 Hz), 7.95 (m, 3H), 7.84 (d, 2H, J = 8.8 Hz), 7.80 (dd, 1H, J = 8.1, 7.9 Hz) ppm; LC/MS: m/z (%): $[\text{M}+\text{MeCN}]^+$ 331.74 (100 %), t_R = 12.11 min, 95.4 % pure (UV).

N-(4-cyanophenyl)-N'-hydroxy-3-(trifluoromethyl)benzimidamide (4) white solid, m.p. 165 – 167 °C; 40 % yield; ^1H NMR (500 MHz, DMSO- d_6): δ = 11.29 (br s, 1H), 9.14 (br s, 1H), 7.78 (d, 1H, J = 7.6 Hz), 7.76 (s, 1H), 7.69 (d, 1H, J = 7.9 Hz), 7.62 (dd, 1H, J = 7.9, 7.6 Hz), 7.53 (d, 2H, J = 9.0 Hz), 6.73 (d, 2H, J = 9.0 Hz) ppm; ^{13}C NMR (125 MHz, DMSO- d_6): δ = 145.9, 145.8, 133.5, 132.8, 131.2, 129.8, 129.6, 129.3 (q, $J_{\text{C-F}}$ = 32.1 Hz), 126.0 (q, $J_{\text{C-F}}$ = 3.7 Hz), 123.9 (q, $J_{\text{C-F}}$ = 272.2 Hz), 123.5 (q, $J_{\text{C-F}}$ = 4.6 Hz), 119.5, 118.2, 101.2 ppm; LC/MS: m/z (%): $[\text{M}+\text{H}]^+$ 305.88 (100 %), t_R = 10.48 min, 96.8 % pure (UV).

N-(4-methoxyphenyl)-3-(trifluoromethyl)benzamide (5a) white solid, m.p. 129 – 131 °C; 79 % yield; ^1H NMR (500 MHz, DMSO- d_6): δ = 10.34 (br s, 1H), 8.26 (m, 2H), 7.95 (d, 1H, J = 7.8 Hz), 7.77 (dd, 1H, J = 7.8, 7.6 Hz), 7.67 (d, 2H, J = 9.0 Hz), 6.94 (d, 2H, J = 9.0 Hz), 3.75 (s, 3H) ppm; LC/MS: m/z (%): $[\text{M}+\text{H}]^+$ 295.87 (100 %), t_R = 11.83 min, 100 % pure (UV).

N'-hydroxy-N-(4-methoxyphenyl)-3-(trifluoromethyl)benzimidamide (5) white solid, m.p. 140 – 142 °C; 53 % yield; ^1H NMR (500 MHz, DMSO- d_6): δ = 10.56 (br s, 1H), 8.20 (br s, 1H), 7.67 (d, 1H, J = 7.6 Hz), 7.64 (s, 1H), 7.56 (d, 1H, J = 7.9 Hz), 7.52 (dd, 1H, J = 7.9, 7.6 Hz), 7.69 (d, 2H, J = 8.8 Hz), 6.63 (d, 2H, J = 8.8 Hz), 3.63 (s, 3H) ppm; ^{13}C NMR (125 MHz, DMSO- d_6): δ = 154.4, 148.8, 133.9, 131.8, 129.2, 128.8 (q, $J_{\text{C-F}}$ = 32.1 Hz), 125.2 (q, $J_{\text{C-F}}$ = 3.7 Hz), 124.1 (q, $J_{\text{C-F}}$ = 3.7 Hz), 123.9 (q, $J_{\text{C-F}}$ = 272.2 Hz), 122.7, 113.8, 55.1 ppm; LC/MS: m/z (%): $[\text{M}+\text{H}]^+$ 310.88 (100 %), t_R = 10.93 min, 95.5 % pure (UV).

N-(4-aminophenyl)-N'-hydroxy-3-(trifluoromethyl)benzimidamide (6) white solid, m.p. 131 – 133 °C; 33 % yield; ^1H NMR (500 MHz, DMSO- d_6): δ = 10.83 (br s, 1H), 9.12 (br s, 1H), 7.71 (d, 1H, J = 7.6 Hz), 7.68 (s, 1H), 7.60 (d, 1H, J = 7.9 Hz), 7.57 (dd, 1H, J = 7.9, 7.6 Hz), 6.93 (d, 2H, J = 8.2 Hz), 6.61 (d, 2H, J = 8.2 Hz), 4.87 (s, 2H) ppm; ^{13}C NMR (125 MHz, DMSO- d_6): δ = 148.3, 138.7, 134.0, 131.5, 130.0, 129.2, 128.9 (q, $J_{\text{C-F}}$ = 32.1 Hz), 128.8, 125.3 (q, $J_{\text{C-F}}$ = 3.7 Hz), 124.0 (q, $J_{\text{C-F}}$ = 3.7 Hz), 123.9 (q, $J_{\text{C-F}}$ = 272.2 Hz), 121.0 ppm; LC/MS: m/z (%): $[\text{M}+\text{H}]^+$ 295.89 (100 %), t_R = 8.98 min, 96.8 % pure (UV).

N-(4-chlorophenyl)-3-(trifluoromethyl)benzamide (7a) white solid, m.p. 136 – 138 °C; 85 % yield; ^1H NMR (500 MHz, DMSO- d_6): δ = 10.58 (br s, 1H), 8.28 (s, 1H), 8.26 (d, 1H, J = 7.6 Hz), 7.97 (d, 1H, J = 7.9 Hz), 7.77 (m, 3H), 7.44 (d, 2H, J = 9.1 Hz) ppm; LC/MS: m/z (%): $[\text{M}+\text{MeCN}]^+$ 340.55 (100 %), t_R = 12.74 min, 99.5 % pure (UV).

N-(4-chlorophenyl)-N'-hydroxy-3-(trifluoromethyl)benzimidamide (7) white solid, m.p. 173 – 175 °C; 50 % yield; ^1H NMR (500 MHz, DMSO- d_6): δ = 10.90 (br s, 1H), 8.64 (br s, 1H), 7.73 (d, 1H, J = 7.6 Hz), 7.69 (s, 1H), 7.62 (d, 1H, J = 7.9 Hz), 7.57 (dd, 1H, J = 7.9, 7.6 Hz), 7.13 (d, 2H, J = 9.0 Hz), 6.65 (d, 2H, J = 9.0 Hz) ppm; ^{13}C NMR (125 MHz, DMSO- d_6): δ = 147.4, 140.1, 133.6, 131.5, 129.5, 129.1 (q, $J_{\text{C-F}}$ = 32.1 Hz), 128.2, 125.6 (q, $J_{\text{C-F}}$ = 3.7 Hz), 124.6, 123.9 (q, $J_{\text{C-F}}$ = 272.2 Hz), 123.8 (q, $J_{\text{C-F}}$ = 3.7 Hz), 121.2 ppm; LC/MS: m/z (%): $[\text{M}+\text{H}]^+$ 314.80 (100 %), t_R = 11.81 min, 99.2 % pure (UV).

N-(3-nitrophenyl)-3-(trifluoromethyl)benzamide (8a) slight yellow solid, m.p. 160 – 162 °C; 69 % yield; ^1H NMR (500 MHz, DMSO- d_6): δ = 10.39 (br s, 1H), 8.78 (dd, 1H, J = 2.2, 2.2 Hz), 8.34 (s, 1H), 8.30 (d, 1H, J = 7.9 Hz), 8.21 (m, 1H), 8.00 (m, 2H), 7.82 (dd, 1H, J = 8.2, 8.2 Hz), 7.69 (dd, 1H, J = 7.9, 7.6 Hz) ppm; LC/MS: m/z (%): $[\text{M}+\text{MeCN}]^+$ 351.55 (100 %), t_R = 12.64 min, 99.2 % pure (UV).

N'-hydroxy-N-(3-nitrophenyl)-3-(trifluoromethyl)benzimidamide (8) slight yellow solid, m.p. 163.0 – 164.4 °C; 40 % yield; ¹H NMR (500 MHz, DMSO-d₆): δ= 11.17 (br s, 1H), 9.08 (br s, 1H), 7.77 (m, 2H), 7.72 (d, 1H, *J* = 7.6 Hz), 7.61 (m, 2H), 7.52 (dd, 1H, *J* = 2.5, 2.2 Hz), 7.36 (dd, 1H, *J* = 8.2, 8.2 Hz), 6.98 (m, 1H) ppm; ¹³C NMR (125 MHz, DMSO-d₆): δ= 147.9, 146.2, 142.6, 133.5, 131.4, 129.8, 129.5, 129.3 (q, *J*_{C-F} = 32.1 Hz), 125.9 (q, *J*_{C-F} = 3.7 Hz), 124.7, 123.9 (q, *J*_{C-F} = 272.2 Hz), 123.7 (q, *J*_{C-F} = 3.7 Hz), 114.6, 112.7 ppm; LC/MS: *m/z* (%): [M+H]⁺ 325.81 (100 %), *t*_R = 11.30 min, 100 % pure (UV).

N-(m-tolyl)-3-(trifluoromethyl)benzamide (9a) white solid, m.p. 116 – 118 °C; 77 % yield; ¹H NMR (500 MHz, DMSO-d₆): δ= 10.38 (br s, 1H), 8.29 (s, 1H), 8.25 (d, 1H, *J* = 7.9 Hz), 7.96 (d, 1H, *J* = 7.8 Hz), 7.78 (dd, 1H, *J* = 7.9, 7.8 Hz), 7.61 (s, 1H), 7.57 (d, 1H, *J* = 8.0 Hz), 7.25 (dd, 1H, *J* = 8.0, 7.5 Hz), 6.95 (d, 1H, *J* = 7.5 Hz), 2.32 (s, 3H) ppm; LC/MS: *m/z* (%): [M+H]⁺ 279.90 (100 %), *t*_R = 12.74 min, 100 % pure (UV).

N'-hydroxy-N-(m-tolyl)-3-(trifluoromethyl)benzimidamide (9) white solid, m.p. 95 – 97 °C; 44 % yield; ¹H NMR (500 MHz, DMSO-d₆): δ= 10.77 (br s, 1H), 8.36 (br s, 1H), 7.71 (d, 1H, *J* = 8.0 Hz), 7.66 (s, 1H), 7.61 (d, 1H, *J* = 7.6 Hz), 7.55 (dd, 1H, *J* = 8.0, 7.6 Hz), 6.93 (dd, 1H, *J* = 7.9, 7.6 Hz), 6.83 (d, 1H, *J* = 7.6 Hz), 6.57 (s, 1H), 6.35 (m, 1H), 2.11 (s, 3H) ppm; ¹³C NMR (125 MHz, DMSO-d₆): δ= 148.0, 140.9, 137.6, 134.0, 131.5, 129.4, 128.9 (q, *J*_{C-F} = 32.1 Hz), 128.2, 125.4 (q, *J*_{C-F} = 3.7 Hz), 123.9 (q, *J*_{C-F} = 272.2 Hz), 123.8 (q, *J*_{C-F} = 4.6 Hz), 121.8, 120.6, 117.2, 21.0 ppm; LC/MS: *m/z* (%): [M+H]⁺ 294.89 (100 %), *t*_R = 11.93 min, 96.7 % pure (UV).

3-(trifluoromethyl)-N-(3-(trifluoromethyl)phenyl)benzamide (10a) white solid, m.p. 126 – 128 °C; 83 % yield; ¹H NMR (500 MHz, CDCl₃): δ= 8.13 (s, 1H), 8.07 (d, 1H, *J* = 7.9 Hz), 8.00 (br s, 1H), 7.94 (s, 1H), 7.88 (d, 1H, *J* = 8.0 Hz), 7.83 (d, 1H, *J* = 7.9 Hz), 7.65 (dd, 1H, *J* = 7.9, 7.9 Hz), 7.51 (dd, 1H, *J* = 8.0, 7.8 Hz), 7.44 (d, 1H, *J* = 7.8 Hz) ppm; LC/MS: *m/z* (%): [M+ MeCN]⁺ 374.63 (100 %), *t*_R = 12.98 min, 99.1 % pure (UV).

N'-hydroxy-3-(trifluoromethyl)-N-(3-(trifluoromethyl)phenyl)benzimidamide (10) white solid, m.p. 104 – 106 °C; 55 % yield; ¹H NMR (500 MHz, CDCl₃): δ= 8.59 (br s, 1H), 7.75 (s, 1H), 7.66 (d, 1H, *J* = 7.8 Hz), 7.57 (d, 1H, *J* = 7.9 Hz), 7.45 (dd, 1H, *J* = 7.9, 7.8 Hz), 7.38 (br s, 1H), 7.21 (m, 2H), 6.91 (s, 1H), 6.77 (d, 1H, *J* = 7.6 Hz) ppm; ¹³C NMR (125 MHz, CDCl₃): δ= 150.2, 139.7, 131.5, 131.4 (q, *J*_{C-F} = 33.0 Hz), 131.2 (q, *J*_{C-F} = 33.0 Hz), 129.5, 129.2, 126.7 (q, *J*_{C-F} = 3.7 Hz), 125.1 (q, *J*_{C-F} = 3.7 Hz), 124.0, 123.6 (q, *J*_{C-F} = 272.2 Hz), 123.5 (q, *J*_{C-F} = 272.2 Hz), 119.6 (q, *J*_{C-F} = 3.7 Hz), 117.6 (q, *J*_{C-F} = 3.7 Hz) ppm; LC/MS: *m/z* (%): [M+H]⁺ 348.70 (100 %), *t*_R = 12.11 min, 100 % pure (UV).

N-(3-cyanophenyl)-3-(trifluoromethyl)benzamide (11a) white solid, m.p. 142 – 144 °C; 80 % yield; ¹H NMR (500 MHz, DMSO-d₆): δ= 10.75 (br s, 1H), 8.30 (s, 1H), 8.27 (d, 1H, *J* = 7.9 Hz),

8.24 (s, 1H), 8.05 (m, 1H), 8.00 (d, 1H, $J = 7.6$ Hz), 7.81 (dd, 1H, $J = 7.9, 7.6$ Hz), 7.60 (m, 2H) ppm; LC/MS: m/z (%): $[M + \text{MeCN}]^+$ 331.92 (100 %), $t_R = 12.10$ min, 98.2 % pure (UV).

N-(3-cyanophenyl)-N'-hydroxy-3-(trifluoromethyl)benzimidamide (11) white solid, m.p. 152 – 154 °C; 45 % yield; ^1H NMR (500 MHz, DMSO- d_6): $\delta = 11.08$ (br s, 1H), 8.90 (br s, 1H), 7.76 (d, 1H, $J = 7.9$ Hz), 7.73 (s, 1H), 7.67 (d, 1H, $J = 7.6$ Hz), 7.60 (dd, 1H, $J = 7.9, 7.6$ Hz), 7.28 (dd, 1H, $J = 8.2, 7.6$ Hz), 7.23 (d, 1H, $J = 7.6$ Hz), 7.05 (s, 1H), 6.88 (d, 1H, $J = 8.2$ Hz) ppm; ^{13}C NMR (125 MHz, DMSO- d_6): $\delta = 146.5, 142.1, 133.4, 131.5, 129.7, 129.6, 129.2$ (q, $J_{\text{C-F}} = 31.2$ Hz), 125.8 (q, $J_{\text{C-F}} = 3.7$ Hz), 123.9 (q, $J_{\text{C-F}} = 272.2$ Hz), 123.8 (q, $J_{\text{C-F}} = 3.7$ Hz), 123.8, 123.7, 121.8, 118.8, 111.1 ppm; LC/MS: m/z (%): $[M + \text{MeCN}]^+$ 346.77 (100 %), $t_R = 10.27$ min, 97.7 % pure (UV).

N-(3-methoxyphenyl)-3-(trifluoromethyl)benzamide (12a) white solid, m.p. 121 – 123 °C; 74 % yield; ^1H NMR (500 MHz, DMSO- d_6): $\delta = 10.43$ (br s, 1H), 8.28 (s, 1H), 8.25 (d, 1H, $J = 8.2$ Hz), 7.96 (d, 1H, $J = 8.2$ Hz), 7.79 (dd, 1H, $J = 8.2, 8.2$ Hz), 7.46 (dd, 1H, $J = 2.4, 2.2$ Hz), 7.37 (d, 1H, $J = 7.9$ Hz), 7.28 (dd, 1H, $J = 8.2, 7.9$ Hz), 6.72 (dd, 1H, $J = 8.2, 2.4$ Hz), 3.76 (s, 3H) ppm; LC/MS: m/z (%): $[M + \text{H}]^+$ 295.84 (100 %), $t_R = 12.32$ min, 96.5 % pure (UV).

N'-hydroxy-N-(3-methoxyphenyl)-3-(trifluoromethyl)benzimidamide (12) white solid, m.p. 109 – 111 °C; 48 % yield; ^1H NMR (500 MHz, DMSO- d_6): $\delta = 10.81$ (br s, 1H), 8.44 (br s, 1H), 7.72 (d, 1H, $J = 8.2, 7.8$ Hz), 8.68 (s, 1H), 7.62 (d, 1H, $J = 7.9$ Hz), 7.56 (dd, 1H, $J = 7.9, 7.9$ Hz), 6.96 (dd, 1H, $J = 3.0$ Hz), 6.38 (dd, 1H, $J = 8.2, 2.3$ Hz), 6.26 (dd, 1H, $J = 2.3, 2.0$ Hz), 6.18 (dd, 1H, $J = 7.9, 2.0$ Hz), 3.55 (s, 3H) ppm; ^{13}C NMR (125 MHz, DMSO- d_6): $\delta = 159.4, 147.9, 142.2, 134.0, 131.6, 129.4, 129.1, 129.0$ (q, $J_{\text{C-F}} = 32.1$ Hz), 125.4 (q, $J_{\text{C-F}} = 3.7$ Hz), 123.9 (q, $J_{\text{C-F}} = 272.2$ Hz), 123.8 (q, $J_{\text{C-F}} = 3.7$ Hz), 112.2, 106.5, 105.7, 54.6 ppm; LC/MS: m/z (%): $[M + \text{H}]^+$ 310.84 (100 %), $t_R = 11.27$ min, 97.4 % pure (UV).

N-(3-aminophenyl)-N'-hydroxy-3-(trifluoromethyl)benzimidamide (13) white solid, m.p. 130 – 132 °C; 40 % yield; ^1H NMR (500 MHz, DMSO- d_6): $\delta = 10.66$ (br s, 1H), 8.01 (br s, 1H), 7.69 (d, 1H, $J = 7.9$ Hz), 7.67 (s, 1H), 7.61 (d, 1H, $J = 7.6$ Hz), 7.54 (dd, 1H, $J = 7.9, 7.6$ Hz), 6.69 (dd, 1H, $J = 8.2, 7.9$ Hz), 6.06 (m, 1H), 6.00 (dd, 1H, $J = 2.2, 1.9$ Hz), 5.75 (dd, 1H, $J = 7.9, 2.2$ Hz), 4.88 (s, 2H) ppm; ^{13}C NMR (125 MHz, DMSO- d_6): $\delta = 148.9, 148.5, 141.6, 134.2, 131.4, 129.2, 128.8$ (q, $J_{\text{C-F}} = 32.1$ Hz), 128.7, 125.3 (q, $J_{\text{C-F}} = 3.7$ Hz), 123.9 (q, $J_{\text{C-F}} = 272.2$ Hz), 123.6 (q, $J_{\text{C-F}} = 4.6$ Hz), 108.8, 107.9, 106.1 ppm; LC/MS: m/z (%): $[M + \text{H}]^+$ 295.88 (100 %), $t_R = 9.46$ min, 100 % pure (UV).

N-phenyl-2-(trifluoromethyl)benzamide (14a) white solid, m.p. 152 – 154 °C; 55 % yield; ^1H NMR (500 MHz, DMSO- d_6): $\delta = 10.54$ (br s, 1H), 7.85 (d, 1H, $J = 7.9$ Hz), 7.79 (dd, 1H, $J = 7.9, 7.6$ Hz), 7.70 (m, 4H), 7.35 (dd, 2H, $J = 8.5, 7.6$ Hz), 7.11 (t, 1H, $J = 7.6$ Hz) ppm; LC/MS: m/z (%): $[M + \text{H}]^+$ 265.98 (100 %), $t_R = 10.95$ min, 99.4 % pure (UV).

N'-hydroxy-N-phenyl-2-(trifluoromethyl)benzimidamide (14) white solid, m.p. 140 – 142 °C; 49 % yield; ¹H NMR (500 MHz, DMSO-d₆): δ= 10.52 (br s, 1H), 8.49 (br s, 1H), 7.78 (m, 1H), 7.60 (m, 2H), 7.40 (m, 1H), 7.00 (dd, 2H, *J* = 7.6, 7.2 Hz), 6.76 (t, 1H, *J* = 7.2 Hz), 6.59 (d, 2H, *J* = 7.6 Hz) ppm; ¹³C NMR (125 MHz, DMSO-d₆): δ= 147.0, 140.2, 132.2, 131.8, 131.5, 129.6, 128.4, 128.3, 128.1 (q, *J*_{C-F} = 30.2 Hz), 126.7 (q, *J*_{C-F} = 4.6 Hz), 123.8 (q, *J*_{C-F} = 274.0 Hz), 121.3, 119.7 ppm; LC/MS: *m/z* (%): [M+H]⁺ 280.98 (100 %), *t*_R= 10.30 min, 97.2 % pure (UV).

N-phenyl-4-(trifluoromethyl)benzamide (15a) white solid, m.p. 210.0 – 211.7 °C; 68 % yield; ¹H NMR (500 MHz, DMSO-d₆): δ= 10.47 (br s, 1H), 8.15 (d, 2H, *J* = 8.4 Hz), 7.91 (d, 2H, *J* = 8.4 Hz), 7.78 (d, 2H, *J* = 8.0 Hz), 7.37 (dd, 2H, *J* = 8.0, 7.4 Hz), 7.13 (t, 1H, *J* = 7.4 Hz) ppm; LC/MS: *m/z* (%): [M+H]⁺ 265.89 (100 %), *t*_R= 12.07 min, 97.4 % pure (UV).

N'-hydroxy-N-phenyl-4-(trifluoromethyl)benzimidamide (15) white solid, m.p. 133 – 136 °C; 44 % yield; ¹H NMR (500 MHz, DMSO-d₆): δ= 10.85 (br s, 1H), 8.45 (br s, 1H), 7.69 (d, 2H, *J* = 8.0 Hz), 7.57 (d, 2H, *J* = 8.0 Hz), 7.08 (dd, 2H, *J* = 7.6, 7.5 Hz), 6.80 (t, 1H, *J* = 7.5 Hz), 6.65 (d, 2H, *J* = 7.6 Hz) ppm; ¹³C NMR (125 MHz, DMSO-d₆): δ= 148.1, 141.0, 137.0, 129.0 (q, *J*_{C-F} = 31.2 Hz), 128.5, 128.3, 125.2 (q, *J*_{C-F} = 3.7 Hz), 124.0 (q, *J*_{C-F} = 272.2 Hz), 120.9, 119.9 ppm; LC/MS: *m/z* (%): [M+H]⁺ 280.96 (100 %), *t*_R= 11.39 min, 93.6 % pure (UV).

3-cyano-N-phenylbenzamide (16a) white solid, m.p. 175 – 177 °C; 82 % yield; ¹H NMR (500 MHz, DMSO-d₆): δ= 10.41 (br s, 1H), 8.40 (dd, 1H, *J* = 1.6, 1.3 Hz), 8.25 (m, 1H), 8.06 (ddd, 1H, *J* = 7.9, 1.6, 1.3 Hz), 7.76 (m, 3H), 7.38 (dd, 2H, *J* = 8.5, 7.6 Hz), 7.13 (t, 1H, *J* = 7.6 Hz) ppm; LC/MS: *m/z* (%): [M+H]⁺ 223.17 (100 %), *t*_R= 10.14 min, 98.5 % pure (UV).

3-cyano-N'-hydroxy-N-phenylbenzimidamide (16) white solid, m.p. 145 – 147 °C; 43 % yield; ¹H NMR (500 MHz, DMSO-d₆): δ= 10.82 (br s, 1H), 8.47 (br s, 1H), 7.81 (ddd, 1H, *J* = 7.6, 1.6, 1.3 Hz), 7.76 (dd, 1H, *J* = 1.6, 1.6 Hz), 7.63 (dt, 1H, *J* = 8.2, 1.6, 1.3 Hz), 7.52 (dd, 1H, *J* = 8.2, 7.6 Hz), 7.09 (dd, 2H, *J* = 8.5, 7.2 Hz), 6.82 (t, 1H, *J* = 7.2 Hz), 6.65 (d, 2H, *J* = 8.5 Hz) ppm; ¹³C NMR (125 MHz, DMSO-d₆): δ= 147.6, 140.9, 134.2, 132.5, 132.3, 131.0, 129.5, 128.4, 121.1, 120.1, 118.4, 111.4 ppm; LC/MS: *m/z* (%): [M+H]⁺ 238.12 (100 %), *t*_R= 9.27 min, 95.2 % pure (UV).

3-chloro-N-phenylbenzamide (17a) white solid, m.p. 142 – 144 °C; 89 % yield; ¹H NMR (500 MHz, DMSO-d₆): δ= 10.34 (br s, 1H), 8.00 (dd, 1H, *J* = 1.9, 1.6 Hz), 7.91 (m, 1H), 7.76 (d, 2H, *J* = 8.0 Hz), 7.66 (m, 1H), 7.57 (dd, 1H, *J* = 7.9, 7.6 Hz), 7.36 (dd, 2H, *J* = 8.0, 7.6 Hz), 7.12 (t, 1H, *J* = 7.6 Hz) ppm; LC/MS: *m/z* (%): [M+H]⁺ 232.06 (100 %), *t*_R= 11.61 min, 99.4 % pure (UV).

3-chloro-N'-hydroxy-N-phenylbenzimidamide (17) white solid, m.p. 102 – 104 °C; 55 % yield; ¹H NMR (500 MHz, DMSO-d₆): δ= 10.72 (br s, 1H), 8.37 (br s, 1H), 7.41 (m, 1H), 7.39 (dd, 1H, *J* = 1.6, 1.6 Hz), 7.34 (dd, 1H, *J* = 7.9, 7.6 Hz), 7.28 (ddd, 1H, *J* = 7.9, 1.6, 1.3 Hz), 7.08 (dd, 2H, *J* = 8.0, 7.6 Hz), 6.80 (t, 1H, *J* = 7.6 Hz), 6.66 (d, 2H, *J* = 8.0 Hz) ppm; ¹³C NMR (125 MHz, DMSO-d₆):

δ = 148.0, 141.1, 135.0, 132.8, 130.1, 128.8, 128.4, 127.2, 126.3, 120.9, 119.8 ppm; LC/MS: m/z (%): $[M+H]^+$ 246.95 (100 %), t_R = 10.73 min, 98.7 % pure (UV).

4-nitro-N-phenyl-3-(trifluoromethyl)benzamide (18a) white solid, m.p. 185 – 187 °C; 51 % yield; 1H NMR (500 MHz, DMSO- d_6): δ = 10.68 (br s, 1H), 8.50 (s, 1H), 8.46 (d, 1H, J = 8.3 Hz), 8.34 (d, 1H, J = 8.3 Hz), 7.76 (d, 2H, J = 8.0 Hz), 7.40 (dd, 2H, J = 8.5, 7.6 Hz), 7.17 (t, 1H, J = 7.3 Hz) ppm; LC/MS: m/z (%): $[M+ MeCN]^+$ 351.41(100 %), t_R = 11.73 min, 100 % pure (UV).

N'-hydroxy-4-nitro-N-phenyl-3-(trifluoromethyl)benzimidamide (18) white solid, m.p. 167 – 169 °C; 47 % yield; 1H NMR (500 MHz, DMSO- d_6): δ = 11.19 (br s, 1H), 8.66 (br s, 1H), 8.10 (d, 1H, J = 8.5 Hz), 7.91 (d, 1H, J = 1.9 Hz), 7.81 (dd, 1H, J = 8.5, 1.9 Hz), 7.13 (dd, 2H, J = 8.0, 7.6 Hz), 6.86 (t, 1H, J = 7.6 Hz), 6.70 (d, 2H, J = 8.0 Hz) ppm; ^{13}C NMR (125 MHz, DMSO- d_6): δ = 146.7, 140.6, 137.8, 132.8, 128.6, 126.5 (q, J_{C-F} = 5.5 Hz), 125.8, 124.0 (q, J_{C-F} = 273.1 Hz), 121.5, 121.4 (q, J_{C-F} = 33.0 Hz), 120.3 ppm; LC/MS: m/z (%): $[M+H]^+$ 325.76 (100 %), t_R = 11.09 min, 98.5 % pure (UV).

4- fluoro -N-phenyl-3-(trifluoromethyl)benzamide (19a) white solid, m.p. 167 – 169 °C; 58 % yield; 1H NMR (500 MHz, DMSO- d_6): δ = 10.46 (br s, 1H), 8.35 (m, 2H), 7.75 (d, 2H, J = 8.0 Hz), 7.71 (dd, 1H, J = 10.4, 8.8 Hz), 7.38 (dd, 2H, J = 8.0, 7.6 Hz), 7.14 (t, 1H, J = 7.6 Hz) ppm; LC/MS: m/z (%): $[M+H]^+$ 283.78 (100 %), t_R = 11.84 min, 100 % pure (UV).

4-fluoro-N'-hydroxy-N-phenyl-3-(trifluoromethyl)benzimidamide (19) white solid, m.p. 136 – 138 °C; 49 % yield; 1H NMR (500 MHz, DMSO- d_6): δ = 10.81 (br s, 1H), 8.52 (br s, 1H), 7.69 (dd, 1H, J = 6.9, 1.9 Hz), 7.65 (m, 1H), 7.47 (dd, 1H, J = 10.4, 9.1 Hz), 7.10 (dd, 2H, J = 8.0, 7.6 Hz), 6.83 (t, 1H, J = 7.6 Hz), 6.67 (d, 2H, J = 8.0 Hz) ppm; ^{13}C NMR (125 MHz, DMSO- d_6): δ = 158.8 (dq, J_{C-F} = 255.7, 1.8 Hz), 147.2, 140.8, 134.3 (d, J_{C-F} = 9.2 Hz), 129.8 (d, J_{C-F} = 3.7 Hz), 128.5, 126.1 (q, J_{C-F} = 4.6 Hz), 122.3 (q, J_{C-F} = 272.2 Hz), 121.2, 120.2, 117.2 (dq, J_{C-F} = 20.6, 12.8 Hz) ppm; LC/MS: m/z (%): $[M+H]^+$ 298.83 (100 %), t_R = 11.13 min, 98.5 % pure (UV).

3-chloro-4-fluoro-N-phenylbenzamide (20a) white solid, m.p. 157 – 159 °C; 71 % yield; 1H NMR (500 MHz, DMSO- d_6): δ = 10.34 (br s, 1H), 8.20 (dd, 1H, J = 8.0, 2.2 Hz), 8.00 (m, 1H), 7.75 (d, 2H, J = 8.2 Hz), 7.59 (dd, 1H, J = 8.8, 8.0 Hz), 7.36 (dd, 2H, J = 8.2, 7.6 Hz), 7.12 (t, 1H, J = 7.6 Hz) ppm; LC/MS: m/z (%): $[M+H]^+$ 249.86 (100 %), t_R = 11.33 min, 99.2 % pure (UV).

3-chloro-4-fluoro-N'-hydroxy-N-phenylbenzimidamide (20) white solid, m.p. 138 – 140 °C; 47 % yield; 1H NMR (500 MHz, DMSO- d_6): δ = 10.74 (br s, 1H), 8.43 (br s, 1H), 7.69 (dd, 1H, J = 7.1, 2.0 Hz), 7.65 (m, 1H), 7.47 (dd, 1H, J = 9.1, 8.8 Hz), 7.10 (dd, 2H, J = 8.0, 7.6 Hz), 6.83 (t, 1H, J = 7.6 Hz), 6.67 (d, 2H, J = 8.0 Hz) ppm; ^{13}C NMR (125 MHz, DMSO- d_6): δ = 157.3 (d, J_{C-F} = 248.4 Hz), 147.3, 141.0, 130.7 (d, J_{C-F} = 3.7 Hz), 129.5, 128.5, 128.4, 121.0, 120.0, 119.4 (d, J_{C-F} = 18.3

Hz), 116.8 (d, $J_{\text{C-F}} = 22.0$ Hz) ppm; LC/MS: m/z (%): $[\text{M}+\text{H}]^+$ 264.80 (100 %), $t_{\text{R}} = 10.70$ min, 97.2 % pure (UV).

4-(trifluoromethyl)-N-(3-(trifluoromethyl)phenyl)benzamide (21a) white solid, m.p. 117 – 119 °C; 77 % yield; ^1H NMR (500 MHz, CDCl_3): $\delta = 7.99$ (d, 2H, $J = 8.0$ Hz), 7.94 (s, 1H), 7.86 (d, 1H, $J = 8.0$ Hz), 7.77 (d, 2H, $J = 8.0$ Hz), 7.51 (dd, 1H, $J = 8.2, 8.0$ Hz), 7.44 (d, 1H, $J = 8.2$ Hz) ppm; LC/MS: m/z (%): $[\text{M}+\text{MeCN}]^+$ 374.65 (100 %), $t_{\text{R}} = 13.04$ min, 99.4 % pure (UV).

N'-hydroxy-4-(trifluoromethyl)-N-(3-(trifluoromethyl)phenyl)benzimidamide (21) white solid, m.p. 147 – 149 °C; 53 % yield; ^1H NMR (500 MHz, CDCl_3): $\delta = 8.82$ (br s, 1H), 7.60 (d, 2H, $J = 8.2$ Hz), 7.55 (d, 1H, $J = 8.2$ Hz), 7.37 (br s, 1H), 7.22 (m, 2H), 6.94 (s, 1H), 6.74 (m, 1H) ppm; ^{13}C NMR (125 MHz, CDCl_3): $\delta = 150.2, 139.8, 134.1, 132.0$ (q, $J_{\text{C-F}} = 33.0$ Hz), 131.6 (q, $J_{\text{C-F}} = 32.5$ Hz), 129.5, 128.6, 125.6 (q, $J_{\text{C-F}} = 3.7$ Hz), 124.0, 123.7 (q, $J_{\text{C-F}} = 272.2$ Hz), 123.5 (q, $J_{\text{C-F}} = 272.2$ Hz), 119.7 (q, $J_{\text{C-F}} = 3.7$ Hz), 117.6 (q, $J_{\text{C-F}} = 3.7$ Hz) ppm; LC/MS: m/z (%): $[\text{M}+\text{H}]^+$ 348.70 (100 %), $t_{\text{R}} = 12.11$ min, 96.8 % pure (UV).

3-chloro-N-(3-methoxyphenyl)benzamide (22a) white solid, m.p. 104 – 106 °C; 74 % yield; ^1H NMR (500 MHz, DMSO-d_6): $\delta = 10.31$ (br s, 1H), 8.00 (dd, 1H, $J = 1.9, 1.6$ Hz), 7.90 (m, 1H), 7.66 (m, 1H), 7.57 (dd, 1H, $J = 7.9, 7.9$ Hz), 7.45 (dd, 1H, $J = 2.5, 2.2$ Hz), 7.36 (m, 1H), 7.26 (dd, 1H, $J = 8.2, 7.9$ Hz), 6.70 (m, 1H), 3.76 (s, 3H) ppm; LC/MS: m/z (%): $[\text{M}+\text{H}]^+$ 262.80 (100 %), $t_{\text{R}} = 11.29$ min, 98.3 % pure (UV).

3-chloro-N'-hydroxy-N-(3-methoxyphenyl)benzimidamide (22) white solid, m.p. 135 – 137 °C; 55 % yield; ^1H NMR (500 MHz, CDCl_3): $\delta = 8.11$ (br s, 1H), 7.50 (dd, 1H, $J = 2.2, 1.6$ Hz), 7.34 (m, 1H), 7.29 (ddd, 1H, $J = 7.9, 1.6, 1.3$ Hz), 7.23 (dd, 1H, $J = 7.9, 7.9$ Hz), 7.21 (br s, 1H), 7.03 (dd, 1H, $J = 8.2, 7.9$ Hz), 6.50 (m, 1H), 6.26 (m, 1H), 6.23 (dd, 1H, $J = 2.2, 2.2$ Hz), 3.63 (s, 3H) ppm; ^{13}C NMR (125 MHz, CDCl_3): $\delta = 154.8, 145.6, 135.3, 129.2, 127.9, 124.6, 124.40, 124.39, 123.0, 121.3, 108.5, 103.5, 101.9, 49.9$ ppm; LC/MS: m/z (%): $[\text{M}+\text{H}]^+$ 277.80 (100 %), $t_{\text{R}} = 10.39$ min, 98.3 % pure (UV).

3-chloro-N-(3-chlorophenyl)benzamide (23a) white solid, m.p. 118 – 120 °C; 83 % yield; ^1H NMR (500 MHz, DMSO-d_6): $\delta = 10.49$ (br s, 1H), 8.00 (dd, 1H, $J = 1.9, 1.6$ Hz), 7.95 (dd, 1H, $J = 1.9, 1.9$ Hz), 7.91 (m, 1H), 7.69 (m, 1H), 7.58 (dd, 1H, $J = 8.2, 7.6$ Hz), 7.39 (dd, 1H, $J = 8.2, 8.2$ Hz), 7.18 (m, 1H), 6.70 (m, 1H) ppm; LC/MS: m/z (%): $[\text{M}+\text{MeCN}]^+$ 306.57 (100 %), $t_{\text{R}} = 13.49$ min, 99.2 % pure (UV).

3-chloro-N-(3-chlorophenyl)-N'-hydroxybenzimidamide (23) white solid, m.p. 127 – 129 °C; 56 % yield; ^1H NMR (500 MHz, CDCl_3): $\delta = 8.62$ (br s, 1H), 7.49 (m, 1H), 7.37 (m, 1H), 7.27 (m, 3H), 7.03 (dd, 1H, $J = 8.2, 8.2$ Hz), 6.93 (m, 1H), 6.73 (dd, 1H, $J = 2.2, 1.9$ Hz), 6.48 (m, 1H) ppm; ^{13}C

NMR (125 MHz, CDCl₃): δ = 150.3, 140.6, 134.6, 132.5, 130.1, 129.8, 128.2, 126.5, 123.1, 121.0, 119.2 ppm; LC/MS: m/z (%): [M+H]⁺ 281.80 (100 %), t_R = 12.38 min, 98.9 % pure (UV).

N-(4-chlorophenyl)-3-cyanobenzamide (24a) white solid, m.p. 206 – 208 °C; 68 % yield; ¹H NMR (500 MHz, DMSO-d₆): δ = 10.53 (br s, 1H), 8.39 (dd, 1H, J = 1.9, 3 Hz), 8.24 (m, 1H), 8.07 (m, 1H), 7.80 (d, 2H, J = 9.1 Hz), 7.76 (dd, 1H, J = 8.5, 7.9 Hz), 7.43 (d, 2H, J = 9.1 Hz) ppm; LC/MS: m/z (%): [M+ MeCN]⁺ 297.85 (100 %), t_R = 10.86 min, 100 % pure (UV).

N-(4-chlorophenyl)-3-cyano-N'-hydroxybenzimidamide (24) white solid, m.p. 164 – 166 °C; 39 % yield; ¹H NMR (500 MHz, DMSO-d₆): δ = 10.92 (br s, 1H), 8.65 (br s, 1H), 7.84 (ddd, 1H, J = 7.9, 1.6, 1.3 Hz), 7.80 (dd, 1H, J = 1.6, 1.3 Hz), 7.62 (ddd, 1H, J = 8.3, 1.6, 1.6 Hz), 7.54 (dd, 1H, J = 8.3, 7.9 Hz), 7.13 (d, 2H, J = 8.8 Hz), 6.65 (d, 2H, J = 8.8 Hz) ppm; ¹³C NMR (125 MHz, DMSO-d₆): δ = 147.1, 140.0, 133.9, 132.6, 132.3, 131.0, 129.6, 128.2, 124.7, 121.3, 118.4, 111.5 ppm; LC/MS: m/z (%): [M+H]⁺ 272.82 (100 %), t_R = 10.18 min, 97.5 % pure (UV).

4-methoxy-N-(4-(trifluoromethyl)phenyl)benzamide (25a) white solid, m.p. 226 – 228 °C; 71 % yield; ¹H NMR (500 MHz, DMSO-d₆): δ = 10.41 (br s, 1H), 7.99 (m, 4H), 7.70 (d, 2H, J = 8.7 Hz), 7.08 (d, 2H, J = 8.7 Hz), 3.85 (s, 3H) ppm; LC/MS: m/z (%): [M+H]⁺ 295.83 (100 %), t_R = 11.89 min, 100 % pure (UV).

N'-hydroxy-4-methoxy-N-(4-(trifluoromethyl)phenyl)benzimidamide (25) white solid, m.p. 139 – 141 °C; 41 % yield; ¹H NMR (500 MHz, DMSO-d₆): δ = 10.70 (br s, 1H), 8.74 (br s, 1H), 7.40 (d, 2H, J = 8.6 Hz), 7.35 (d, 2H, J = 9.1 Hz), 6.93 (d, 2H, J = 9.1 Hz), 6.76 (d, 2H, J = 8.6 Hz), 3.76 (s, 3H) ppm; ¹³C NMR (125 MHz, DMSO-d₆): δ = 165.2, 162.1, 142.9, 129.7, 126.7, 125.7 (q, J_{C-F} = 3.6 Hz), 125.2, 124.3 (q, J_{C-F} = 271.3 Hz), 123.2 (q, J_{C-F} = 32.1 Hz), 119.9, 55.4 ppm; LC/MS: m/z (%): [M+H]⁺ 311.04 (100 %), t_R = 10.33 min, 99.0 % pure (UV).

N-phenyl-3-(trifluoromethyl)benzamide (26a) white solid, m.p. 145 – 147 °C; 87 % yield; ¹H NMR (500 MHz, DMSO-d₆): δ = 10.46 (br s, 1H), 8.30 (s, 1H), 8.26 (d, 1H, J = 8.2 Hz), 7.97 (d, 1H, J = 7.6 Hz), 7.78 (m, 3H), 7.38 (dd, 2H, J = 8.5, 7.6 Hz), 6.75 (t, 1H, J = 7.6 Hz) ppm; ¹³C NMR (125 MHz, DMSO-d₆): δ = 164.0, 138.8, 135.8, 131.8, 129.7, 129.1 (q, J_{C-F} = 32.1 Hz), 128.6, 128.1 (q, J_{C-F} = 3.7 Hz), 124.2 (q, J_{C-F} = 3.7 Hz), 124.0, 123.9 (q, J_{C-F} = 273.1 Hz), 120.5 ppm; LC/MS: m/z (%): [M+H]⁺ 265.91 (100 %), t_R = 11.65 min, 100 % pure (UV).

N'-methoxy-N-phenyl-3-(trifluoromethyl)benzimidamide (26) colorless oil; 62 % yield; ¹H NMR (500 MHz, CDCl₃): δ = 7.76 (s, 1H), 7.59 (d, 1H, J = 7.6 Hz), 7.56 (d, 1H, J = 7.9 Hz), 7.39 (dd, 1H, J = 7.9, 7.6 Hz), 7.17 (br s, 1H), 7.12 (t, 2H, J = 7.9, 7.6 Hz), 6.95 (t, 1H, J = 7.6 Hz), 6.65 (d, 2H, J = 7.9 Hz), 4.00 (s, 3H) ppm; ¹³C NMR (125 MHz, CDCl₃): δ = 149.8, 139.3, 132.1, 131.7, 131.0 (q, J_{C-F} = 32.1 Hz), 128.9, 128.8, 126.2 (q, J_{C-F} = 3.7 Hz), 125.2 (q, J_{C-F} = 3.7 Hz), 123.7 (q, J_{C-F} = 272.2 Hz), 120.5 ppm; LC/MS: m/z (%): [M+H]⁺ 265.91 (100 %), t_R = 11.65 min, 100 % pure (UV).

Hz), 123.2, 121.5, 61.9 ppm; LC/MS: m/z (%): $[M+H]^+$ 294.86 (100 %), t_R = 10.39 min, 96.9 % pure (UV).

N-phenyl-3-(trifluoromethyl)benzohydrazonamide (27) white solid, m.p. 143 – 145 °C; 23 % yield; 1H NMR (500 MHz, DMSO- d_6): δ = 7.72 (m, 2H), 7.40 (m, 5H), 7.26 (dd, 2H, J = 7.6, 7.6 Hz), 7.14(t, 1H, J = 7.6 Hz), 6.98(d, 2H, J = 7.6 Hz) ppm; ^{13}C NMR (125 MHz, DMSO- d_6): δ = 153.8, 147.6, 134.7, 132.8, 130.8, 130.6, 130.4, 129.7 (q, J_{C-F} = 31.2 Hz), 128.8, 128.2, 126.9 (q, J_{C-F} = 3.2 Hz), 125.2 (q, J_{C-F} = 4.3 Hz), 124.1 (q, J_{C-F} = 272.4 Hz) ppm; LC/MS: m/z (%): $[M+H]^+$ 279.93 (100 %), t_R = 6.74 min, 94.0 % pure (UV). This unsealed compound turns red and forms dimer (the mixture analyzed by LC/MS) after days under room temperature.

Synthesis of 2-amino-1-(3-(trifluoromethyl)phenyl)ethanone hydrochloride (28a) (4). To a stirred solution of 3-(trifluoromethyl) acetophenone (5.20 g, 27.6 mmol) in CH_2Cl_2 (80 mL) at 0 °C was carefully added a solution of bromine (4.40 g, 27.6 mmol) in CH_2Cl_2 (75 mL). The reaction was warmed to room temperature and stirred for 1.5 h. The solvent was reduced under reduced pressure and the after the addition was completed and then crude α -bromoketone was used without further purification. The α -bromoketone was dissolved in CCl_4 (100 mL), hexamethylenetetramine (4.20 g, 30.7 mmol) was added. The mixture was stirred overnight, the precipitate was filtered and washed with CCl_4 (2 x 40 mL). The white solid (ca. 9.2 g) was treated with EtOH (150 mL) and concentrated HCl (21 mL) and stirred for 16 h. The mixture was filtered and the precipitate was washed with EtOH (2 x 50 mL). The filtrate was concentrated and the residue was crystallized from 4M HCl. The amino hydrochloride **28a** was obtained as colorless needles. Yield: 57 %. 1H NMR (500 MHz, DMSO- d_6): δ = 8.65 (br s, 3H, NH_3), 8.32 (m, 1H), 8.29 (dd, 1H, J = 2.0, 2.0 Hz), 8.09 (m, 1H), 7.84 (dd, 1H, J = 7.9, 7.9 Hz), 4.69 (s, 2 H, CH_2) ppm. ^{13}C NMR (500 MHz, d_6 -DMSO): δ = 192.3 (C=O), 134.5, 132.2, 130.7 (q, J_{C-F} = 3.7 Hz), 130.4, 129.7 (q, J_{C-F} = 32.1 Hz), 124.7 (q, J_{C-F} = 3.7 Hz), 123.7 (q, J_{C-F} = 272.2 Hz), 45.0 ppm.

Synthesis of 1-phenyl-5-(3-(trifluoromethyl)phenyl)-1H-imidazole-2(3H)-thione (28) (5). A mixture of the amino hydrochloridebromide **28a** (1.00 g, 3.38 mmol), phenylisothiocyanate (440 mg, 3.38 mmol) and triethylamine (342 mg, 3.38 mmol) in EtOH (10 mL) was refluxed in a sealed tube for 2 h. The clear solution was cooled to room temperature and the precipitate was filtered and washed with EtOH (2 x 5 mL). The 4-imidazoline-2-thione **28** was obtained as colorless crystals. Yield: 72%; m.p. 125.3 – 128.4 °C; 1H NMR (500 MHz, DMSO- d_6): δ = 12.70 (br s, 1H), 7.56 (d, 1H, J = 7.3 Hz), 7.55 (s, 1H), 7.44 (m, 4H), 7.38 (d, 1H, J = 7.9 Hz), 7.26 (m, 3H) ppm; ^{13}C NMR (125 MHz, DMSO- d_6): δ = 164.4, 136.4, 131.1, 129.5, 129.4, 129.3, 129.1 (q, J_{C-F} = 31.6 Hz), 129.0, 128.9, 128.6, 124.1 (q, J_{C-F} = 3.7 Hz), 123.7 (q, J_{C-F} = 272.2 Hz), 123.5 (q, J_{C-F} = 4.6 Hz), 115.0 ppm; LC/MS: m/z (%): $[M+H]^+$ 321.05 (100 %), t_R = 10.94 min, 98.4 % pure (UV).

Synthesis of 3-(trifluoromethyl)benzohydrazide (29a). A mixture of 3-(trifluoromethyl)benzoyl chloride (4.75 g, 22.8 mmol) and hydrazine hydrate (4.56 g, 91.2 mmol) in EtOH (15 mL) was refluxed overnight and cooled to room temperature. The clear solution was decanted from the oily residue and poured into ice water. The precipitate was filtered and washed with water (2 x 20 mL). The solid was dissolved in EtOAc (40 mL) washed with saturated NaCl (2 x 30 mL), dried over MgSO₄ and concentrated. The crude material (3.30 g) was crystallized from benzene/*n*-hexane (2:1, 120 mL) and washed with *n*-hexane (2 x 20 mL). The hydrazide **29a** was obtained as a colorless solid. Yield: 3.05 g, 66 %; ¹H NMR (500 MHz, DMSO-*d*₆): δ= 10.04 (br s, 1H, CONH), 8.15 (dd, 1H, *J* = 2.0, 2.0 Hz), 8.11 (m, 1H), 7.88 (m, 1H), 7.71 (dd, 1H, *J* = 7.9, 7.9 Hz), 4.58 (br s, 2H, NH₂) ppm. ¹³C NMR: δ= 164.2 (CONH), 134.2, 131.0, 129.6, 129.2 (q, *J*_{C-F} = 32.1 Hz), 127.6 (q, *J*_{C-F} = 3.7 Hz), 123.9 (q, *J*_{C-F} = 272.2 Hz), 123.6 (q, *J*_{C-F} = 3.7 Hz) ppm.

Synthesis of N-phenyl-2-(3-(trifluoromethyl)benzoyl)hydrazinecarbothioamide (29b). A mixture of 3-trifluoromethyl benzoic acid hydrazide (714 mg, 3.50 mmol) and phenylisothiocyanate (473 mg, 3.50 mmol) in EtOH (5 mL) was refluxed for 2 h. The solution was cooled to room temperature, the precipitate was filtered and washed with Et₂O (2 x 10 mL). The thiosemicarbazide **29b** was obtained as a white solid. Yield: 550 mg, 46 %; ¹H NMR (500 MHz, DMSO-*d*₆): δ= 10.82 (br s, 1H, NH), 9.86 (br s, 1H, NH), 9.78 (br s, 1H, NH), 8.30 (dd, 1H, *J* = 2.0, 2.0 Hz), 8.24 (m, 1H), 7.97 (m, 1H), 7.77 (dd, 1H, *J* = 7.8, 7.8 Hz), 7.43 (m, 2H), 7.34 (m, 2H), 7.17 (m, 1 H) ppm; ¹³C NMR (125 MHz, DMSO-*d*₆): δ= 181.1 (C=S), 164.7 (C=O), 139.1, 133.5, 131.9, 129.6, 129.0 (q, *J*_{C-F} = 32.1 Hz), 128.3 (q, *J*_{C-F} = 2.8 Hz), 128.0 (q, *J*_{C-F} = 2.8 Hz), 126.2, 125.2, 124.5, 123.9 (q, *J*_{C-F} = 272.2 Hz) ppm.

Synthesis of 4-phenyl-3-(3-(trifluoromethyl)phenyl)-1H-1,2,4-triazole-5(4H)-thione (29) (6). The semicarbazide **29b** (300 mg, 0.88 mmol) was suspended in an aqueous solution of NaOH (5 wt%, 15 mL) and heated under reflux. After the solid was completely dissolved the pale yellow solution was stirred for 2 h. The solution was cooled to 0 °C and acidified with 2M HCl. The precipitate was filtered, washed with water (3 x 30 mL) and air-dried. The crude material was crystallized from *n*-hexane/EtOH (2:1). **29** was obtained as colorless needles, m.p. 155.3 – 156.7 °C; 65 % yield; ¹H NMR (500 MHz, DMSO-*d*₆): δ= 14.25 (br s, 1H), 7.78 (d, 1H, *J* = 7.6 Hz), 7.65 (d, 1H, *J* = 7.9 Hz), 7.60 (dd, 1H, *J* = 7.9, 7.6 Hz), 7.51 (m, 4H), 7.40 (m, 2H) ppm; ¹³C NMR (125 MHz, DMSO-*d*₆): δ= 168.8, 149.2, 134.2, 132.2, 129.8, 129.6, 129.4, 129.1 (q, *J*_{C-F} = 32.1 Hz), 128.7, 126.9 (q, *J*_{C-F} = 3.7 Hz), 126.8, 124.7 (q, *J*_{C-F} = 3.7 Hz), 123.5 (q, *J*_{C-F} = 272.2 Hz) ppm; LC/MS: *m/z* (%): [M+H]⁺ 322.05 (100 %), *t*_R = 11.11 min, 98.3 % pure (UV).

Synthesis of N-(3-(trifluoromethyl)benzylidene)aniline (30a). A solution of 3-(trifluoromethyl)benzaldehyde (4.85 g, 27.9 mmol) and aniline (2.76 g, 27.9 mmol) in EtOH (30 mL) was refluxed for 2 h. The solution was cooled to room temperature and the solvent was removed under reduced pressure. The imine **30a** was obtained as yellow oil and used in the next

step without further purification. ^1H NMR (500 MHz, CDCl_3): δ = 8.42 (s, 1H, CHN), 8.12 (dd, J = 2.0, 2.0 Hz, 1H), 8.01 (m, 1H), 7.66 (m, 1H), 7.52 (dd, J = 7.7, 7.7 Hz, 1H), 7.34 (m, 2H), 7.21–7.14 (m, 3 H) ppm; ^{13}C NMR (125 MHz, CDCl_3): δ = 158.4 (CHN), 151.4, 136.9, 131.9, 131.4 (q, $J_{\text{C-F}}$ = 32.8 Hz), 129.3, 129.2, 127.7 (q, $J_{\text{C-F}}$ = 3.7 Hz), 126.5, 125.4 (q, $J_{\text{C-F}}$ = 3.7 Hz), 123.9 (q, $J_{\text{C-F}}$ = 272.0 Hz), 120.8 ppm.

Synthesis of 1-phenyl-5-(3-(trifluoromethyl)phenyl)-1H-imidazole (30) (7). To a solution of the imine **30a** (1.54 g, 6.18 mmol) in MeOH (30 mL) and DME (15 mL) was added K_2CO_3 (4.15 g, 13.0 mmol) and *p*-toluenesulfonylmethylisocyanide (1.45 g, 7.42 mmol). The reaction mixture was refluxed for 6 h. After cooling to room temperature, the solvent was removed under reduced pressure, and the residue was partitioned between EtOAc (50 mL) and saturated NaCl (50 mL). The organic layer was washed with saturated NaCl (2 x 30 mL), dried over MgSO_4 and concentrated. The crude material was purified by flash chromatography (SiO_2 , *n*-hexane / EtOAc 2:1→1:1). The imidazole **30** was obtained as a pale yellow solid, m.p. 110.8 – 111.7 °C; 65 % yield; ^1H NMR (500 MHz, DMSO-d_6): δ = 8.07 (d, 1H, J = 1.0 Hz), 7.60 (d, 1H, J = 7.6 Hz), 7.53 (dd, 1H, J = 7.9, 7.6 Hz), 7.48 (m, 5H), 7.39 (s, 1H), 7.30 (m, 2H) ppm; ^{13}C NMR (125 MHz, DMSO-d_6): δ = 140.2, 135.9, 131.3, 130.6, 130.2, 129.6, 129.5, 129.1 (q, $J_{\text{C-F}}$ = 32.1 Hz), 128.4, 125.8, 123.8 (q, $J_{\text{C-F}}$ = 273.1 Hz), 123.7 (q, $J_{\text{C-F}}$ = 3.7 Hz), 123.6 (q, $J_{\text{C-F}}$ = 3.7 Hz) ppm; LC/MS: m/z (%): $[\text{M}+\text{H}]^+$ 288.90 (100 %), t_R = 12.59 min, 98.2 % pure (UV).

Validation of iron chelating property. 1) **Color test with iron (III) chloride:** All compounds were dissolved as 0.01 M solution in ethanol and FeCl_3 was prepared as 0.01 M solution in water. The same volume of ethanolic solutions were mixed up with ferric chloride solution and taken same amount of ethanol as a blank control (8).

2) **Determine the complex stability constants:** The experiment was performed by potentiometric titration. Thereby, it was uncovered that already under acidic conditions (pH = 4) the formation of $\text{Fe}(\text{OH})_3$ was observed indicating that the CBR compounds cannot form stable Fe(III) complexes under biological conditions (Data supplied by Professor Hegetschweiler's group).

Biology.

Transcription Inhibition Assay. The transcription inhibition experiments were performed as described earlier (9, 10). Purification and quantification of transcripts as well as the determination of IC_{50} values was performed as described by Haupenthal and colleagues (11).

Minimal inhibitory concentration (MIC) determinations. MIC values for *E. coli TolC* were determined for all compounds. Selected compounds were tested in *E. coli K12*, *Bacillus subtilis subsp. subtilis*, *Pseudomonas aeruginosa PAO1* and *Staphylococcus aureus subsp. aureus* (Newman strain). As a bacteria start OD_{600} we used 0.03 in a total volume of 200 μL in lysogeny broth (LB)

containing the compounds predissolved in DMSO (maximal DMSO concentration in the experiment: 1 %). Final compound concentrations prepared from serial dilutions ranged from 0.02 to 100 µg/mL (double values for each concentration) and were adapted for each compound depending on their antibacterial activity and the observation of compound precipitation in the growth medium. The ODs were determined after addition of the compounds and again after incubation for 16 h at 37 °C and 50 rpm (200 rpm for *PAOI*) in 96 well plates (Sarstedt, Nümbrecht, Germany) using a PolarStar Omega (BMG labtech, Ortenberg, Germany). Given MIC values are means of two independent determinations (three if MIC < 10 µg/mL). They are defined as the lowest concentration of compounds that reduced OD₆₀₀ by ≥ 95 % and were read off the inhibition curves. Standard deviation was less than 25 % (most cases: < 15 %).

Influence of iron (III) on the antibacterial activity of CBR703. The effect of DMSO, deferoxamine mesylate (DFO) (25 µg/mL) and CBR703 (3 µg/mL) on the growth of *E.coli TolC* was determined after 16 h (growth conditions as described in the MIC determinations section) by OD₆₀₀ measurement in a PolarStar Omega. The experiment was performed in parallel either in presence or absence of 250 µM Fe (III) citrate. The DMSO concentration was kept at 1 % for all samples.

Cytotoxicity assay. HEK 293 cells (2x10⁵ cells per well) were seeded in 24-well, flat-bottomed plates. Culturing of cells, incubations and OD measurements were performed as described previously (12) with small modifications. 24 h after seeding the cells the incubation was started by the addition of compounds in a final DMSO concentration of 1 %. The living cell mass was determined after 24 and 72 h followed by the calculation of LD₅₀ values.

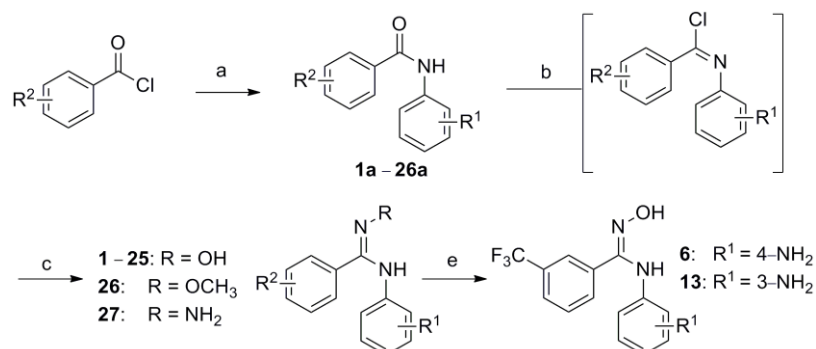
Precipitation experiment. CBR703 was diluted to different concentrations (0 – 400 µg/mL) in MHB in a total volume of 200 µL in a 96 well plate and a maximal DMSO concentration of 2 %. After 25 minutes the precipitation-derived turbidity was measured at 600 nm in a PolarStar Omega. The experiment was performed twice in quadruplicates.

Microtiter plate biofilm tests. 96-well biofilm assays were carried out in sterile clear flat bottom untreated microtiter plates (Nunc, Wiesbaden, Germany) in a volume of 100 µL. Aerobic overnight cultures were generated from a glycerol stock at 37 °C in 10 ml Medium T. Serial dilutions of the compounds with final concentrations from 7.3 to 400 µg/mL were added to a homogenized suspension of the clinical *S. aureus* isolate 11-02670 (MSSA ST30 strain) with an OD₆₀₀ of 0.2 (final OD₆₀₀ of 0.1). The plates were incubated for 17 h at 37 °C in a moist atmosphere. The optical density was determined at 600 nm. 20 µL of supernatant was removed with the pipetting robot Evolution P3 (PerkinElmer, Waltham, MA), transferred to a 396-well microtiter plate (Corning, Tewksbury, MA) and the optical density of planctonic bacteria was determined at 600 nm. Biofilm was quantified in the original 96-well plate by adding 10 µL of a solution of FITC in DMSO (1

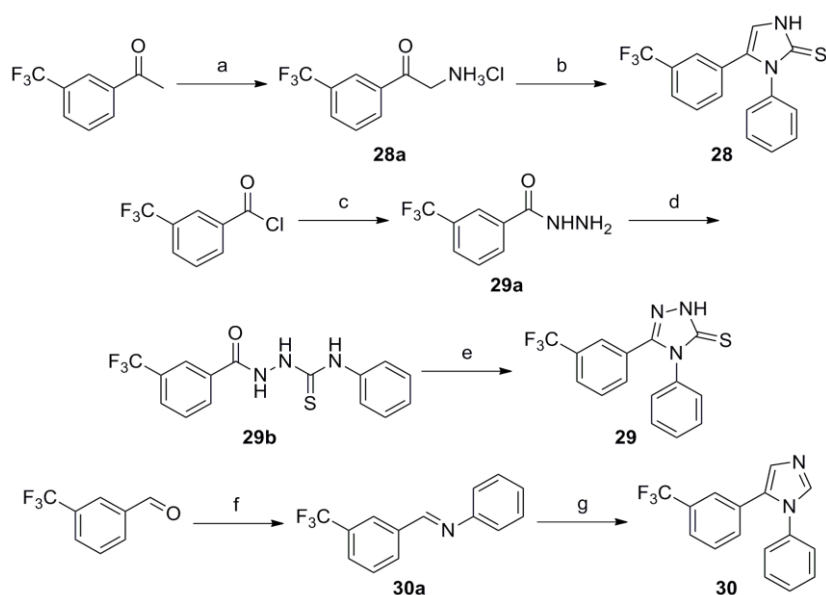
mg/mL) to the wells followed by an incubation for 1 h. Planctonic bacteria were removed by three washes of 45, 30 and 15 min with 0.9 % NaCl. The washing was carried out by carefully submerging the plates in an upright orientation into the washing solution and slowly swirling the container at room temperature. The final wash contained 0.5 % peroxy acetic acid to decontaminate the plates before they were placed in the reader for fluorescence determination (excitation 485 nm, emission 535 nm).

REFERENCES

1. **Li L, Chen X, Fan P, Mihalic JT, Cutler ST.** 2001. Synthesis, antibacterial activity and RNA polymerase inhibition of phenylamidine derivs. PCT Int. Appl. WO 2001051456 A2 20010719.
2. **Krajete A, Steiner G, Kopacka H, Ongania KH, Wurst K, Kristen MO, Preishuber-Pflugl P, Bildstein B.** 2004. Iminohydroxamate early and late transition metal halide complexes-new precatalysts for aluminosiloxane-cocatalyzed olefin insertion polymerization. *Eur. J. Inorg. Chem.* **8**:1740–1752.
3. **Bellamy FD, Ou K.** 1984. Selective reduction of aromatic nitro compounds with stannous chloride in nonacidic and nonaqueous medium. *Tetrahedron Lett.* **25**:839–842.
4. (a) **Weintraub PM, Meyer DR, Aiman CE.** 1980. Evidence for 1, 2-dehydroadamantane as a gas-phase product in time-resolved field-ionization mass spectrometry of 2-adamantyl trifluoroacetate. *J. Org. Chem.* **45**:4990–4992; (b) **Martinet SJ, Larsen L, Street JD, Joule JA.** 1988. Synthesis of 6-hydroxy-1,4-dimethylisoquinoline and of ethyl 7-hydroxy-6-methoxy-1-methylisoquinoline-3-carboxylate. *J. Chem. Soc., Perkin Trans. 1.* **7**:1705–1710; (c) **Shafik RM, Askar A-FAA.** 1979. New biphenyl derivatives. II: 1-(4-Biphenyl)-1-hydroxy-2-aminoethanes and 1-(4-biphenyl)-1-chloro-2-aminoethanes as potential β -adrenoceptor blocking agents. *J. Pharm. Sci.* **68**:776–780.
5. **Korohoda MJ, Bojarska AB.** 1991. Methylation of 4-imidazoline-2-thiones. *J. Prakt. Chem.* **333**:355–360.
6. **Plech T, Wujec M, Siwek A, Kosikowska U, Malm A.** 2011. Synthesis and antimicrobial activity of thiosemicarbazides, s-triazoles and their Mannich bases bearing 3-chlorophenyl moiety. *Eur. J. Med. Chem.* **46**:241–248.
7. **Almansa C, Alfón J, de Arriba AF, Cavalcant FL, Escamilla I, Gómez LA, Miralles A, Soliva R, Bartrolí J, Carceller E, Merlos M, García-Rafanell J.** 2003. Synthesis and Structure-Activity Relationship of a New Series of COX-2 Selective Inhibitors: 1,5-Diarylimidazoles. *J. Med. Chem.* **46**:3463–3475.
8. **Johnson JE, Carvallo C, Dolliver DD, Sanchez N, Garza V, Canseco DC, Eggleton GL, Fronczek FR.** 2007. Bisamidoximes: Synthesis and Complexation with Iron(III). *Aust. J. Chem.* **60**:685–690.
9. **Hinsberger S, Hüsecken K, Groh M, Negri M, Haupenthal J, Hartmann RW.** 2013. Discovery of novel bacterial RNA polymerase inhibitors: pharmacophore-based virtual screening and hit optimization. *J. Med. Chem.* **56**:8332–8338.
10. **Sahner JH, Groh M, Negri M, Haupenthal J, Hartmann RW.** 2013. Novel small molecule inhibitors targeting the "switch region" of bacterial RNAP: structure-based optimization of a virtual screening hit. *Eur J Med Chem.* **65**:223–231.
11. **Haupenthal J, Hüsecken K, Negri M, Maurer CK, Hartmann RW.** 2012. Influence of DNA template choice on transcription and inhibition of Escherichia coli RNA polymerase. *Antimicrob. Agents Chemother.* **56**:4536–4539.
12. **Haupenthal J, Baehr C, Zeuzem S, Piiper A.** 2007. RNase A-like enzymes in serum inhibit the anti-neoplastic activity of siRNA targeting polo-like kinase 1. *Int. J. Cancer.* **121**:206–210.

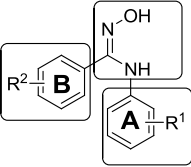
SCHEME S1 Synthesis of compounds **1** – **27**.

Reagents and conditions: (a) appropriate aniline, Et₃N, CH₂Cl₂, 0 °C to r. t. for 2 h; (b) PCl₅, 1,2-dichloroethane, 70 °C for 5 h; (c) RNH₂·HCl, Et₃N, acetonitrile, 0 °C to r. t., overnight; (d) SnCl₂·2H₂O, EtOH, N₂, 70 °C for 30 min.

SCHEME S2 Synthesis of compound **28** – **30**.

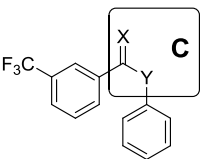
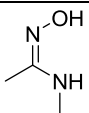
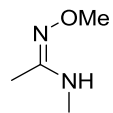
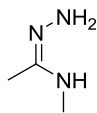
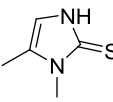
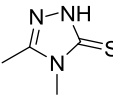
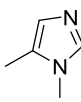
Reagents and conditions: (a) 1) Br₂, CH₂Cl₂, 0 °C to r. t. 2) Hexamethylenetetramine, CCl₄. 3) HCl, EtOH, r. t. (b) PhNCS, NEt₃, EtOH, reflux. (c) Hydrazine hydrate, EtOH, reflux. (d) PhNCS, EtOH, reflux. (e) NaOH, H₂O, reflux. (f) Aniline, EtOH, reflux. (g) TOSMIC, K₂CO₃, MeOH, DME.

TABLE S1 RNAP inhibition and antibacterial activities of derivatives of **CBR703**.

Compound			% Inhibition of <i>E. coli</i> RNAP (at 50 μ M)	MIC <i>E. coli TolC</i> (μ g/mL) ^c
	R ¹	R ²		
CBR703	H	3-CF ₃	18 μ M ^a	14
1	4-NO ₂	3-CF ₃	16	>50
2	4-CH ₃	3-CF ₃	26	14
3	4-CF ₃	3-CF ₃	18 ^b	8
4	4-CN	3-CF ₃	n. i.	>25
5	4-OCH ₃	3-CF ₃	n. i.	>25
6	4-NH ₂	3-CF ₃	10	>100
7	4-Cl	3-CF ₃	35	9
8	3-NO ₂	3-CF ₃	12	>50
9	3-CH ₃	3-CF ₃	24	12
10	3-CF ₃	3-CF ₃	15 ^b	22
11	3-CN	3-CF ₃	n. i.	42
12	3-OCH ₃	3-CF ₃	12	24
13	3-NH ₂	3-CF ₃	10	>100
14	H	2-CF ₃	n. i.	>100
15	H	4-CF ₃	n. i.	23
16	H	3-CN	n. i.	>100
17	H	3-Cl	32	41
18	H	3-CF ₃ -, 4-NO ₂	23 μ M ^a	20
19	H	3-CF ₃ -, 4-F	19 μ M ^a	21
20	H	3-Cl-, 4-F	34	39
21	3-CF ₃	4-CF ₃	n. i.	8
22	3-OCH ₃	3-Cl	20	45
23	3-Cl	3-Cl	25	9
24	4-Cl	3-CN	n. i.	68
25	4-CF ₃	4-OCH ₃	n. i.	15

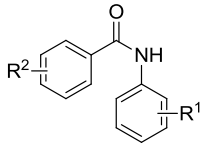
^a: IC₅₀ value; ^b: Compound was tested at 20 μ M limited due to insufficient solubility of the compounds; ^c >: MIC-determination was limited due to insufficient solubility of the compound; n.i. = no inhibition (<10 % inhibition). The SD in these experiments was < 25 % (most cases: < 15 %).

TABLE S2 RNAP inhibition and antibacterial activities of derivatives of CBR703.

Compound		% Inhibition of <i>E. coli</i> RNAP (at 50 μ M)	MIC <i>E. coli TolC</i> (μ g/mL) ^b
CBR703		18 μ M ^a	14
26		29	24
27		n.i.	23
28		n.i.	>50
29		n.i.	>50
30		n.i.	>25

^a: IC₅₀ value; ^b >: MIC-determination was limited due to insufficient solubility of the compound; n.i. = no inhibition (<10 % inhibition). The SD in these experiments was < 25 % (most cases: < 15 %).

TABLE S3 Biological activities of synthetic intermediates.

Compound			% Inhibition of <i>E. coli</i> RNAP (at 50 µM)	MIC <i>E. coli TolC</i> (µg/mL) ^a
	R ¹	R ²		
1a	4-NO ₂	3-CF ₃	n. i.	>100
2a	4-CH ₃	3-CF ₃	n. i.	>25
3a	4-CF ₃	3-CF ₃	n. i.	2
4a	4-CN	3-CF ₃	n. i.	>25
5a	4-OCH ₃	3-CF ₃	n. i.	>25
7a	4-Cl	3-CF ₃	n. i.	7
8a	3-NO ₂	3-CF ₃	n. i.	>25
9a	3-CH ₃	3-CF ₃	n. i.	>25
10a	3-CF ₃	3-CF ₃	n. i.	4
11a	3-CN	3-CF ₃	n. i.	24
12a	3-OCH ₃	3-CF ₃	n. i.	28
14a	H	2-CF ₃	n. i.	>25
15a	H	4-CF ₃	n. i.	23
16a	H	3-CN	n. i.	>25
17a	H	3-Cl	n. i.	>25
18a	H	3-CF ₃ -, 4-NO ₂	n. i.	>25
19a	H	3-CF ₃ -, 4-F	n. i.	>50
20a	H	3-Cl-, 4-F	n. i.	>25
21a	3-CF ₃	4-CF ₃	n. i.	3
22a	3-OCH ₃	3-Cl	n. i.	>25
23a	3-Cl	3-Cl	n. i.	7
24a	4-Cl	3-CN	n. i.	>25
25a	4-CF ₃	4-OCH ₃	n. i.	>25
26a	H	3-CF ₃	n. i.	>25

^a >: MIC-determination was limited due to insufficient solubility of the compound; n.i. = no inhibition (<10 % inhibition). The SD in these experiments was < 25 % (most cases: < 15 %).

TABLE S4 Inhibition of *E. coli TolC* growth in absence or presence of FCS.

Compound	<i>E. coli TolC</i> MIC (µg/mL) ^a	
	LB	LB + 10 % FCS
CBR703	14	>25
7	9	>25
19	21	50
26	24	>25
3a	2	14

The antibacterial activity of the tested compounds was abolished or drastically reduced by addition of FCS, which suggested the cytotoxicities of our compounds are even more pronounced in the absence of serum. FCS: Fetal calf serum; ^a >: MIC-determination was limited due to insufficient solubility of the compound. The SD in these experiments was < 25 % (most cases: < 15 %).

TABLE S5 Color test with iron (III) chloride.

compound	Color change reaction with Fe (III)
CBR703	positive
26	negative

For **CBR703** bearing an amidoxime moiety we observed a color variation (positive effect). In contrast the esterified **26** lacking a color change indicated that the free hydroxyl group was necessary to form complexes.

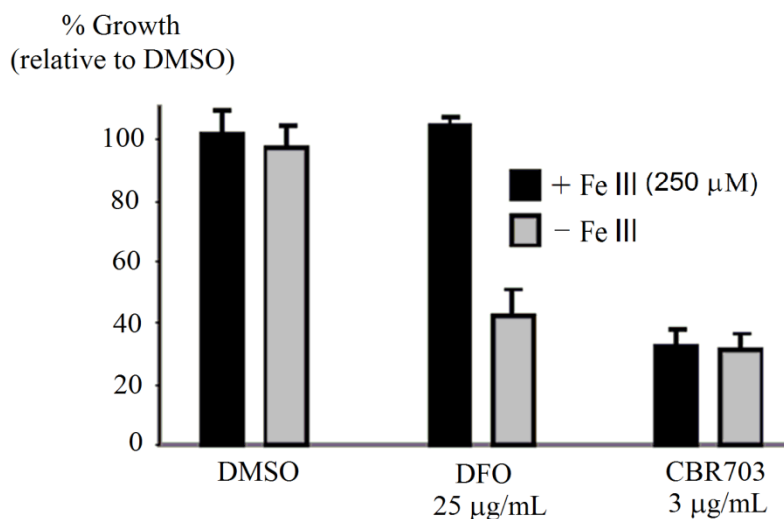


FIG. S1 Effect of **CBR703** and deferoxamine mesylate (DFO) on growth of *E. coli TolC* (OD_{600} determined after 16 h incubation) in presence or absence of Fe III. The antibacterial activity of DFO was eliminated by addition of Fe III, in contrast, no such effect was observed for **CBR703**.

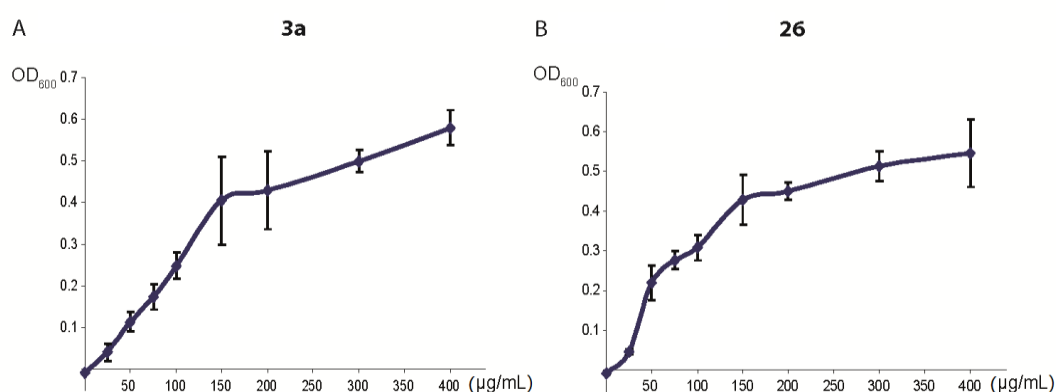


FIG. S2 Concentration dependent precipitation of **3a** and **26** in MHB.

6.3 Supplemental Information for Chapter III

Potent 11 β -Hydroxylase Inhibitors with Inverse Metabolic Stability in Human Plasma and Hepatic S₉ Fractions to Promote Wound Healing

1. Biological tests procedures.

Inhibition of CYP11B1 and CYP11B2

V79MZh cells expressing human or rat CYP11B1 or CYP11B2 were incubated with [1,2-³H]-11-deoxycorticosterone (100 nM) as the substrate and the inhibitor at different concentrations. The assay was performed as previously described.^{s1}

CYP17 preparation and assay

Human CYP17 was expressed in *E. coli* (coexpressing human CYP17 and NADPH-P450 reductase), and the assay was performed using the method previously described with progesterone (25 μ M) as the substrate and NADPH as the cofactor.^{s2}

CYP19 preparation and assay

Human CYP19 was obtained from microsomal preparations of human placenta and the assay was performed using the 3H₂O-method as previously described with [1 β ³H]androstenedione (500 nM) as the substrate.^{s3}

Metabolic Stability Tests in Human Liver S₉ Fraction.

The compound (1 μ M) was incubated with 1 mg/mL pooled human liver S₉ fraction (BD Gentest), 2 mM NADPH regenerating system, 1 mM UDPGA, and 0.1 mM PAPS at 37 °C for 0, 5, 15, and 60 min. The incubation was stopped by precipitation of S₉ enzymes with 2 volumes of cold acetonitrile containing internal standard. Concentration of the remaining test compound at the different time points was analyzed by LC-MS/MS and used to determine half-life ($t_{1/2}$).^{s4}

Metabolic Stability Tests in Human Plasma.

The compound (1 μ M) was incubated with human plasma (pooled, heparinized) at 37 °C for 0, 10, 30, 60, and 150 min. The incubation was stopped by precipitation of plasma proteins with 5 volumes of cold acetonitrile containing an internal standard, and the remaining compound concentration was analyzed by LC-MS/MS.^{s4}

Ames II mutagenicity assay.

The Ames II assay was performed with *S. typhimurium* TA98 and TAMix (containing TA7001, 7002, 7003, 7004, 7005 and 7006) according to the Ames II kit manual instructions of Xenometrix AG, Switzerland (Materials and “Instructions for use, Version 4.5_L January 2012”), with the positive controls of 2-nitrofluorene, 4-nitroquinoline-N-oxide and 2-aminoanthracene. Compound **34** was tested at the following concentrations: 100 μ M, 33 μ M, 11 μ M, 3.7 μ M, 1.2 μ M and 0.4 μ M.

s1. (a) Denner, K.; Doehmer, J.; Bernhardt, R. Cloning of CYP11B1 and CYP11B2 from normal human adrenal and their functional expression in COS-7 and V79 chinese hamster cells. *Endocr.Res.* **1995**, *21*, 443–448. (b) Ehmer, P. B.; Bureik, M.; Bernhardt, R.; Muller, U.; Hartmann, R. W. Development of a test system for inhibitors of human aldosterone synthase (CYP11B2): Screening

in fission yeast and evaluation of selectivity in V79 cells. *J. Steroid Biochem. Mol. Biol.* **2002**, *81*, 173–179.

s2. (a) Ehmer, P. B.; Jose, J.; Hartmann, R. W. Development of a simple and rapid assay for the evaluation of inhibitors of human 17 α -hydroxylase-C(17,20)-lyase (P450c17) by coexpression of P450c17 with NADPH-cytochrome-P450-reductase in *Escherichia coli*. *J. Steroid Biochem. Mol. Biol.* **2000**, *75*, 57–63. (b) Hutschenreuter, T. U.; Ehmer, P. E.; Hartmann, R. W. Synthesis of hydroxy derivatives of highly potent non-steroidal CYP 17 Inhibitors as potential metabolites and evaluation of their activity by a non cellular assay using recombinant human enzyme. *J. Enzyme Inhib. Med. Chem.* **2004**, *19*, 17–32.

s3. Hartmann, R. W.; Batzl, C. Aromatase inhibitors. Synthesis and evaluation of mammary tumorinhibiting activity of 3-alkylated 3-(4-aminophenyl)piperidine-2,6-diones. *J. Med. Chem.* **1986**, *29*, 1362–1369.

s4. Emmerich, J.; Hu, Q; Hanke, N; Hartmann, R.W. Cushing's syndrome: development of highly potent and selective CYP11B1 inhibitors of the (pyridylmethyl)pyridine type. *J. Med. Chem.* **2013**, *56*, 6022–32.

2. Synthetic procedures and characterization

General Methods

Proton nuclear magnetic resonance (^1H NMR) and carbon NMR (^{13}C NMR) spectra were recorded on a Bruker Fourier spectrometer (500 or 300 MHz) at ambient temperature with the chemical shifts recorded as δ values in ppm units by reference to the hydrogenated residues of deuterated solvent as internal standard. Coupling constants (J) are given in Hz and signal patterns are indicated as follows: s, singlet; d, doublet; t, triplet; m, multiplet, br, broad signal. The melting points (mp) were determined on a Stuart Scientific SMP3 apparatus and are uncorrected. The Spectra Systems-LC-system consisted of a pump, an autosampler, and a UV detector. Mass spectrometry was performed on a MSQ electro spray mass spectrometer (Thermo Fisher, Dreieich, Germany). The system was operated with the standard software Xcalibur. A RP C18 NUCLEODUR 100-5 (125 x 3 mm) column (Macherey-Nagel GmbH, Dueren, Germany) was used as stationary phase. Solvent system: In a gradient run the percentage of acetonitrile (containing 0.1% trifluoroacetic acid) in 0.1% trifluoroacetic acid was increased from an initial concentration of 3% at 0 min to 100% at 15 min and kept at 100% for 10 min. The injection volume was 10 μL and flow rate was set to 800 $\mu\text{L}/\text{min}$. MS analysis was carried out at a spray voltage of 3800 V, a capillary temperature of 350 $^\circ\text{C}$ and a source CID of 10 V. Spectra were acquired in positive mode from 100 to 1000 m/z and at 254 nm for the UV trace. Column chromatography was performed using silica-gel 60 (50 – 200 μm), and reaction progress was determined by TLC analysis on Alugram SIL G/UV254 (Macherey-Nagel). Commercially available reagents and solvents (from Acros, sigma-aldrich and ABCR) were used directly without further purification.

Method A: Suzuki Coupling.

The corresponding brominated aromatic compound (0.5 mmol, 1.0 equiv) and the boronic acid (1.0 – 2.0 equiv) were dissolved in 1,2-dimethoxyethane (12 mL), water (4 mL) and Na_2CO_3 (3.0 – 5.0 equiv). The mixture was degassed under reduced pressure and flushed with N_2 for three times before $\text{Pd}(\text{PPh}_3)_4$ (5 – 10 mol%) was added. The resulting suspension was then heated under reflux (95 $^\circ\text{C}$) for 4 – 8 h. After cooling down, water (20 mL) and EtOAc (40 mL) were added. The phases were separated, and the aqueous phase was extracted two times with EtOAc (40 mL). The combined organic extracts were dried over MgSO_4 and concentrated under reduced pressure to give the crude product, which was purified with flash chromatography on silica gel.

Method B: Sulfonylation Reaction.

To the solution of corresponding brominated aromatic amine (1 mmol, 1.0 equiv), 4-dimethylaminopyridine (DMAP, 0.2 equiv) and pyridine (3.0 – 5.0 equiv) in dry THF (8 mL) was added dropwise corresponding sulfonyl chloride (1.0 – 2.0 equiv) at room temperature or. Then the mixture was stirred at room temperature or heated to 60 $^\circ\text{C}$ for 1 – 6 h and the reaction was detected by TLC until the raw material disappeared. Then the mixture was cooled to ambient temperature and quenched by addition of a cold mixture of concentrated hydrochloric acid (6.0 – 10.0 equiv) and water. It was extracted with EtOAc (3 x 30 mL). The combined organic extracts were dried over MgSO_4 and concentrated under reduced pressure to give the crude product, which was purified with flash chromatography on silica gel.

Method C: Sulfonylation Reaction.

60% gas-volumetric NaH (40 mg, 1 mmol) was added to a stirred solution of **16a** (105 mg, 0.5 mmol) in 6 mL of dry THF at 0 $^\circ\text{C}$ under N_2 . After stirring at room temperature for 1 h, corresponding sulfonyl chloride (1.0 mmol) was added slowly. The reaction mixture was stirred for an additional 30 min and heated to 60 $^\circ\text{C}$ for 4 h and then poured into 20 mL of 5% aq. NaHCO_3

and extracted with CH₂Cl₂ (3 x 25 mL). The combined organic layers were dried over MgSO₄, and the solvent was removed under reduced pressure to get the crude product which was purified by flash chromatography on silica gel.

5-Pyridin-3-yl-2,3-dihydro-1H-indole (3a). The title compound was synthesized according to Method A using 5-bromoindoline (0.99 g, 5 mmol), pyridin-3-ylboronic acid (0.94 g, 7.5 mmol), Na₂CO₃ (2.12 g, 2.0 mmol), Pd(PPh₃)₄ (434 mg, 0.38 mmol) and 1,2-dimethoxyethane (120 mL) / water (40 mL) to yield the crude product, which was purified by flash chromatography on silica gel (CH₂Cl₂ / MeOH, 500:1 to 62.5:1) to yield a brown solid (760 mg, 78%). ¹H-NMR (500 MHz, CDCl₃): δ 8.79 (dd, *J* = 2.3, 0.6 Hz, 1H), 8.49 (dd, *J* = 4.8, 1.6 Hz, 1H), 7.80 (dt, *J* = 7.9, 2.1 Hz, 1H), 7.35 (d, *J* = 1.2 Hz, 1H), 7.29 (m, 1H), 7.25 (m, 1H), 6.71 (d, *J* = 8.1 Hz, 1H), 3.64 (t, *J* = 8.4 Hz, 2H), 3.11 (t, *J* = 8.4 Hz, 2H).

5-bromo-1-((3-methoxyphenyl)sulfonyl)-2,3-dihydro-1H-pyrrolo[2,3-b]pyridine (9a) The title compound was synthesized according to Method B using 5-bromo-2,3-dihydro-1H-pyrrolo[2,3-b]pyridine (200 mg, 1.0 mmol), 3-methoxybenzene-1-sulfonyl chloride (207 mg, 1.0 mmol), DMAP (24 mg, 0.2 mmol), pyridine (310 mg, 4.0 mmol) and dry THF (8 mL) to yield the crude product, which was purified by flash chromatography on silica gel (n-hexane / EtOAc, 10:1) to yield a white solid (315 mg, 85%). ¹H-NMR (500 MHz, CDCl₃): δ 8.19 (m, 1H), 7.65 (m, 1H), 7.62 (m, 1H), 7.46 (m, 1H), 7.38 (dd, *J* = 8.8, 7.9 Hz, 1H), 7.10 (m, 1H), 4.06 (t, *J* = 8.5 Hz, 2H), 3.84 (s, 3H), 3.04 (t, *J* = 8.5 Hz, 2H). ¹³C-NMR (125 MHz, CDCl₃): δ 159.7, 155.0, 147.4, 138.6, 136.0, 129.8, 126.5, 120.2, 120.0, 113.8, 112.5, 55.7, 48.8, 25.1.

N-(4-bromophenyl)-3-methoxybenzenesulfonamide (11a) The title compound was synthesized according to Method B using 4-bromoaniline (172 mg, 1.0 mmol), 3-methoxybenzene-1-sulfonyl chloride (207 mg, 1.0 mmol), DMAP (24 mg, 0.2 mmol), pyridine (310 mg, 4.0 mmol) and dry THF (8 mL) to yield the crude product, which was purified by flash chromatography on silica gel (n-hexane / EtOAc, 8:1) to yield a white solid (274 mg, 80%). ¹H-NMR (300 MHz, CDCl₃): δ 7.34 (m, 4H), 7.28 (m, 1H), 7.07 (m, 1H), 6.99 (d, *J* = 8.8 Hz, 2H), 3.76 (s, 3H).

N-(4-bromophenyl)-3-methoxy-N-methylbenzenesulfonamide (12a) The title compound was synthesized according to Method B using 4-bromo-N-methylaniline (186 mg, 1.0 mmol), 3-methoxybenzene-1-sulfonyl chloride (207 mg, 1.0 mmol), DMAP (24 mg, 0.2 mmol), pyridine (310 mg, 4.0 mmol) and dry THF (8 mL) to yield the crude product, which was purified by flash chromatography on silica gel (n-hexane / EtOAc, 10:1) to yield a white solid (338 mg, 95%). ¹H-NMR (300 MHz, CDCl₃): δ 7.42 (d, *J* = 8.8 Hz, 2H), 7.37 (dd, *J* = 8.1, 7.9 Hz, 1H), 7.12 (m, 2H), 6.99 (m, 3H), 3.75 (s, 3H), 3.16 (s, 3H).

6-bromo-1-((3-methoxyphenyl)sulfonyl)-1,2,3,4-tetrahydroquinoline (14a) The title compound was synthesized according to Method B using 6-bromo-1,2,3,4-tetrahydroquinoline (212 mg, 1.0 mmol), 3-methoxybenzene-1-sulfonyl chloride (207 mg, 1.0 mmol), DMAP (24 mg, 0.2 mmol), pyridine (230 mg, 3.0 mmol) and dry THF (8 mL) to yield the crude product, which was purified by flash chromatography on silica gel (n-hexane / EtOAc, 10:1) to yield a white solid (340 mg, 89%). ¹H-NMR (500 MHz, DMSO): δ 7.56 (d, *J* = 8.8 Hz, 1H), 7.48 (dd, *J* = 8.2, 7.9 Hz, 1H), 7.38 (dd, *J* = 8.8, 2.5 Hz, 1H), 7.31 (m, 1H), 7.24 (m, 1H), 7.17 (m, 1H), 7.00 (m, 1H), 3.75 (m, 2H), 3.72 (s, 3H), 2.43 (t, *J* = 6.6 Hz, 2H), 1.55 (m, 2H). ¹³C-NMR (125 MHz, DMSO): δ 159.4, 139.6, 135.7, 133.3, 131.7, 130.8, 129.1, 125.7, 119.4, 118.7, 117.2, 111.5, 55.5, 46.2, 25.8, 20.5.

6-(pyridin-3-yl)-1,2,3,4-tetrahydroquinoline (16a) The title compound was synthesized according to Method A using 6-bromo-1,2,3,4-tetrahydroquinoline (212 mg, 1.0 mmol), pyridin-3-ylboronic acid (250 mg, 2.0 mmol), Na₂CO₃ (316 mg, 3.0 mmol), Pd(PPh₃)₄ (65 mg, 5.6 mol %) and 1,2-dimethoxyethane (24 mL) / water (8 mL) to yield the crude product, which was purified by flash chromatography on silica gel (CH₂Cl₂ / MeOH, 500:1 to 62.5:1) to yield a slight red solid (95–143 mg, 45–68%). ¹H-NMR (300 MHz, CDCl₃): δ 8.78 (m, 1H), 8.47 (d, *J* = 4.8 Hz, 1H), 7.79 (m, 1H),

7.28 (m, 1H), 7.20 (m, 2H), 6.56 (d, $J = 7.7$ Hz, 1H), 3.35 (m, 2H), 2.84 (t, $J = 6.3$ Hz, 2H), 1.98 (m, 2H).

6-bromo-1-((3-(trifluoromethoxy)phenyl)sulfonyl)-1,2,3,4-tetrahydroquinoline (20a) The title compound was synthesized according to Method B using 6-bromo-1,2,3,4-tetrahydroquinoline (212 mg, 1.0 mmol), 3-(trifluoromethoxy)benzene-1-sulfonyl chloride (260 mg, 1.0 mmol), DMAP (24 mg, 0.2 mmol), pyridine (230 mg, 3.0 mmol) and dry THF (8 mL) to yield the crude product, which was purified by flash chromatography on silica gel (n-hexane / EtOAc, 10:1) to yield a white solid (265 mg, 61%). $^1\text{H-NMR}$ (300 MHz, CDCl_3): δ 7.67 (d, $J = 8.8$ Hz, 1H), 7.48 (m, 3H), 7.39 (d, $J = 7.5$ Hz, 1H), 7.32 (d, $J = 8.8$ Hz, 1H), 7.17 (m, 1H), 3.79 (m, 2H), 2.41 (t, $J = 6.7$ Hz, 2H), 1.61 (m, 2H).

6-bromo-1-((4-(trifluoromethoxy)phenyl)sulfonyl)-1,2,3,4-tetrahydroquinoline (21a) The title compound was synthesized according to Method B using 6-bromo-1,2,3,4-tetrahydroquinoline (212 mg, 1.0 mmol), 4-(trifluoromethoxy)benzene-1-sulfonyl chloride (260 mg, 1.0 mmol), DMAP (24 mg, 0.2 mmol), pyridine (230 mg, 3.0 mmol) and dry THF (8 mL) to yield the crude product, which was purified by flash chromatography on silica gel (n-hexane / EtOAc, 10:1) to yield a white solid (314 mg, 72%). $^1\text{H-NMR}$ (300 MHz, CDCl_3): δ 7.68 (m, 3H), 7.33 (d, $J = 8.8$ Hz, 1H), 7.27 (d, $J = 7.4$ Hz, 2H), 7.19 (m, 1H), 3.80 (m, 2H), 2.45 (t, $J = 6.4$ Hz, 2H), 1.64 (m, 2H).

6-bromo-1-((3-(trifluoromethyl)phenyl)sulfonyl)-1,2,3,4-tetrahydroquinoline (26a) The title compound was synthesized according to Method B using 6-bromo-1,2,3,4-tetrahydroquinoline (212 mg, 1.0 mmol), 3-(trifluoromethyl)benzene-1-sulfonyl chloride (245 mg, 1.0 mmol), DMAP (24 mg, 0.2 mmol), pyridine (230 mg, 3.0 mmol) and dry THF (8 mL) to yield the crude product, which was purified by flash chromatography on silica gel (n-hexane / EtOAc, 10:1) to yield a white solid (294 mg, 70%). $^1\text{H-NMR}$ (300 MHz, CDCl_3): δ 7.90 (s, 1H), 7.81 (d, $J = 7.8$ Hz, 1H), 7.73 (d, $J = 7.6$ Hz, 1H), 7.68 (d, $J = 8.8$ Hz, 1H), 7.57 (dd, $J = 7.8, 7.6$ Hz, 1H), 7.33 (d, $J = 8.8$ Hz, 1H), 7.17 (m, 1H), 3.81 (m, 2H), 2.41 (t, $J = 6.7$ Hz, 2H), 1.63 (m, 2H).

6-bromo-1-((4-(trifluoromethyl)phenyl)sulfonyl)-1,2,3,4-tetrahydroquinoline (27a) The title compound was synthesized according to Method B using 6-bromo-1,2,3,4-tetrahydroquinoline (212 mg, 1.0 mmol), 4-(trifluoromethyl)benzene-1-sulfonyl chloride (245 mg, 1.0 mmol), DMAP (24 mg, 0.2 mmol), pyridine (230 mg, 3.0 mmol) and dry THF (8 mL) to yield the crude product, which was purified by flash chromatography on silica gel (n-hexane / EtOAc, 10:1) to yield a white solid (328 mg, 78%). $^1\text{H-NMR}$ (300 MHz, CDCl_3): δ 7.88 (m, 1H), 7.68 (m, 3H), 7.33 (d, $J = 8.8$ Hz, 1H), 7.28 (d, $J = 7.6$ Hz, 2H), 3.80 (m, 2H), 2.44 (t, $J = 6.6$ Hz, 2H), 1.63 (m, 2H).

6-(pyridin-4-ylmethyl)-1,2,3,4-tetrahydroquinoline (33b) The title compound was synthesized according to Method A using **33a** (194 mg, 0.75 mmol), 4-(bromomethyl)pyridine hydrobromide (190 mg, 0.75 mmol), Na_2CO_3 (380 mg, 3.6 mmol), $\text{Pd}(\text{PPh}_3)_4$ (65 mg, 7.5 mol%) and 1,2-dimethoxyethane (18 mL) / water (6 mL) to yield the crude product, which was purified by flash chromatography on silica gel (CH_2Cl_2 / MeOH, 500:1 to 62.5:1) to yield a slight red solid (81 mg, 48%). $^1\text{H-NMR}$ (300 MHz, CDCl_3): δ 8.47 (d, $J = 5.4$ Hz, 2H), 7.10 (d, $J = 5.4$ Hz, 2H), 6.74 (m, 2H), 6.42 (d, $J = 8.0$ Hz, 1H), 3.80 (s, 2H), 3.28 (m, 2H), 2.72 (t, $J = 6.3$ Hz, 2H), 1.92 (m, 2H).

6-(pyridin-3-ylmethyl)-1,2,3,4-tetrahydroquinoline (34b) The title compound was synthesized according to Method A using **33a** (194 mg, 0.75 mmol), 3-(bromomethyl)pyridine hydrobromide (190 mg, 0.75 mmol), Na_2CO_3 (380 mg, 3.6 mmol), $\text{Pd}(\text{PPh}_3)_4$ (65 mg, 7.5 mol %) and 1,2-dimethoxyethane (18 mL) / water (6 mL) to yield the crude product, which was purified by flash chromatography on silica gel (CH_2Cl_2 / MeOH, 500:1 to 62.5:1) to yield a slight red solid (86 mg, 51%). $^1\text{H-NMR}$ (300 MHz, CDCl_3): δ 8.48 (d, $J = 2.0$ Hz, 1H), 8.42 (dd, $J = 4.8, 1.5$ Hz, 1H), 7.47 (m, 1H), 7.18 (m, 1H), 6.75 (m, 2H), 6.41 (d, $J = 8.3$ Hz, 1H), 3.82 (s, 2H), 3.27 (m, 2H), 2.71 (t, $J = 6.3$ Hz, 2H), 1.91 (m, 2H).

1-((3-methoxyphenyl)sulfonyl)-5-(pyridin-3-yl)indoline (3) The title compound was synthesized according to Method B using **3a** (98 mg, 0.5 mmol), 3-methoxybenzene-1-sulfonyl chloride (155 mg, 0.75 mmol), DMAP (12 mg, 0.1 mmol), pyridine (155 mg, 2.0 mmol) and dry THF (4 mL) to yield the crude product, which was purified by flash chromatography on silica gel (CH₂Cl₂ / MeOH, 500:1 to 62.5:1) to yield a white solid (135 mg, 74%). mp: 136 – 138 °C; HPLC: 98% pure; MS (ESI) m/z = 367 [M⁺+H]; ¹H-NMR (500 MHz, DMSO-d₆): δ 8.82 (s, 1H), 8.52 (d, J = 4.0 Hz, 1H), 7.99 (d, J = 8.0 Hz, 1H), 7.59 – 7.58 (m, 2H), 7.55 (s, 1H), 7.51 (t, J = 7.9 Hz, 1H), 7.43 – 7.41 (m, 2H), 7.25 – 7.23 (m, 2H), 3.97 (t, J = 8.5 Hz, 2H), 3.76 (s, 3H), 2.99 (t, J = 8.5 Hz, 2H); ¹³C-NMR (125 MHz, DMSO-d₆): δ 159.4, 148.0, 147.2, 141.3, 137.0, 134.9, 133.6, 132.6, 130.7, 126.2, 123.9, 123.7, 119.5, 119.0, 114.4, 111.8, 55.5, 50.2, 27.1.

1-((3-fluorophenyl)sulfonyl)-5-(pyridin-3-yl)indoline (4) The title compound was synthesized according to Method B using **3a** (98 mg, 0.5 mmol), 3-fluorobenzene-1-sulfonyl chloride (146 mg, 0.75 mmol), DMAP (12 mg, 0.1 mmol), pyridine (155 mg, 2.0 mmol) and dry THF (4 mL) to yield the crude product, which was purified by flash chromatography on silica gel (CH₂Cl₂ / MeOH, 500:1 to 62.5:1) to yield a slight yellow solid (126 mg, 71%). mp: 146 – 148 °C; HPLC: 98% pure; MS (ESI) m/z = 355 [M⁺+H]; ¹H-NMR (500 MHz, DMSO-d₆): δ 8.82 (d, J = 1.7 Hz, 1H), 8.52 (dd, J = 4.7, 1.7 Hz, 1H), 7.99 – 7.98 (m, 1H), 7.70 – 7.71 (m, 2H), 7.66 – 7.65 (m, 1H), 7.57 – 7.55 (m, 4H), 7.43 – 7.42 (m, 1H), 3.96 (t, J = 8.5 Hz, 2H), 3.03 (t, J = 8.5 Hz, 2H); ¹³C-NMR (125 MHz, DMSO-d₆): δ 161.8 (d, J_{C-F} = 249.2 Hz), 148.2, 147.3, 141.0, 138.0 (d, J_{C-F} = 6.5 Hz), 134.9, 133.7, 133.3, 132.8, 132.0 (d, J_{C-F} = 8.0 Hz), 126.4, 124.1, 123.8, 123.4 (d, J_{C-F} = 2.9 Hz), 121.1 (d, J_{C-F} = 21.2 Hz), 114.3, 114.2 (d, J_{C-F} = 24.1 Hz), 50.3, 27.2.

1-(methylsulfonyl)-5-(pyridin-3-yl)indoline (5) The title compound was synthesized according to Method B using **3a** (196 mg, 1.0 mmol), methanesulfonyl chloride (171 mg, 1.5 mmol), DMAP (24 mg, 0.2 mmol), pyridine (310 mg, 4.0 mmol) and dry THF (8 mL) to yield the crude product, which was purified by flash chromatography on silica gel (CH₂Cl₂ / MeOH, 500:1 to 62.5:1) to yield a slight yellow solid (134 mg, 49%). mp: 128 – 130 °C; HPLC: 98% pure; MS (ESI) m/z = 275 [M⁺+H]; ¹H-NMR (500 MHz, MeOH-d₄): δ 8.77 (d, J = 2.5 Hz, 1H), 8.48 (dd, J = 5.0, 1.6 Hz, 1H), 8.04 – 8.07 (m, 1H), 7.57 (d, J = 0.9 Hz, 1H), 7.47 – 7.52 (m, 3H), 4.04 (t, J = 8.5 Hz, 2H), 3.24 (t, J = 8.5 Hz, 2H), 2.96 (s, 3H); ¹³C-NMR (125 MHz, MeOH-d₄): δ 148.5, 148.1, 144.0, 138.3, 136.3, 134.6, 134.2, 125.5, 125.3, 115.2, 51.8, 34.6, 28.8.

1-(ethylsulfonyl)-5-(pyridin-3-yl)indoline (6) The title compound was synthesized according to Method B using **3a** (196 mg, 1.0 mmol), ethanesulfonyl chloride (192 mg, 1.5 mmol), DMAP (24 mg, 0.2 mmol), pyridine (310 mg, 4.0 mmol) and dry THF (8 mL) to yield the crude product, which was purified by flash chromatography on silica gel (CH₂Cl₂ / MeOH, 500:1 to 62.5:1) to yield a dark red solid (121 mg, 42%). mp: 113 – 115 °C; HPLC: 98% pure; MS (ESI) m/z = 289 [M⁺+H]; ¹H-NMR (500 MHz, MeOH-d₄): δ 8.76 (s, 1H), 8.48 (d, J = 4.1 Hz, 1H), 8.06 – 8.03 (m, 1H), 7.54 (d, J = 1.3 Hz, 1H), 7.50 – 7.44 (m, 3H), 3.26 – 3.18 (m, 4H), 4.08 (t, J = 8.6 Hz, 2H), 1.34 (t, J = 7.4 Hz, 3H); ¹³C-NMR (125 MHz, MeOH-d₄): δ 148.4, 148.1, 144.1, 138.3, 136.2, 134.3, 133.8, 127.8, 125.5, 125.3, 115.1, 51.7, 44.7, 28.8, 8.0.

1-(isopropylsulfonyl)-5-(pyridin-3-yl)indoline (7) The title compound was synthesized according to Method B using **3a** (196 mg, 1.0 mmol), propane-2-sulfonyl chloride (213 mg, 1.5 mmol), DMAP (24 mg, 0.2 mmol), pyridine (310 mg, 4.0 mmol) and dry THF (8 mL) to yield the crude product, which was purified by flash chromatography on silica gel (CH₂Cl₂ / MeOH, 500:1 to 62.5:1) to yield a white solid (133 mg, 44%). mp: 104 – 106 °C; HPLC: 99% pure; MS (ESI) m/z = 303 [M⁺+H]; ¹H-NMR (500 MHz, MeOH-d₄): δ 8.76 (d, J = 1.3 Hz, 1H), 8.48 (d, J = 4.1 Hz, 1H), 8.03 – 8.05 (m, 1H), 7.53 (s, 1H), 7.41 – 7.49 (m, 3H), 4.12 (t, J = 8.7 Hz, 2H), 3.57 (sept, J = 6.8 Hz, 1H), 3.24 (t, J = 8.7 Hz, 2H), 1.35 (s, 3H), 1.34 (s, 3H); ¹³C-NMR (125 MHz, MeOH-d₄): δ 148.3, 148.0, 144.5, 138.2, 136.1, 133.8, 133.3, 127.6, 125.5, 125.2, 114.9, 54.3, 51.9, 28.8, 16.9.

1-(isobutylsulfonyl)-5-(pyridin-3-yl)indoline (8) The title compound was synthesized according to Method B using **3a** (196 mg, 1.0 mmol), 2-methylpropane-1-sulfonyl chloride (234 mg, 1.5 mmol),

DMAP (24 mg, 0.2 mmol), pyridine (310 mg, 4.0 mmol) and dry THF (8 mL) to yield the crude product, which was purified by flash chromatography on silica gel (CH₂Cl₂ / MeOH, 500:1 to 62.5:1) to yield a white solid (126 mg, 40%). mp: 120 – 122 °C; HPLC: 98% pure; MS (ESI) m/z = 317 [$M^+ + H$]; ¹H-NMR (500 MHz, MeOH-*d*₄): δ 8.75 (d, J = 1.7 Hz, 1H), 8.47 (dd, J = 4.7, 1.7 Hz, 1H), 8.05 – 8.02 (m, 1H), 7.53 (s, 1H), 7.46 – 7.42 (m, 3H), 4.05 (t, J = 8.5 Hz, 2H), 3.22 (t, J = 8.5 Hz, 2H), 3.00 (d, J = 6.7 Hz, 2H), 2.28 (sept, J = 6.7 Hz, 1H), 1.10 (s, 3H), 1.09 (s, 3H); ¹³C-NMR (125 MHz, MeOH-*d*₄): δ 148.3, 148.0, 144.0, 138.2, 136.2, 134.4, 133.8, 127.8, 125.5, 125.2, 115.0, 56.6, 51.5, 28.8, 25.7, 22.8.

1-(3-methoxyphenyl)sulfonyl-5-(pyridin-4-yl)-2,3-dihydro-1H-pyrrolo[2,3-*b*]pyridine (9) The title compound was synthesized according to Method A using **9a** (184 mg, 0.5 mmol), pyridin-4-ylboronic acid (125 mg, 1.0 mmol), Na₂CO₃ (212 mg, 2.0 mmol), Pd(PPh₃)₄ (58 mg, 0.05 mmol) and 1,2-dimethoxyethane (12 mL) / water (4 mL) to yield the crude product, which was purified by flash chromatography on silica gel (CH₂Cl₂ / MeOH, 500:1 to 62.5:1) to yield a slight yellow solid (133 mg, 73%). mp: 120 – 122 °C; HPLC: 96% pure; MS (ESI) m/z = 368 [$M^+ + H$]; ¹H-NMR (500 MHz, CDCl₃): δ 8.64 (d, J = 5.9 Hz, 2H), 8.44 (s, 1H), 7.72 (s, 1H), 7.68 (d, J = 7.6 Hz, 1H), 7.62 (s, 1H), 7.40 – 7.38 (m, 3H), 7.10 (dd, J = 8.2, 2.2 Hz, 1H), 4.12 (t, J = 8.4 Hz, 2H), 3.84 (s, 3H), 3.14 (t, J = 8.4 Hz, 2H); ¹³C-NMR (125 MHz, CDCl₃): δ 159.7, 156.8, 150.2, 145.6, 145.3, 138.8, 131.7, 129.8, 128.4, 125.0, 121.1, 120.2, 120.0, 112.5, 55.7, 48.7, 25.2.

1-((3-methoxyphenyl)sulfonyl)-5-(pyridin-3-yl)-2,3-dihydro-1H-pyrrolo[2,3-*b*]pyridine (10) The title compound was synthesized according to Method A using **9a** (184 mg, 0.5 mmol), pyridin-3-ylboronic acid (125 mg, 1.0 mmol), Na₂CO₃ (212 mg, 2.0 mmol), Pd(PPh₃)₄ (58 mg, 0.05 mmol) and 1,2-dimethoxyethane (12 mL) / water (4 mL) to yield the crude product, which was purified by flash chromatography on silica gel (CH₂Cl₂ / MeOH, 500:1 to 62.5:1) to yield a white solid (104 mg, 57%). mp: 135 – 137 °C; HPLC: 98% pure; MS (ESI) m/z = 368 [$M^+ + H$]; ¹H-NMR (500 MHz, CDCl₃): δ 8.73 (d, J = 1.6 Hz, 1H), 8.60 (dd, J = 4.7, 1.6 Hz, 1H), 8.37 – 8.36 (m, 1H), 7.78 – 7.75 (m, 1H), 7.73 – 7.72 (m, 1H), 7.69 – 7.67 (m, 1H), 7.57 – 7.56 (m, 1H), 7.39 (dd, J = 8.2, 7.9 Hz, 1H), 7.37 – 7.35 (m, 1H), 7.11 – 7.09 (m, 1H), 4.12 (t, J = 8.4 Hz, 2H), 3.84 (s, 3H), 3.13 (t, J = 8.4 Hz, 2H); ¹³C-NMR (125 MHz, CDCl₃): δ 159.7, 156.2, 148.9, 147.8, 145.5, 138.9, 134.0, 133.5, 131.9, 129.8, 128.4, 124.9, 123.7, 120.2, 120.0, 112.5, 55.7, 48.7, 25.3.

3-methoxy-N-(4-(pyridin-3-yl)phenyl)benzenesulfonamide (11) The title compound was synthesized according to Method A using **11a** (256 mg, 0.75 mmol), pyridin-3-yl-boronic acid (188 mg, 1.5 mmol), Na₂CO₃ (318 mg, 3.0 mmol), Pd(PPh₃)₄ (90 mg, 0.08 mmol) and 1,2-dimethoxyethane (18 mL) / water (6 mL) to yield the crude product, which was purified by flash chromatography on silica gel (CH₂Cl₂ / MeOH, 500:1 to 62.5:1) to yield a slight yellow solid (186 mg, 73%). mp: 208 – 210 °C; HPLC: 99% pure; MS (ESI) m/z = 341 [$M^+ + H$]; ¹H-NMR (500 MHz, *d*₆-DMSO): δ 10.48 (s, 1H), 8.81 (d, J = 1.9 Hz, 1H), 8.51 (dd, J = 4.7, 1.6 Hz, 1H), 8.00 – 7.97 (m, 1H), 7.63 (d, J = 8.8 Hz, 2H), 7.48 (dd, J = 8.2, 7.9 Hz, 1H), 7.44 – 7.42 (m, 1H), 7.38 – 7.36 (m, 1H), 7.30 (dd, J = 2.5, 1.6 Hz, 1H), 7.22 (d, J = 8.8 Hz, 2H), 7.19 – 7.17 (m, 1H), 3.77 (s, 3H); ¹³C-NMR (125 MHz, *d*₆-DMSO): δ 159.3, 148.2, 147.3, 140.7, 137.7, 134.6, 133.6, 132.5, 130.6, 127.6, 123.8, 120.2, 118.7, 118.6, 111.6, 55.5.

3-methoxy-N-methyl-N-(4-(pyridin-3-yl)phenyl)benzenesulfonamide (12) The title compound was synthesized according to Method A using **12a** (178 mg, 0.5 mmol), pyridin-3-ylboronic acid (125 mg, 1.0 mmol), Na₂CO₃ (212 mg, 2.0 mmol), Pd(PPh₃)₄ (58 mg, 0.05 mmol) and 1,2-dimethoxyethane (15 mL) / water (5 mL) to yield the crude product, which was purified by flash chromatography on silica gel (CH₂Cl₂ / MeOH, 500:1 to 62.5:1) to yield a white solid (147 mg, 83%). mp: 108 – 110 °C; HPLC: 95% pure; MS (ESI) m/z = 396 [$M^+ + MeCN$]; ¹H-NMR (500 MHz, CDCl₃): δ 8.82 (d, J = 2.0 Hz, 1H), 8.60 (dd, J = 4.9, 2.0 Hz, 1H), 7.86 – 7.84 (m, 1H), 7.53 (d, J = 8.5 Hz, 2H), 7.40 – 7.36 (m, 2H), 7.24 (d, J = 8.5 Hz, 2H), 7.20 – 7.18 (m, 1H), 7.12 – 7.10 (m, 1H), 7.04 – 7.03 (m, 1H), 3.73 (s, 3H), 3.22 (s, 3H); ¹³C-NMR (125 MHz, CDCl₃): δ 159.7, 148.8, 148.2, 141.6, 137.6, 136.8, 135.6, 134.2, 129.8, 127.5, 127.1, 123.6, 120.0, 119.5, 112.4, 55.6, 38.1.

N-benzyl-3-methoxy-N-(4-(pyridin-3-yl)phenyl)benzenesulfonamide (13) To a suspension of 60% gas-volumetric NaH (24 mg, 0.6 mmol) in dry DMF (2 mL), at 0 °C, was added a solution of **11** (136 mg, 0.4 mmol) in DMF (2 mL) and the reaction mixture stirred at rt for 1 h. The reaction mixture was cooled to 0 °C, the benzyl bromide (55 µL, 0.45 mmol) was added dropwise and the reaction mixture warmed to 80 °C over 10 h. Then the mixture was cooled to ambient temperature and quenched by addition of H₂O (12 mL) and EtOAc (25 mL) which was partitioned and the aqueous layer was extracted with EtOAc (2 x 25 mL). The combined organic layer was washed with 1 M HCl solution (2 x 10 mL), H₂O (2 x 20 mL), brine (1 x 20 mL), dried over (MgSO₄) and the solvent was removed under reduced pressure to give the crude product, which was purified by flash chromatography on silica gel (n-hexane/EtOAc, 20:1 to 2:1) to yield a yellow solid (43 mg, 25%). mp: 99 – 101 °C; HPLC: 100% pure; MS (ESI) m/z = 472 [M^+ +MeCN]; ¹H-NMR (500 MHz, (CD₃)₂CO): δ 8.82 (s, 1H), 8.57 (d, J = 3.8 Hz, 1H), 7.99 – 7.97 (m, 1H), 7.61 (d, J = 8.8 Hz, 2H), 7.53 (dd, J = 8.2, 7.9 Hz, 2H), 7.43 – 7.41 (m, 1H), 7.36 – 7.34 (m, 2H), 7.31 – 7.29 (m, 1H), 7.28 – 7.25 (m, 4H), 7.22 – 7.19 (m, 1H), 7.17 – 7.16 (m, 1H), 4.91 (s, 2H), 3.82 (s, 3H); ¹³C-NMR (125 MHz, (CD₃)₂CO): δ 160.9, 149.7, 148.8, 140.7, 140.1, 137.9, 137.4, 134.8, 131.2, 130.2, 129.3, 129.2, 128.4, 128.1, 124.5, 120.6, 120.1, 113.1, 56.0, 54.8.

1-((3-methoxyphenyl)sulfonyl)-6-(pyridin-4-yl)-1,2,3,4-tetrahydroquinoline (14) The title compound was synthesized according to Method A using **14a** (190 mg, 0.5 mmol), pyridin-4-ylboronic acid (125 mg, 1.0 mmol), Na₂CO₃ (212 mg, 2.0 mmol), Pd(PPh₃)₄ (58 mg, 0.05 mmol) and 1,2-dimethoxyethane (15 mL) / water (5 mL) to yield the crude product, which was purified by flash chromatography on silica gel (CH₂Cl₂ / MeOH, 500:1 to 62.5:1) to yield a slight yellow solid (121 mg, 64%). mp: 116 – 118 °C; HPLC: 95% pure; MS (ESI) m/z = 381 [M^+ +H]; ¹H-NMR (500 MHz, CDCl₃): δ 8.63 (dd, J = 4.4, 1.7 Hz, 2H), 7.93 (d, J = 8.2 Hz, 1H), 7.48 (dd, J = 8.8, 2.5 Hz, 1H), 7.46 (dd, J = 4.4, 1.7 Hz, 2H), 7.33 (dd, J = 8.2, 7.9 Hz, 1H), 7.32 – 7.31 (m, 1H), 7.25 – 7.23 (m, 1H), 7.10 (dd, J = 2.2, 1.8 Hz, 1H), 7.07 – 7.05 (m, 1H), 3.86 – 3.84 (m, 2H), 3.69 (s, 3H), 2.56 (t, J = 6.6 Hz, 2H), 1.73 – 1.68 (m, 2H); ¹³C-NMR (125 MHz, CDCl₃): δ 159.7, 150.3, 147.3, 140.5, 137.8, 134.3, 131.1, 130.1, 127.6, 125.1, 125.0, 121.2, 119.4, 119.1, 111.6, 55.5, 46.7, 26.9, 21.5.

1-((3-methoxyphenyl)sulfonyl)-6-(pyridin-3-yl)-1,2,3,4-tetrahydroquinoline (15) The title compound was synthesized according to Method A using **14a** (190 mg, 0.5 mmol), pyridin-3-ylboronic acid (125 mg, 1.0 mmol), Na₂CO₃ (212 mg, 2.0 mmol), Pd(PPh₃)₄ (58 mg, 0.05 mmol) and 1,2-dimethoxyethane (15 mL) / water (5 mL) to yield the crude product, which was purified by flash chromatography on silica gel (CH₂Cl₂ / MeOH, 500:1 to 62.5:1) to yield a slight yellow solid (146 mg, 77%). mp: 107 – 109 °C; HPLC: 99% pure; MS (ESI) m/z = 381 [M^+ +H]; ¹H-NMR (500 MHz, CDCl₃): δ 8.80 (d, J = 2.2 Hz, 1H), 8.56 (dd, J = 4.7, 1.6 Hz, 1H), 7.91 (d, J = 8.8 Hz, 1H), 7.85 – 7.82 (m, 1H), 7.42 (dd, J = 8.5, 2.2 Hz, 1H), 7.36 – 7.32 (m, 2H), 7.26 – 7.24 (m, 2H), 7.08 – 7.05 (m, 2H), 3.85 – 3.83 (m, 2H), 3.69 (s, 3H), 2.54 (t, J = 6.6 Hz, 2H), 1.72 – 1.67 (m, 2H); ¹³C-NMR (125 MHz, CDCl₃): δ 159.7, 148.4, 148.0, 140.5, 137.0, 135.7, 134.2, 134.0, 131.2, 130.0, 127.6, 125.3, 125.2, 123.5, 119.4, 119.2, 111.5, 55.5, 46.7, 26.8, 21.5.

1-(phenylsulfonyl)-6-(pyridin-3-yl)-1,2,3,4-tetrahydroquinoline (16) The title compound was synthesized according to Method C using **16a** (105 mg, 0.5 mmol), 60% gas-volumetric NaH (40 mg, 1.0 mmol), benzenesulfonyl chloride (176 mg, 1.0 mmol) and dry THF (6 mL) to yield the crude product, which was purified by flash chromatography on silica gel (CH₂Cl₂ / MeOH, 500:1 to 62.5:1) to yield a slight brown oil (122 mg, 70%). HPLC: 100% pure; MS (ESI) m/z = 351 [M^+ +H]; ¹H-NMR (500 MHz, CDCl₃): δ 8.81 (dd, J = 2.2, 1.0 Hz, 1H), 8.56 (dd, J = 4.7, 1.6 Hz, 1H), 7.91 (d, J = 8.8 Hz, 1H), 7.86 – 7.84 (m, 1H), 7.67 – 7.65 (m, 2H), 7.57 – 7.53 (m, 1H), 7.45 – 7.41 (m, 3H), 7.36 – 7.33 (m, 1H), 7.25 – 7.24 (m, 1H), 3.86 – 3.84 (m, 2H), 2.54 (t, J = 6.6 Hz, 2H), 1.70 – 1.66 (m, 2H); ¹³C-NMR (125 MHz, CDCl₃): δ 148.4, 148.0, 139.6, 136.9, 135.7, 134.2, 134.0, 132.9, 131.0, 129.1, 127.6, 127.0, 125.3, 125.2, 123.5, 46.8, 26.8, 21.5.

1-((4-methoxyphenyl)sulfonyl)-6-(pyridin-3-yl)-1,2,3,4-tetrahydroquinoline (17) The title compound was synthesized according to Method C using **16a** (105 mg, 0.5 mmol), 60% gas-volumetric NaH (40 mg, 1.0 mmol), 4-methoxybenzene-1-sulfonyl chloride (206 mg, 1.0 mmol) and dry THF (6 mL) to yield the crude product, which was purified by flash chromatography on silica gel (CH₂Cl₂ / MeOH, 500:1 to 62.5:1) to yield a white solid (139 mg, 73%). mp: 98 – 100 °C; HPLC: 98% pure; MS (ESI) m/z = 381 [M⁺+H]; ¹H-NMR (500 MHz, CDCl₃): δ 8.81 (dd, J = 2.5, 1.0 Hz, 1H), 8.56 (dd, J = 4.7, 1.6 Hz, 1H), 7.91 (d, J = 8.5 Hz, 1H), 7.86 – 7.83 (m, 1H), 7.58 (d, J = 9.0 Hz, 2H), 7.41 (dd, J = 8.5, 2.2 Hz, 1H), 7.36 – 7.33 (m, 1H), 7.24 – 7.23 (m, 1H), 6.88 (d, J = 9.0 Hz, 2H), 3.84 – 3.82 (m, 5H), 2.57 (t, J = 6.6 Hz, 2H), 1.71 – 1.66 (m, 2H); ¹³C-NMR (125 MHz, CDCl₃): δ 163.0, 148.4, 148.0, 137.1, 135.8, 134.0, 131.2, 130.9, 129.2, 127.6, 125.3, 125.1, 123.5, 114.2, 55.6, 46.5, 26.9, 21.4.

6-(pyridin-3-yl)-1-(*m*-tolylsulfonyl)-1,2,3,4-tetrahydroquinoline (18) The title compound was synthesized according to Method C using **16a** (105 mg, 0.5 mmol), 60% gas-volumetric NaH (40 mg, 1 mmol), 3-methylbenzene-1-sulfonyl chloride (190 mg, 1 mmol) and dry THF (6 mL) to yield the crude product, which was purified by flash chromatography on silica gel (CH₂Cl₂ / MeOH, 500:1 to 62.5:1) to yield a yellow solid (120 mg, 66%). mp: 112 – 114 °C; HPLC: 100% pure; MS (ESI) m/z = 365 [M⁺+H]; ¹H-NMR (500 MHz, CDCl₃): δ 8.81 (dd, J = 2.5, 1.0 Hz, 1H), 8.56 (dd, J = 4.7, 1.6 Hz, 1H), 7.88 (d, J = 8.8 Hz, 1H), 7.87 – 7.83 (m, 1H), 7.48 (s, 1H), 7.43 (d, J = 7.6 Hz, 1H), 7.41 (dd, J = 8.2, 2.2 Hz, 1H), 7.36 – 7.33 (m, 2H), 7.30 (dd, J = 8.2, 7.6 Hz, 1H), 7.25 – 7.24 (m, 1H), 3.85 – 3.83 (m, 2H), 2.56 (t, J = 6.6 Hz, 2H), 2.34 (s, 3H), 1.73 – 1.68 (m, 2H); ¹³C-NMR (125 MHz, CDCl₃): δ 148.4, 148.0, 139.4, 139.2, 137.0, 135.8, 134.1, 134.0, 133.6, 131.0, 128.9, 127.6, 127.4, 125.2, 125.1, 124.2, 123.5, 46.6, 26.9, 21.6, 21.3.

6-(pyridin-3-yl)-1-tosyl-1,2,3,4-tetrahydroquinoline (19) The title compound was synthesized according to Method C using **16a** (105 mg, 0.5 mmol), 60% gas-volumetric NaH (40 mg, 1.0 mmol), 4-methylbenzene-1-sulfonyl chloride (190 mg, 1.0 mmol) and dry THF (6 mL) to yield the crude product, which was purified by flash chromatography on silica gel (CH₂Cl₂ / MeOH, 500:1 to 62.5:1) to yield a yellow oil (129 mg, 71%). HPLC: 97% pure; MS (ESI) m/z = 365 [M⁺+H]; ¹H-NMR (500 MHz, CDCl₃): δ 8.81 (dd, J = 2.5, 1.0 Hz, 1H), 8.56 (dd, J = 4.7, 1.9 Hz, 1H), 7.90 (d, J = 8.5 Hz, 1H), 7.86 – 7.83 (m, 1H), 7.53 (d, J = 8.5 Hz, 2H), 7.40 (dd, J = 8.5, 2.5 Hz, 1H), 7.36 – 7.33 (m, 1H), 7.24 – 7.21 (m, 3H), 3.84 – 3.82 (m, 2H), 2.56 (t, J = 6.6 Hz, 2H), 2.38 (s, 3H), 1.71 – 1.66 (m, 2H); ¹³C-NMR (125 MHz, CDCl₃): δ 148.3, 148.0, 143.7, 137.0, 136.6, 135.7, 134.0, 130.9, 129.6, 127.6, 127.1, 125.2, 125.1, 123.5, 46.5, 26.9, 21.5, 21.4.

6-(pyridin-3-yl)-1-((3-(trifluoromethoxy)phenyl)sulfonyl)-1,2,3,4-tetrahydroquinoline (20) The title compound was synthesized according to Method A using **20a** (256 mg, 0.5 mmol), pyridin-3-ylboronic acid (125 mg, 1.0 mmol), Na₂CO₃ (212 mg, 2.0 mmol), Pd(PPh₃)₄ (58 mg, 0.05 mmol) and 1,2-dimethoxyethane (12 mL) / water (4 mL) to yield the crude product, which was purified by flash chromatography on silica gel (CH₂Cl₂ / MeOH, 500:1 to 62.5:1) to yield a yellow solid (89 mg, 41%). mp: 112 – 114 °C; HPLC: 100% pure; MS (ESI) m/z = 475 [M⁺+MeCN]; ¹H-NMR (500 MHz, CDCl₃): δ 8.81 (d, J = 2.5 Hz, 1H), 8.58 (dd, J = 5.0, 1.6 Hz, 1H), 7.89 (d, J = 8.5 Hz, 1H), 7.85 – 7.83 (m, 1H), 7.61 – 7.59 (m, 1H), 7.50 – 7.47 (m, 2H), 7.43 (dd, J = 8.5, 2.5 Hz, 1H), 7.40 – 7.38 (m, 1H), 7.37 – 7.34 (m, 1H), 7.25 – 7.24 (m, 1H), 3.87 – 3.85 (m, 2H), 2.54 (t, J = 6.6 Hz, 2H), 1.72 – 1.67 (m, 2H); ¹³C-NMR (125 MHz, CDCl₃): δ 149.2 (q, J_{C-F} = 1.7 Hz), 148.3, 147.8, 141.4, 136.4, 135.8, 134.7, 134.3, 131.3, 130.7, 127.8, 125.5, 125.4, 125.3, 125.2, 123.6, 122.2 (q, J_{C-F} = 259.2 Hz), 119.7, 46.8, 26.7, 21.5.

6-(pyridin-3-yl)-1-((4-(trifluoromethoxy)phenyl)sulfonyl)-1,2,3,4-tetrahydroquinoline (21) The title compound was synthesized according to Method A using **21a** (256 mg, 0.5 mmol), pyridin-3-ylboronic acid (125 mg, 1.0 mmol), Na₂CO₃ (212 mg, 2.0 mmol), Pd(PPh₃)₄ (58 mg, 0.05 mmol) and 1,2-dimethoxyethane (12 mL) / water (4 mL) to yield the crude product, which was purified by flash chromatography on silica gel (CH₂Cl₂ / MeOH, 500:1 to 62.5:1) to yield a white solid (128 mg,

59%). mp: 80 – 82 °C; HPLC: 100% pure; MS (ESI) m/z = 475 [M^+ +MeCN]; $^1\text{H-NMR}$ (500 MHz, CDCl_3): δ 8.82 (dd, J = 2.5, 0.6 Hz, 1H), 8.58 (dd, J = 5.0, 1.6 Hz, 1H), 7.89 (d, J = 8.5 Hz, 1H), 7.86 – 7.84 (m, 1H), 7.72 – 7.70 (m, 2H), 7.43 (dd, J = 8.5, 2.5 Hz, 1H), 7.37 – 7.35 (m, 1H), 7.27 – 7.26 (m, 2H), 7.26 – 7.25 (m, 1H), 3.86 – 3.84 (m, 2H), 2.57 (t, J = 6.6 Hz, 2H), 1.74 – 1.69 (m, 2H); $^{13}\text{C-NMR}$ (125 MHz, CDCl_3): δ 152.5 (q, $J_{\text{C-F}}$ = 1.7 Hz), 148.7, 148.2, 138.1, 136.8, 135.8, 134.8, 134.3, 131.4, 129.4, 128.0, 125.6, 125.5, 123.8, 122.5 (q, $J_{\text{C-F}}$ = 259.8 Hz), 121.1, 47.0, 27.0, 21.8.

1-((3-fluorophenyl)sulfonyl)-6-(pyridin-3-yl)-1,2,3,4-tetrahydroquinoline (22) The title compound was synthesized according to Method C using **16a** (105 mg, 0.5 mmol), 60% gas-volumetric NaH (40 mg, 1.0 mmol), 3-fluorobenzene-1-sulfonyl chloride (194 mg, 1.0 mmol) and dry THF (6 mL) to yield the crude product, which was purified by flash chromatography on silica gel (CH_2Cl_2 / MeOH, 500:1 to 62.5:1) to yield a yellow solid (134 mg, 73%). mp: 100 – 102 °C; HPLC: 99% pure; MS (ESI) m/z = 369 [M^+ +H]; $^1\text{H-NMR}$ (500 MHz, d_6 -DMSO): δ 8.80 (dd, J = 2.5, 1.0 Hz, 1H), 8.54 (dd, J = 4.7, 1.9 Hz, 1H), 8.07 – 8.04 (m, 1H), 7.71 (d, J = 1.0 Hz, 1H), 7.66 – 7.49 (m, 6H), 7.47 – 7.45 (m, 1H), 3.85 – 3.83 (m, 2H), 2.58 (t, J = 6.6 Hz, 2H), 1.68 – 1.63 (m, 2H); $^{13}\text{C-NMR}$ (125 MHz, d_6 -DMSO): δ 162.6 (d, $J_{\text{C-F}}$ = 251.9 Hz), 148.7, 148.3, 141.8 (d, $J_{\text{C-F}}$ = 7.0 Hz), 136.8, 135.9, 134.8, 134.3, 131.3, 131.1 (d, $J_{\text{C-F}}$ = 7.6 Hz), 128.0, 125.6, 125.4, 123.8, 123.1 (d, $J_{\text{C-F}}$ = 3.5 Hz), 120.3 (d, $J_{\text{C-F}}$ = 21.3 Hz), 114.7 (d, $J_{\text{C-F}}$ = 24.6 Hz), 46.4, 26.1, 21.0.

1-((4-fluorophenyl)sulfonyl)-6-(pyridin-3-yl)-1,2,3,4-tetrahydroquinoline (23) The title compound was synthesized according to Method C using **16a** (105 mg, 0.5 mmol), 60% gas-volumetric NaH (40 mg, 1.0 mmol), 4-fluorobenzene-1-sulfonyl chloride (194 mg, 1.0 mmol) and dry THF (6 mL) to yield the crude product, which was purified by flash chromatography on silica gel (CH_2Cl_2 / MeOH, 500:1 to 62.5:1) to yield a yellow solid (104 mg, 56%). mp: 115 – 117 °C; HPLC: 100% pure; MS (ESI) m/z = 369 [M^+ +H]; $^1\text{H-NMR}$ (500 MHz, CDCl_3): δ 8.82 (dd, J = 2.2, 0.8 Hz, 1H), 8.57 (dd, J = 4.8, 1.8 Hz, 1H), 7.90 (d, J = 8.5 Hz, 1H), 7.86 – 7.83 (m, 1H), 7.68 – 7.65 (m, 2H), 7.42 (dd, J = 8.5, 2.3 Hz, 1H), 7.37 – 7.34 (m, 1H), 7.26 – 7.25 (m, 1H), 7.13 – 7.09 (m, 2H), 3.86 – 3.83 (m, 2H), 2.56 (t, J = 6.6 Hz, 2H), 1.73 – 1.67 (m, 2H); $^{13}\text{C-NMR}$ (125 MHz, CDCl_3): δ 165.2 (d, $J_{\text{C-F}}$ = 255.2 Hz), 148.5, 148.1, 136.7, 135.6 (d, $J_{\text{C-F}}$ = 2.8 Hz), 134.4, 134.1, 131.1, 129.8 (d, $J_{\text{C-F}}$ = 9.4 Hz), 127.7, 125.4, 125.3, 123.6, 116.4 (d, $J_{\text{C-F}}$ = 22.6 Hz), 46.7, 26.8, 21.5.

1-((3-chlorophenyl)sulfonyl)-6-(pyridin-3-yl)-1,2,3,4-tetrahydroquinoline (24) The title compound was synthesized according to Method C using **16a** (105 mg, 0.5 mmol), 60% gas-volumetric NaH (40 mg, 1.0 mmol), 3-chlorobenzene-1-sulfonyl chloride (211 mg, 1.0 mmol) and dry THF (6 mL) to yield the crude product, which was purified by flash chromatography on silica gel (CH_2Cl_2 / MeOH, 500:1 to 62.5:1) to yield a yellow solid (98 mg, 50%). mp: 78 – 80 °C; HPLC: 100% pure; MS (ESI) m/z = 426 [M^+ +MeCN]; $^1\text{H-NMR}$ (500 MHz, CDCl_3): δ 8.81 (d, J = 1.9 Hz, 1H), 8.56 (dd, J = 4.7, 1.6 Hz, 1H), 7.87 – 7.83 (m, 2H), 7.66 (dd, J = 2.2, 1.6 Hz, 1H), 7.52 – 7.49 (m, 2H), 7.42 (dd, J = 8.5, 2.2 Hz, 1H), 7.37 (d, J = 7.6 Hz, 1H), 7.36 – 7.33 (m, 1H), 7.26 – 7.25 (m, 1H), 3.86 – 3.83 (m, 2H), 2.57 (t, J = 6.6 Hz, 2H), 1.75 – 1.70 (m, 2H); $^{13}\text{C-NMR}$ (125 MHz, CDCl_3): δ 148.4, 148.0, 141.2, 136.5, 135.6, 135.2, 134.5, 134.0, 133.0, 131.1, 130.3, 127.7, 127.1, 125.3, 125.1, 125.0, 123.5, 46.8, 26.8, 21.6.

1-((4-chlorophenyl)sulfonyl)-6-(pyridin-3-yl)-1,2,3,4-tetrahydroquinoline (25) The title compound was synthesized according to Method C using **16a** (105 mg, 0.5 mmol), 60% gas-volumetric NaH (40 mg, 1.0 mmol), 4-chlorobenzene-1-sulfonyl chloride (210 mg, 1.0 mmol) and dry THF (6 mL) to yield the crude product, which was purified by flash chromatography on silica gel (CH_2Cl_2 / MeOH, 500:1 to 62.5:1) to yield a white solid (102 mg, 53%). mp: 125 – 127 °C; HPLC: 96% pure; MS (ESI) m/z = 426 [M^+ +MeCN]; $^1\text{H-NMR}$ (500 MHz, CDCl_3): δ 8.82 (dd, J = 2.2, 0.8 Hz, 1H), 8.58 (dd, J = 4.9, 1.6 Hz, 1H), 7.89 (d, J = 8.5 Hz, 1H), 7.86 – 7.83 (m, 1H), 7.58 (d, J = 8.8 Hz, 2H), 7.44 – 7.39 (m, 3H), 7.37 – 7.34 (m, 1H), 7.26 – 7.25 (m, 1H), 3.86 – 3.83 (m, 2H), 2.57 (t, J = 6.6 Hz, 2H), 1.74 – 1.67 (m, 2H); $^{13}\text{C-NMR}$ (125 MHz, CDCl_3): δ 148.5, 148.1,

141.2, 139.5, 138.1, 136.6, 135.6, 134.5, 134.0, 131.1, 129.4, 128.5, 127.8, 125.4, 125.3, 123.6, 46.7, 26.9, 21.6.

6-(pyridin-3-yl)-1-((3-(trifluoromethyl)phenyl)sulfonyl)-1,2,3,4-tetrahydroquinoline (26)

The title compound was synthesized according to Method A using **26a** (248 mg, 0.5 mmol), pyridin-3-ylboronic acid (125 mg, 1.0 mmol), Na₂CO₃ (212 mg, 2.0 mmol), Pd(PPh₃)₄ (58 mg, 0.05 mmol) and 1,2-dimethoxyethane (12 mL) / water (4 mL) to yield the crude product, which was purified by flash chromatography on silica gel (CH₂Cl₂ / MeOH, 500:1 to 62.5:1) to yield a white solid (119 mg, 57%). mp: 132 – 134 °C; HPLC: 99% pure; MS (ESI) *m/z* = 419 [M⁺+H]; ¹H-NMR (500 MHz, CDCl₃): δ 8.80 (dd, *J* = 2.5, 1.0 Hz, 1H), 8.58 (dd, *J* = 4.7, 1.9 Hz, 1H), 7.90 – 7.89 (m, 2H), 7.85 – 7.79 (m, 3H), 7.58 (dd, *J* = 8.5, 7.9 Hz, 1H), 7.44 (dd, *J* = 8.5, 2.5 Hz, 1H), 7.37 – 7.34 (m, 1H), 7.25 – 7.24 (m, 1H), 3.88 – 3.86 (m, 2H), 2.53 (t, *J* = 6.6 Hz, 2H), 1.73 – 1.69 (m, 2H); ¹³C-NMR (125 MHz, CDCl₃): δ 148.6, 148.1, 140.6, 136.3, 135.6, 134.9, 134.1, 131.7 (q, *J*_{C-F} = 33.6 Hz), 131.3, 130.1, 129.8, 129.4 (q, *J*_{C-F} = 3.6 Hz), 127.8, 125.5, 125.3, 124.2 (q, *J*_{C-F} = 4.0 Hz), 123.9 (q, *J*_{C-F} = 273.1 Hz), 123.6, 46.9, 26.7, 21.6.

6-(pyridin-3-yl)-1-((4-(trifluoromethyl)phenyl)sulfonyl)-1,2,3,4-tetrahydroquinoline (27) The title compound was synthesized according to Method A using **27a** (248 mg, 0.5 mmol), pyridin-3-ylboronic acid (125 mg, 1.0 mmol), Na₂CO₃ (212 mg, 2.0 mmol), Pd(PPh₃)₄ (58 mg, 0.05 mmol) and 1,2-dimethoxyethane (12 mL) / water (4 mL) to yield the crude product, which was purified by flash chromatography on silica gel (CH₂Cl₂ / MeOH, 500:1 to 62.5:1) to yield a white solid (115 mg, 55%). mp: 124 – 126 °C; HPLC: 99% pure; MS (ESI) *m/z* = 459 [M⁺+MeCN]; ¹H-NMR (500 MHz, CDCl₃): δ 8.82 (d, *J* = 1.8 Hz, 1H), 8.58 (dd, *J* = 4.8, 1.5 Hz, 1H), 7.91 (d, *J* = 8.5 Hz, 1H), 7.87 – 7.84 (m, 1H), 7.79 (d, *J* = 8.3 Hz, 2H), 7.71 (d, *J* = 8.3 Hz, 2H), 7.44 (dd, *J* = 8.5, 2.2 Hz, 1H), 7.38 – 7.34 (m, 1H), 7.27 – 7.26 (m, 1H), 3.89 – 3.86 (m, 2H), 2.56 (t, *J* = 6.6 Hz, 2H), 1.74 – 1.68 (m, 2H); ¹³C-NMR (125 MHz, CDCl₃): δ 148.6, 148.0, 143.1, 136.4, 135.6, 135.0 (q, *J*_{C-F} = 31.7 Hz), 134.7, 134.1, 131.1, 127.8, 127.6, 126.2 (q, *J*_{C-F} = 3.9 Hz), 125.4, 125.2, 123.8 (q, *J*_{C-F} = 272.6 Hz), 123.6, 48.8, 26.8, 21.7.

3-((6-(pyridin-3-yl)-3,4-dihydroquinolin-1(2H)-yl)sulfonyl)benzonitrile (28) The title compound was synthesized according to Method C using **16a** (105 mg, 0.5 mmol), 60% gas-volumetric NaH (40 mg, 1.0 mmol), 3-cyanobenzene-1-sulfonyl chloride (200 mg, 1.0 mmol) and dry THF (6 mL) to yield the crude product, which was purified by flash chromatography on silica gel (CH₂Cl₂ / MeOH, 500:1 to 62.5:1) to yield a white solid (133 mg, 71%). mp: 138 – 140 °C; HPLC: 98% pure; MS (ESI) *m/z* = 376 [M⁺+H]; ¹H-NMR (500 MHz, CDCl₃): δ 8.82 (dd, *J* = 2.5, 1.0 Hz, 1H), 8.58 (dd, *J* = 4.7, 1.6 Hz, 1H), 8.00 – 7.97 (m, 1H), 7.88 – 7.87 (d, *J* = 8.5 Hz, 1H), 7.86 – 7.82 (m, 3H), 7.58 (dd, *J* = 8.5, 7.9 Hz, 1H), 7.44 (dd, *J* = 8.5, 2.2 Hz, 1H), 7.37 – 7.35 (m, 1H), 7.27 – 7.26 (m, 1H), 3.88 – 3.86 (m, 2H), 2.59 (t, *J* = 6.6 Hz, 2H), 1.76 – 1.71 (m, 2H); ¹³C-NMR (125 MHz, CDCl₃): δ 148.6, 148.0, 141.2, 136.1, 135.9, 135.5, 135.0, 134.1, 131.1, 130.9, 130.6, 130.2, 125.2, 123.6, 117.0, 113.7, 127.9, 125.6, 46.9, 26.8, 21.7.

4-((6-(pyridin-3-yl)-3,4-dihydroquinolin-1(2H)-yl)sulfonyl)benzonitrile (29) The title compound was synthesized according to Method C using **16a** (105 mg, 0.5 mmol), 60% gas-volumetric NaH (40 mg, 1.0 mmol), 4-cyanobenzene-1-sulfonyl chloride (201 mg, 1.0 mmol) and dry THF (6 mL) to yield the crude product, which was purified by flash chromatography on silica gel (CH₂Cl₂ / MeOH, 500:1 to 62.5:1) to yield a yellow solid (116 mg, 62%). mp: 162 – 164 °C; HPLC: 100% pure; MS (ESI) *m/z* = 376 [M⁺+H]; ¹H-NMR (400 MHz, CDCl₃): δ 8.82 (d, *J* = 2.0 Hz, 1H), 8.58 (dd, *J* = 4.8, 1.5 Hz, 1H), 7.89 (d, *J* = 8.5 Hz, 1H), 7.86 – 7.83 (m, 1H), 7.77 – 7.72 (m, 4H), 7.44 (dd, *J* = 8.5, 2.3 Hz, 1H), 7.38 – 7.35 (m, 1H), 7.27 – 7.26 (m, 1H), 3.88 – 3.85 (m, 2H), 2.56 (t, *J* = 6.6 Hz, 2H), 1.73 – 1.68 (m, 2H); ¹³C-NMR (100 MHz, CDCl₃): δ 148.6, 148.0, 143.7, 136.2, 135.4, 134.9, 134.1, 132.9, 131.2, 127.9, 127.7, 125.5, 125.3, 123.6, 117.2, 116.4, 46.9, 26.8, 21.7.

6-(pyridin-3-yl)-1-(thiophen-2-ylsulfonyl)-1,2,3,4-tetrahydroquinoline (30) The title compound was synthesized according to Method C using **16a** (105 mg, 0.5 mmol), 60% gas-volumetric NaH (40 mg, 1.0 mmol), thiophene-2-sulfonyl chloride (182 mg, 1.0 mmol) and dry THF (6 mL) to yield the crude product, which was purified by flash chromatography on silica gel (CH₂Cl₂ / MeOH, 500:1 to 62.5:1) to yield a brown solid (110 mg, 62%). mp: 101 – 103 °C; HPLC: 99% pure; MS (ESI) m/z = 357 [M⁺+H]; ¹H-NMR (500 MHz, CDCl₃): 8.82 (dd, J = 2.2, 0.8 Hz, 1H), 8.58 (dd, J = 4.8, 1.5 Hz, 1H), 7.93 (d, J = 8.5 Hz, 1H), 7.87 – 7.84 (m, 1H), 7.53 (dd, J = 5.0, 1.2 Hz, 1H), 7.45 – 7.42 (m, 2H), 7.37 – 7.34 (m, 1H), 7.28 – 7.27 (m, 1H), 7.04 – 7.02 (m, 1H), 3.90 – 3.87 (m, 2H), 2.59 (t, J = 6.5 Hz, 2H), 1.78 – 1.72 (m, 2H); ¹³C-NMR (125 MHz, CDCl₃): δ 148.5, 148.1, 139.5, 136.4, 135.7, 134.5, 134.0, 132.2, 132.1, 131.4, 127.6, 127.3, 125.6, 125.3, 123.5, 47.0, 27.0, 21.5.

1-(naphthalen-2-ylsulfonyl)-6-(pyridin-3-yl)-1,2,3,4-tetrahydroquinoline (31) The title compound was synthesized according to Method C using **16a** (105 mg, 0.5 mmol), 60% gas-volumetric NaH (40 mg, 1.0 mmol), naphthalene-2-sulfonyl chloride (226 mg, 1.0 mmol) and dry THF (6 mL) to yield the crude product, which was purified by flash chromatography on silica gel (CH₂Cl₂ / MeOH, 500:1 to 62.5:1) to yield a slight brown oil (106 mg, 53%). HPLC: 100% pure; MS (ESI) m/z = 401 [M⁺+H]; ¹H-NMR (500 MHz, CDCl₃): δ 8.81 (d, J = 1.8 Hz, 1H), 8.57 (dd, J = 4.8, 1.2 Hz, 1H), 8.32 (d, J = 2.0, 1H), 7.97 (d, J = 8.5 Hz, 1H), 7.92 – 7.83 (m, 4H), 7.65 – 7.57 (m, 2H), 7.54 (dd, J = 8.6, 1.9 Hz, 1H), 7.43 (dd, J = 8.5, 2.3 Hz, 1H), 7.36 – 7.33 (m, 1H), 7.23 – 7.22 (m, 1H), 3.92 – 3.89 (m, 2H), 2.52 (t, J = 6.6 Hz, 2H), 1.72 – 1.66 (m, 2H); ¹³C-NMR (125 MHz, CDCl₃): δ 148.4, 148.0, 137.0, 136.6, 135.8, 134.8, 134.2, 134.0, 132.1, 131.0, 129.4, 129.3, 128.9, 128.5, 127.9, 127.7, 127.6, 125.3, 125.2, 123.6, 122.2, 46.7, 26.9, 21.7.

1-(cyclohexylsulfonyl)-6-(pyridin-3-yl)-1,2,3,4-tetrahydroquinoline (32) The title compound was synthesized according to Method C using **16a** (105 mg, 0.5 mmol), 60% gas-volumetric NaH (40 mg, 1.0 mmol), cyclohexanesulfonyl chloride (182 mg, 1.0 mmol) and dry THF (6 mL) to yield the crude product, which was purified by flash chromatography on silica gel (CH₂Cl₂ / MeOH, 500:1 to 62.5:1) to yield a white solid (78 mg, 44%). mp: 157 – 159 °C; HPLC: 100% pure; MS (ESI) m/z = 357 [M⁺+H]; ¹H-NMR (500 MHz, CDCl₃): δ 8.83 (s, 1H), 8.57 (s, 1H), 7.85 – 7.83 (m, 1H), 7.69 (d, J = 8.5 Hz, 1H), 7.37 – 7.33 (m, 3H), 3.82 – 3.80 (m, 2H), 3.24 – 3.18 (m, 1H), 2.92 (t, J = 6.6 Hz, 2H), 2.16 – 2.14 (m, 2H), 2.09 – 2.04 (m, 2H), 1.91 – 1.88 (m, 2H), 1.68 – 1.60 (m, 3H), 1.31 – 1.20 (m, 3H); ¹³C-NMR (125 MHz, CDCl₃): δ 148.2, 147.9, 137.8, 133.9, 132.6, 128.6, 128.3, 125.2, 123.5, 121.7, 61.9, 47.1, 27.5, 26.4, 25.2, 25.0, 22.9.

1-((3-methoxyphenyl)sulfonyl)-6-(pyridin-4-ylmethyl)-1,2,3,4-tetrahydroquinoline (33) The title compound was synthesized according to Method B using **33b** (56 mg, 0.25 mmol), 3-methoxybenzene-1-sulfonyl chloride (103 mg, 0.5 mmol), DMAP (6 mg, 0.05 mmol), pyridine (100 mg, 1.2 mmol) and dry THF (4 mL) to yield the crude product, which was purified by flash chromatography on silica gel (n-hexane / EtOAc, 20:1 to 4:1) to yield a brown oil (62 mg, 63%). HPLC: 98% pure; MS (ESI) m/z = 395 [M⁺+H]; ¹H-NMR (500 MHz, CDCl₃): δ 8.50 (d, J = 4.1 Hz, 2H), 7.74 (d, J = 8.5 Hz, 1H), 7.31 (dd, J = 7.9, 7.9 Hz, 1H), 7.22 – 7.20 (m, 1H), 7.08 (dd, J = 5.7 Hz, 2H), 7.05 – 7.02 (m, 2H), 6.98 (dd, J = 2.5, 1.6 Hz, 1H), 6.81 (s, 1H), 3.88 (s, 2H), 3.80 – 3.77 (m, 2H), 3.62 (s, 3H), 2.39 (t, J = 6.6 Hz, 2H), 1.64 – 1.59 (m, 2H); ¹³C-NMR (125 MHz, CDCl₃): δ 159.7, 149.9, 149.8, 140.6, 135.7, 135.5, 131.2, 129.9, 129.5, 127.2, 125.3, 119.4, 119.2, 111.5, 55.4, 46.6, 40.6, 26.6, 21.5.

1-((3-methoxyphenyl)sulfonyl)-6-(pyridin-3-ylmethyl)-1,2,3,4-tetrahydroquinoline (34) The title compound was synthesized according to Method B using **34b** (56 mg, 0.25 mmol), 3-methoxybenzene-1-sulfonyl chloride (103 mg, 0.5 mmol), DMAP (6 mg, 0.05 mmol), pyridine (100 mg, 1.2 mmol) and dry THF (4 mL) to yield the crude product, which was purified by flash chromatography on silica gel (n-hexane / EtOAc, 20:1 to 4:1) to yield a slight brown oil (70 mg, 72%). HPLC: 97% pure; MS (ESI) m/z = 395 [M⁺+H]; ¹H-NMR (500 MHz, CDCl₃): δ 8.47 – 8.46 (m, 2H), 7.72 (d, J = 8.2 Hz, 1H), 7.47 – 7.45 (m, 1H), 7.30 (dd, J = 8.4, 7.7 Hz, 1H), 7.22 – 7.18 (m, 2H), 7.04 – 7.01 (m, 2H), 6.97 – 6.96 (m, 1H), 6.81 – 6.80 (m, 1H), 3.90 (s, 2H), 3.78 – 3.76 (m,

2H), 3.61 (s, 3H), 2.37 (t, $J = 6.6$ Hz, 2H), 1.63 – 1.58 (m, 2H); ^{13}C -NMR (125 MHz, CDCl_3): δ 159.6, 150.1, 147.7, 140.6, 136.7, 136.3, 136.2, 135.3, 131.2, 130.0, 129.3, 127.0, 125.3, 123.4, 119.4, 119.2, 111.4, 55.4, 46.6, 38.4, 26.6, 21.4.

3. HPLC Purity Control of Final Compounds

The SurveyorR-LC-system consisted of a pump, an autosampler, and a PDA detector. Mass spectrometry was performed on a TSQR Quantum (Thermo Electron Corporation, Dreieich, Germany). The triple quadrupole mass spectrometer was equipped with an electrospray interface (ESI). The system was operated by the standard software XcaliburR. A RP C18 NUCLEODURR 100-5 (125 × 3 mm) column (Macherey-Nagel GmbH, Dueren, Germany) was used as stationary phase. All solvents were HPLC grade. In a gradient run the percentage of acetonitrile (containing 0.1% trifluoro-acetic acid) in water was increased from an initial concentration of 3% at 0 min to 100% at 15 min and kept at 100% for 10 min.

The injection volume was 10 µL and flow rate was set to 800 µL / min. MS analysis was carried out at a spray voltage of 3800 V, a capillary temperature of 350 °C and a source CID of 10 V. Spectra were acquired in positive mode from 100 to 1000 *m/z* and at 254 nm for the UV trace. In some cases APC ionization had to be applied.

Comp.	RT (min)	Purity (%)
3	10.39	98.1
4	10.29	98.3
5	8.61	97.8
6	9.29	98.3
7	8.46	99.2
8	9.54	98.0
9	9.97	95.5
10	9.89	98.4
11	10.22	98.8
12	10.45	95.1
13	9.58	100
14	12.18	95.0
15	11.55	98.9
16	8.09	99.7
17	9.80	100
18	8.56	100
19	8.12	100
20	8.63	100
21	8.08	97.8
22	8.50	99.6
23	8.96	100
24	13.28	99.0
25	9.66	100
26	8.36	97.8
27	11.83	97.3
28	8.16	100
29	8.35	100
30	9.38	95.9
31	9.87	99.1
32	9.74	100
33	12.47	97.6
34	12.12	97.2

4. Table S1 Inhibition of CYP11B2 by compounds **3** – **34**

Compd.	IC ₅₀ (nM) ^a	Compd.	IC ₅₀ (nM) ^a
1	60	18	205
2	608	19	555
metirapone	72	20	322
3	251	21	47% ^b
4	850	22	196
5	320	23	260
6	500	24	344
7	34% ^b	25	469
8	41% ^b	26	607
9	8% ^b	27	22% ^b
10	38% ^b	28	429
11	850	29	557
12	239	30	259
13	10% ^b	32	28% ^b
14	7% ^b	32	47% ^b
15	85	33	5
16	295	34	8
17	519		

^a Mean value of at least three independent tests, standard deviation less than 25%. Hamster fibroblasts expressing human CYP11B2; substrate 11-deoxycorticosterone, 100 nM. ^b Inhibition percentage with a compound concentration of 500 nM

6.4 Curriculum Vitae

Persönliche Daten

Name: Weixing Zhu

E-Mail: w.zhu@mx.uni-saarland.de

Geschlecht: weiblich

Geburtsjahr: 1982

Geburtsort: Hengyang, Provinz Hunan, V.R. China

Staatsangehörigkeit: chinesisch

Familienstand: verheiratet

Schulbildung

09/1990–06/1996	Grundschule
09/1996–06/2002	Gymnasium
2002	Abitur

Berufsausbildung/Studium

09/2002–06/2006	Institut für der medizinischen, Hunan Normal University, V.R. China
2006	Abschluss als Bachelor
09/2007–06/2010	Institut für Pharmazie, Central South University, V.R. China
2010	Abschluss als Master
09/2010–	Helmholtz-Institut für Pharmazeutische Forschung Saarland (HIPS) und Institut Pharmazeutische und Medizinische Chemie, Universität des Saarlandes, Deutschland, Doktorandin